

TRADE AND THE END OF ANTIQUITY*

Johannes Boehm[†]

Geneva Graduate Institute

Thomas Chaney[‡]

USC

August 2024

Preliminary draft

Abstract

What caused the end of antiquity, the shift of economic activity away from the Mediterranean towards northern Europe? We assemble a large database of coin flows between the 4th and 10th century and use it to document the shifting patterns of exchange during this time period. We build a dynamic model of trade and money where coins gradually diffuse along trade routes. We estimate the parameters of this model and recover time-varying bilateral trade flows and real consumption from data on the spatial and temporal distribution of coins. Our estimates suggest that technical progress, increased minting, and to a lesser degree the fall in trade flows over the newly formed border between Islam and Christianity contributed to the relative growth of Muslim Spain and the Frankish lands of northern Europe and the decline of the Roman-Byzantine world. Our estimates are consistent with the increased urbanization of western and northern Europe relative to the eastern Mediterranean from the 8th to the 10th century.

JEL Classification: F1, O1, N73.

Keywords: Gravity Models, International Trade, Market Access, Diffusion.

*We thank Marek Jankowiak, Reka Juhasz, Ezra Oberfield, Kevin O'Rourke, and Pseudoerasmus for helpful comments. Malo Cadudal-Ily, Jinpei Tuchel, and in particular Ye Sun provided excellent research assistance. Boehm gratefully acknowledges financial support from the Banque de France/Sciences Po partnership, and Chaney from the European Research Council (ERC grant 884847). All remaining mistakes are our own.

[†]johannes.boehm@graduateinstitute.ch.

[‡]thomas.chaney@gmail.com.

Introduction

We quantify the contribution of disruptions in technology, coin production, and trade to the end of classical antiquity —the decline of Roman and Greek civilizations in the Mediterranean, and subsequent shift of political and economic power to northwestern Europe and the Middle East.

What caused the end of antiquity has been a central question for centuries (see for instance [Montesquieu, 1734](#); [Voltaire, 1756](#); [Gibbon, 1789](#)). Most contemporary historians believe that the conquest of Rome by Germanic invaders in the fifth century did not lead to an immediate end of Roman institutions and commerce, as local institutions remained largely in place ([Pirenne, 1927, 1939](#); [Findlay and O'Rourke, 2009](#); [McCormick, 2001](#)). The archaeological evidence points to a shift in the economic activity to the north-west of Europe and away from the Mediterranean between the fifth and the eighth century. The timing, extent, and reasons remains debated, but when Charlemagne was crowned as Emperor at the end of the eighth century, the political and economic power in Europe is no longer centered around the Mediterranean, but in the Frankish lands of northwestern Europe. Famously, historian Henri Pirenne proposes that the expansion of the Arab Caliphate along the southern Mediterranean coast and into the Iberian peninsula disrupted commerce and political ties in the Mediterranean, and turned the emerging Carolingian Empire into a northern European power (“without Mohammed, Charlemagne would have been inconceivable,” [Pirenne, 1939](#), p.234). The evidence for these disruptions brought forward by Pirenne is mainly related to the disappearance of certain luxury goods north of the Mediterranean.¹

In this paper, we study the changing economic geography during Late Antiquity using the tools of modern quantitative trade models and novel data on the circulation of ancient coins. Our evidence suggests that Mediterranean trade was indeed disrupted by the emergence of the Arab Caliphate. This had a large negative impact on the heartlands of the Byzantine empire, initially very open to trade. But this trade disruption played only a minor role in northwestern Europe, which was not very open to trade. Instead, the growth of northwestern Europe is almost entirely fueled by improved technology and an increase in seigniorage-financed consumption. The relative decline of the Mediterranean world is therefore shaped by a combination of all three forces.

Our first contribution is to assemble a large database of coin finds from hoards that were deposited between AD 325 and AD 950, with observations from hundreds of thousands of coins found in hoards across Europe, North Africa, and the Middle East. Coins offer rich quantitative information in a generally data-scarce setting,² as numismatists and archaeologists have deciphered,

¹Pirenne’s argument is the near *absence* of mentions of silk and spices in historical texts written north of the Mediterranean, and the disuse of gold for coinage and papyrus for writings. These fragments of evidence, along with new archaeological findings, have been extensively studied and discussed by historians since Pirenne. See [Lopez \(1943\)](#), [Ashtor \(1970\)](#), [Hodges and Whitehouse \(1983\)](#), and, in particular, [McCormick \(2001\)](#)’s monumental work that synthesizes the existing literary and archaeological evidence on changes around the Mediterranean, including patterns of change in the flows of communications, objects, and travellers. The synthesis of [Wickham \(2006\)](#) interprets the evidence through the lens of social structures.

²Due to the fact that no comprehensive data on production, consumption, trade, or demographics exists for the

catalogued, and classified ancient coinage for over 200 years. We collect information about where and when coins were minted and buried, and present three stylized facts: (*i*) bilateral coin flows are disrupted by distance and political borders just like trade flows are, (*ii*) unlike traded goods, coins are in use over many years and older coins tend to travel farther, and (*iii*) the geography of coin flows across the Mediterranean changes abruptly around the time of the Arab conquests.

Our second contribution is to build and estimate a dynamic model of trade where agents use coins for transactions. Within each period, trade is governed by comparative advantages as in [Eaton and Kortum \(2002\)](#), and coins flow in opposite direction to trade. After being minted, the same coin can then be saved as a store of value and re-used for subsequent transactions. We first show that with saving, coin flows within a period inherit the same gravity structure as trade flows, up to a single multiplicative constant. We then characterize the full dynamics of coin flows, as coins are minted, saved, used for multiple transactions, and gradually percolate through the trade network.³ Those results allow us the estimate the parameters governing coin creation (minting) and trade in goods (trade and production costs).⁴ Our estimates for minting output are in line with known historical evidence, and our estimate for the travel time elasticity of trade is similar to that for Roman trade in ceramics ([Flückiger et al., 2022](#)). Our estimates reveal a large cost associated with crossing the newly erected border between Islamic and non-Islamic regions.

Our third contribution is to reconstruct time series for real consumption per capita for every 20-year period from the 4th to the 10th century for every region, fully partitioned into three economically meaningful terms: trade openness (as in [Eaton and Kortum, 2002](#); [Arkolakis et al., 2012](#)), technology, and seigniorage-financed trade deficits (similar to [Dekle et al., 2007](#)). We are able to recover real consumption series using solely data on coins, because coin flows contain information on (nominal) trade flows, which contain information on (relative) prices. Our estimates suggest that real consumption in the heartlands of the Byzantine empire collapsed in part due to the fall in trade flows in and out of regions newly conquered by the Arabs. But outside of Byzantium, fluctuations in trade openness contributed relatively little to changes in real consumption, simply because ancient regions were not open enough for trade to play a large role.⁵ We attribute instead most of the variations in real consumption to changes in technology and seigniorage-financed trade deficits. For instance, western and northern Europe including Islamic Spain witness a spectacular

first millennium AD, historians of this period rely to a large extent on literary sources.

³This dynamic model allows us to identify trade flows even with sparse coin data. Our estimation leverages the fact that a coin used for multiple transactions contains information on trade flows over multiple periods.

⁴As recognized by numismatists, whether a coin hoard is created (deliberately or accidentally buried), found by archaeologists, and documented by numismatists, depends on a series of endogenous events. To purge our estimation from those endogenous events we use only information on the *shares* of different coins within a hoard.

⁵Our estimates show a surprisingly large degree of trade openness in the first millennium AD; on average, regions import 20% of their consumption in AD 460-620, and 15% in AD 700-900. Yet unless the trade elasticity were very low (we use $\theta = 4$ from [Simonovska and Waugh, 2014](#)), a fall in import shares from 20 to 15% has only a small impact on consumption. We also note that our evidence comes solely from coins, so corresponds solely to monetized exchanges. Any non-monetized (barter) transaction is missing. To the extent that non-monetized exchanges are more likely to be local, we possibly underestimate aggregate consumption, and over-estimate trade openness.

rise in real consumption fueled by technical progress and a commensurate increase in minting output. Finally, in the absence of virtually any systematic evidence on ancient production, consumption, or trade, we show that our estimates on real consumption changes from pre- to post-AD 700 are remarkably consistent with measures of European urbanization post-AD 700.

While our paper is focused primarily on ancient trade, this does not necessarily mean that trade was a primary driver of economic activity in Late Antiquity. We use (estimates of) trade as a *tool* to learn about the economic geography of the ancient world. Our results suggest that while ancient trade was substantial, it had a minor impact on real consumption outside of Byzantium.

Related literature. Our paper relates to the literature on the role of market access in shaping economic outcomes across space, specifically in historical settings. Fogel (1964), Donaldson and Hornbeck (2016) and Hornbeck and Rotemberg (forthcoming) evaluate the impact of the US railroad on economic growth, Donaldson (2018) the impact of railroads in colonial India on relative welfare, and Nagy (2023) the impact of the westward expansion of the US on growth; Pascali (2017) evaluates the impact of steamships on maritime trade and relative development; Redding and Sturm (2008) study the impact of the iron curtain on comparative development in Germany, and Ahlfeldt et al. (2015) the impact of the Berlin wall on the urban structure of Berlin; Juhász (2018) studies the impact of the trade disruption brought by the Napoleonic blockade on industrial development; Flückiger et al. (2022) study the impact of the Roman transportation network on trade in ceramics (*terra sigillata*) from the 1st century BC to the 3rd century AD, and the persistent impact of the Roman network on European economic integration, while Michaels and Rauch (2018) study changes in the transportation and urban networks after the fall of the Western Roman Empire; Barjamovic et al. (2019) use shipment records from Assyrian merchant archives in Bronze Age Anatolia to estimate the location of ancient lost cities and their size. Within this literature, our paper is closest to several which use a structural approach (in particular Donaldson and Hornbeck, 2016; Hornbeck and Rotemberg, forthcoming; Donaldson, 2018; Nagy, 2023; Redding and Sturm, 2008; Ahlfeldt, Redding, Sturm, and Wolf, 2015; Barjamovic, Chaney, Coşar, and Hortaçsu, 2019). In contrast to this literature, we do not observe prices, trade costs, or even trade flows. Instead, we recover trade flows and relative factor prices from data on the movement of coins over space and time, which we structurally interpret through the lens of a dynamic model of trade and money. Liu and Tsvyanski (2024) feature a related mechanism where the dynamic transmission of shocks in an input-output network is subject to adjustment costs. Finally our paper speaks to a literature in economic history on the changes in Late Antiquity and early medieval times. This literature frequently uses numismatic evidence, mostly in a descriptive manner. A notable exception is Noonan (1980)'s study of Islamic coin finds of different vintages and origins in Eastern Europe and Scandinavia, which is similar in spirit to our exercise, but stops short of using a formal econometric model. Closest to our paper Persson and Sharp (2015) discuss

Pirenne's thesis and economic integration in Europe through the lens of a gravity model.⁶

The remainder of the paper is structured as follows. Section 1 lays out the historical context, describes our data, and presents three stylized facts on ancient coin flows. Section 2 presents and estimates our dynamic model of trade and money. Section 3 discusses our empirical results.

1 Historical context, data, and stylized facts

1.1 Historical context

We study the economic and political developments that occurred in the Mediterranean between the 4th and the 1st century AD. At the start of this period, the fourth century, the Mediterranean was still entirely under control of the Roman Empire, albeit at times with multiple emperors and conflict between them, and under mounting pressure from Germanic invasions. The death of the eastern emperor Theodosius I in 395 divided the Roman Empire into a western and an eastern half. The fifth century saw increased Germanic incursions in the east and west, culminating with the Ostrogothic king Odoacer deposing the last West Roman emperor Romulus Augustulus in 476 and ending the Western Roman Empire. Italy was ruled by the Ostrogoths until the 550s, and later by the Lombards; Spain was taken over by the Visigoths, France by the Merovingian dynasty of the Franks, and North Africa, Sicily, and Sardinia by the Vandals. The Eastern Roman (Byzantine) Empire at times reconquered parts of the former Western Roman territory, but in the sixth century became increasingly under pressure by wars with the Sasanian Empire in the east. The Byzantine-Sasanian wars of 602–628 depleted the resources of both empires, leaving a vacuum that was filled by the emerging Arab caliphate.

Figure 1 shows the rapid Arab expansion, starting in 622. By 634 the Arabs controlled the entire Arabian Peninsula. The Levant followed in the late 630's and Egypt in the 640's. By the end of the Rashidun Caliphate in 661, the Arabs controlled a territory from Tripoli in the west to Balkh in the east. The expansion continued under the Umayyad dynasty. In 698 the Arab army razed Carthage and by 709 they had fully conquered the Maghreb. In 711 they crossed the Strait of Gibraltar and defeated the Visigoths at the Battle of Guadalete. In 732 they were stopped by Charles Martel at Tours, and driven back across the Pyrenees. When the Abbasid family overthrew the ruling Umayyads in 750, the Umayyads retained control of most of Iberia (al-Andalus). While the Arab conquest ended Sasanian rule in the east, advances into Byzantine territory in Anatolia did not lead to sustained shifts in the land border. Meanwhile the Arabs strengthened their naval capabilities, ended the Byzantine naval control of the western Mediterranean and contested its control of the east. Arab sea raids on Mediterranean cities became frequent.

Two other notable (and overlapping) events have been linked to economic and political changes: the Plague of Justinian (541-549), which, according to contemporary literary sources led to large

⁶See Shatzmiller (2018) for a qualitative application of the gravity model to medieval trade in the Middle East.

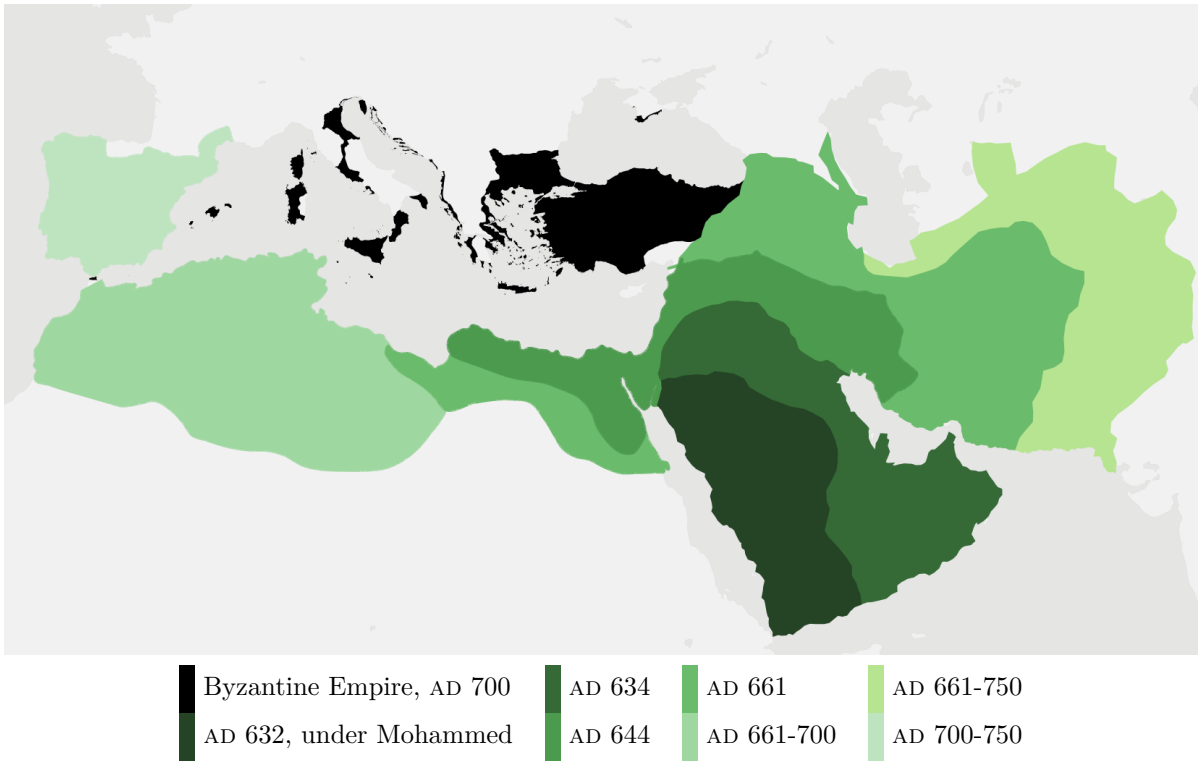


Figure 1: The Arab Conquests, AD 623-750

declines in population, and the temperature anomaly known as the “Late Antique Little Ice Age” (536–560), likely due to volcanic eruptions, which caused temperatures in the northern hemisphere to drop by about one degree Celsius (Peregrine, 2020). The size and quantitative relevance of these two events is heavily debated among historians. We will think of both these events as potentially affecting population and productivity levels, which our estimation strategy accounts for.

1.2 Data

We construct a large dataset on the flows of coins around the Mediterranean between AD 325 and AD 950.⁷ For the period from AD 325 to AD 725 we mostly rely on data from the *Framing the Late Antique and Early Medieval Economy* project (FLAME, 2023b),⁸ a large-scale effort by historians and numismatists to record harmonized information on the location, dating, and composition of coin finds up to the year 725. FLAME covers hoards⁹ from the Mediterranean and beyond, contributed by specialists working on the coinage of their geographical and temporal expertise. We use the most recent release of FLAME (January 2023) which covers 9,831 coin hoards. We remove hoards that fall outside our area of interest, continental western Europe up to the modern-day German-Polish border and including Bohemia, southern Europe up to the line

⁷Appendix B contains extensive information on the assembly, harmonization, and cleaning of the coin flow data.

⁸<https://coinage.princeton.edu/>

⁹FLAME also includes finds from excavations and single finds. Unless explicitly mentioned, we will treat all records in the same way and just use the word “hoard” to describe deposits of any size.

between Vienna and Odessa, and North Africa and the Middle East up to the maximum extent and area of influence of the Umayyad Caliphate (stretching from the Maghreb in the West to the Indus in the east, and up to Bulgar in the north).¹⁰ We also remove all hoards that only consist of incompletely described coins (no mint location or mint date information).

We supplement FLAME’s data, in particular for the period after AD 725, with hand-coded records of 106,373 coins from 824 finds, which we assemble using hoard catalogues from the numismatic literature, similarly to the source documents that underlie FLAME. These additional records include the time period of the Caliphate, so that we can assess the impacts of these changes on the patterns of exchange in the Mediterranean. Together these data cover the vast majority of published information on coin finds in our geographic and temporal scope.

No.	MINT	DATE	DIAM.	WEIGHT	NUMB.
51	الأندلس	114	29.	2.93	4
52	"	115	29.5	2.92	1
53	"	116	26.5	2.92	3

Figure 2: Coin hoard data, an example from al ’Ush (1972)

Notes: The figure shows an excerpt of an original publication from which we assemble hoard data: al ’Ush (1972) gives the content of the Damascus silver hoard in tabular form. From left to right, for the first row: the record number (51), the mint (al-Andalus), the date (year 114 of the Hijri calendar), diameter (29mm), weight (2.93g), and the number of coins with these attributes (4). The issuing dynasty (Umayyad) is given in the table headings and the denomination and material (silver *dirham*) is stated in the text.

The structure of the coin hoard data is ideally suited for an analysis of dynamic bilateral spatial flows. Each unit of observation—a coin—contains the following attributes: (*i*) the location where the coin has been minted, “mint” (birth place), (*ii*) a year interval when the coin was minted, “mint date” (birth date), (*iii*) the identifier and the location of the hoard that the coin is part of (death place), (*iv*) a year interval when the hoard—and therefore the coin—was deposited (death date). These pieces of information are typically recorded by the author of the original numismatic or archaeological publication. Figure 2 shows an example. Mints are usually inferred from mint marks on the coins.¹¹ The mint date is often indicated on the coin. When this is not the case, it can be approximated from the ruler (or dynasty or empire) under whose authority the coin was issued and other information, like the mint mark. Finally, we follow the common approach of historians to estimate the date of deposit of each hoard using the *terminus post quem*, or *tpq* for short, the date of the youngest object in the hoard that can be dated. In our case that is typically

¹⁰See figure 6 below for a map of our area of study. The precise definition and construction is given in Appendix C. We exclude the Viking lands, and therefore do not speak to the discussion on the potential role of the Vikings (and the inflow of Islamic silver through trade via eastern and northern Europe) in the changing economic geography during Late Antiquity (Bolin, 1953). Recent archaeometric studies indicate that Carolingian silver is largely not of Arab origin (Sarah, 2008; Sarah et al., 2008; Kershaw et al., 2024), suggesting a limited role for silver inflows via the Viking route in affecting Carolingian mint output.

¹¹Mint marks have been in use since ancient Greek times to monitor the weight and metal content of coins.

the most recent end year of the time intervals of the coins in the hoard.

In coding the mint location and date we typically follow the coding of the author of the original publication which catalogues the hoard.¹² In some cases this information is imprecise: the author of the publication may not have been able to inspect the coin or inspected only a fragment. We conduct robustness checks to investigate whether our findings are driven by endogenous selection.

We have data on 5,609 hoards and 494,311 coins that fall into our geographic boundary and have tpq between 325 and 950. After removing from FLAME large hoards found in the 19th century or earlier for which not much besides rough coin counts is known, 270,500, or 54.7% of coins are complete with a mint and minting year interval; on average 86% of coins in a hoard are complete. We define the age of coins at time of deposit as the difference between the midpoint of the coin’s minting interval and the tpq of the hoard. Figure 3a shows the temporal distributions of the number of hoard by tpq , and figure 3b shows the distribution of coin ages within a hoard.¹³

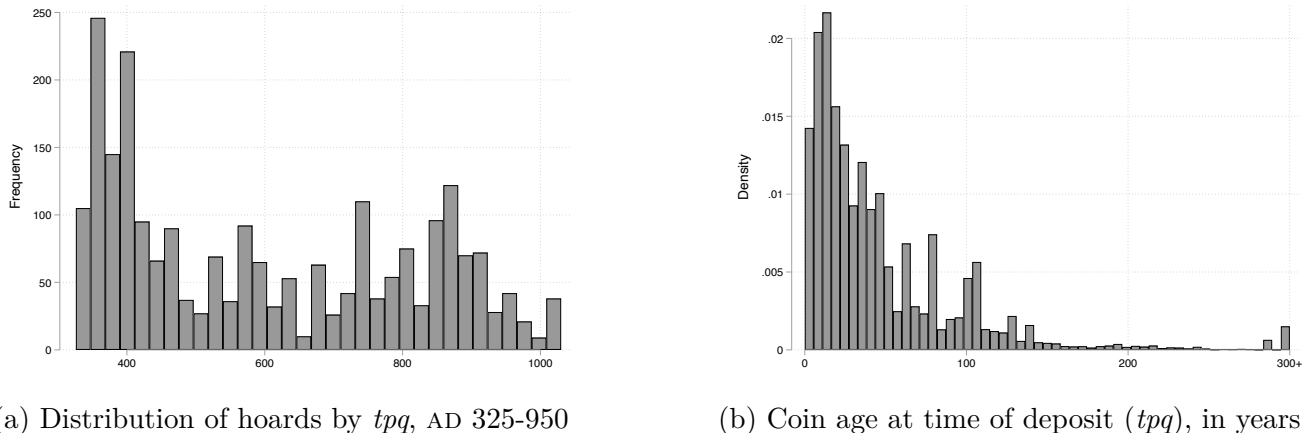


Figure 3: Number of hoards over time and ages of coins within hoards

Notes: Panel (a) shows the number of hoards per 20-year period. Panel (b) displays the (annual) density of coins of different ages. Coin age is defined as the difference between the midpoint of the coin’s minting interval and the tpq of the hoard it is found in.

Coins are deposited on average 47 years after they are struck, with some coins that are hundreds of years old. On average, hoards contain fewer older coins than younger coins. Appendix tables B.1 and B.2 contain additional summary statistics on coins and hoards.

Discussion. The interpretation of coin flows as relating to trade, despite having a long tradition among numismatists and historians,¹⁴ deserves some discussion. The Roman and subsequently Byzantine empire were generally fairly monetized economies, with coinage taking a pre-eminent

¹²Sometimes these interpretations are critically evaluated and corrected by subsequent scholars. Appendix B lists the extensive sources we use for each of the hand-coded hoards.

¹³To further support the view that the hoards in our data reflect coin circulation during Late Antiquity, Appendix figure A.1 compares the coin age distribution in our hoards with the one in twelve Byzantine hoards that Banaji (2016) labels as circulation hoards, i.e. that are known to have originated from coins that were in circulation.

¹⁴See, in particular, the discussions by Grierson (1959) and, more recently, Naismith (2014).

role and credit being very limited (Morrisson, 2002).¹⁵ The situation was similar in the caliphate (Bessard, 2020) and in the Carolingian empire (Coupland, 2014). The fact that coins were light, durable, and—because they were made from precious metal, which could be easily reminted—accepted within and across borders made them particularly suitable for long-distance trade.¹⁶ This is particularly the case for gold coins, traded throughout the Mediterranean and valued for their weight in gold (Banaji, 2016).¹⁷ Of course coins did not travel solely because of commerce; theft, gift-exchange, tribute, dowry, and ransom are other explanations for coin flows. We subsume those alternative motives for exchanges within a model of trade driven by comparative advantages.¹⁸

A potential source of bias comes from the fact that our data do not cover the universe of coin flows, but instead only hoards that have been created (i.e. the coins were either deliberately or accidentally deposited, which may depend on warfare, natural disasters, and property rights protection), found (which may depend on modern-day institutions, such as whether metal detecting is allowed, and modern-day market prices for historical coins), and documented by experts (which may depend on the local presence of experts, the ‘novelty’ of the hoards’ contents, and the demand for research on these topics).¹⁹ Our model-based estimation in section 2 is designed to correct those statistical biases, and differs from the more descriptive methods employed by historians.

Finally, an important characteristic of our data is that—in contrast to standard trade data—we do not observe flows at each point in time, but only when and where a coin was minted, and where and when a coin is deposited into a hoard. Our structural model in section 2 is specifically designed to identify the parameters governing trade flows from data on coin stocks, and to reconstruct the possibly numerous successive trips a coin took throughout its life.

1.3 Three stylized facts on ancient coins

We present reduced-form evidence on three stylized facts, which inform our model in section 2.

Distance and political borders disrupt trade. The bilateral structure of our dataset, with a mint-origin and hoard-destination for each coin, allows us to explore the geography of coin flows in reduced form. We aggregate hoard (h) and mint (m) to $1^\circ \times 1^\circ$ cells across all periods, and

¹⁵A possible exception was the eighth century, where Byzantine mint output collapsed.

¹⁶Examples of the use of currency in foreign empires abound. Bates (1991) discusses how Byzantine coins kept circulating (and even being minted) in Egypt following the Arab takeover in 641. Tribute and ransom payments between the Arabs and Byzantines following periods of conflict often included domestic currency. See also Chapter 12 of McCormick (2001), who discusses the circulation of Arab and Byzantine coins in the west.

¹⁷We conduct robustness checks of our main results that restricting the sample to gold coins.

¹⁸Other data-driven approaches used by economic historians to measure economic activity include urbanization rates, the flows of consumption goods, notably ceramics (Wickham, 2006, Flückiger et al., 2022), communication flows and movements of people (McCormick, 2001), pollen grain measurements (Izdebski et al., 2016), and ice core readings (McConnell et al., 2018, Loveluck et al., 2018). Coin flows bring several econometric advantages and are plausibly more directly related to comprehensive patterns of exchange than ceramics or communications flows. We estimate similar distance elasticities from gravity regressions on coin and ceramic flows in appendix figure A.2.

¹⁹FLAME (2023a) discusses potential sources of biases, which also apply to our combined data.

model coin flows between cells as a function of distance and a political border dummy,

$$\text{count}_{mhp} = \exp(a_{mp} + a_h + b_1 \log \text{distance}_{mh} + b_2 \text{PoliticalBorder}_{hp} + u_{mhp}). \quad (1)$$

We estimate this model by PPML using data on all triplets (m, h, p) for mint cell m in political block b and hoard cell h . The political border dummy is one if the region where the center of the hoard cell h is located in has never and to no extent been under the political control of p .²⁰

Table 1: Distance and Border Effects in Coin Flows

	Dep. var.: # Coins _{mdh}				Dep. var.: Value _{mdh}	
	(1)	(2)	(3)	(4)	(5)	(6)
Log Distance	-1.138*** (0.12)	-1.002*** (0.13)	-1.139*** (0.10)	-0.954*** (0.077)	-1.146*** (0.076)	-0.991*** (0.069)
Political border		-1.945*** (0.62)		-2.071*** (0.47)		-1.516*** (0.27)
Hoard Cell FE	Yes	Yes	Yes	Yes	Yes	Yes
Mint × Empire Cell FE	Yes	Yes	Yes	Yes	Yes	Yes
Sample	All	All	Gold only	Gold only	Gold and Silver	Gold and Silver
Estimator	PPML	PPML	PPML	PPML	PPML	PPML
Pseudo- R^2	0.767	0.778	0.809	0.824	0.800	0.810
Observations	217748	217748	57457	57457	146766	146766

Standard errors in parentheses, clustered at mint cell × empire and hoard cell level.

* $p < 0.10$, ** $p < 0.05$, *** $p < 0.01$

Notes: This table presents various specifications of equation (1). The dependent variable is the number of coins in a hoard cell h from a mint cell m issued by a political entity p in columns 1-4, and the value of coins in columns 5-6. Hoard and mint cells are $1^\circ \times 1^\circ$. Political entities here are categorized into fourteen divisions. Columns 1 and 2 use all coins. Columns 1-2 use data on all coins, columns 3-4 gold only, and columns 6-7 gold and silver.

Table 1 shows the results. Distance between mint and hoard is negatively correlated with coin flows, and crossing a political border is equivalent to a ten-fold increase in distance.²¹ Columns 3 and 4 show almost identical results when restricting the sample to gold coins, which were universally valued throughout the Mediterranean for their metal content and were therefore particularly favored for long-distance trade. Despite accounting for only 7% of the coins in our sample, distance and border effects for gold coins are remarkably similar. Column 5 and 6 also show almost identical results when using silver and gold coins and weighing them by their relative value.²²

²⁰See appendix C for our division of the combined Arab and Mediterranean world into 13 regions.

²¹The distance and border effects are robust to using only the intensive margin of coin flows see appendix table A.1. An alternative explanation for the significance of the border effect would be that coins first get administratively redistributed within a political entity before entering circulation. Appendix table A.2 shows gravity regressions with hoard × empire fixed effects that suggest that this is unlikely to be the case at a large scale.

²²We calculate the equivalent gold weight of silver coins in two steps. First, we code the reference weights of coins of different denominations in our data, noting that coins are often clipped, broken, debased, or abraded. Second, we convert this reference weight into a gold-equivalent weight assuming a constant conversion ratio of 12g of silver for 1g of gold, which should be seen as a rough approximation given the fluctuations of the gold-silver

While purely reduced form, those results suggest that coin flows contain information related to trade costs (e.g. distance and border effects).²³ The key contribution of our model in section 2 is to isolate features of the geography of coin flows that are driven by trade.

Older coins travel further. Coins are found, on average, in hoards 800 kilometers from their mint. But within hoards, older coins are also coins that have on average travelled farther. Table 2 shows results from a regression of log distance between a coin’s mint and hoard place on the log age between minting and the hoard’s tpq , with hoard fixed effects to isolate within hoard variations.

Table 2: Coin age and distance travelled

	Dependent variable: Log Distance between Mint and Hoard				
	(1)	(2)	(3)	(4)	(5)
Log Age of Coin	0.146*** (0.044)	0.0831*** (0.026)	0.0750** (0.030)	0.160*** (0.043)	0.0486** (0.020)
Sample				No non-hoards	No non-hoards
Hoard FE	Yes	Yes	Yes	Yes	Yes
Mint × 50-year-interval FE		Yes			
Mint × 25-year-interval FE			Yes		Yes
R^2	0.762	0.863	0.869	0.775	0.898
Observations	287257	287040	286884	250161	249835

Standard errors in parentheses, clustered at the hoard level.

* $p < 0.10$, ** $p < 0.05$, *** $p < 0.01$

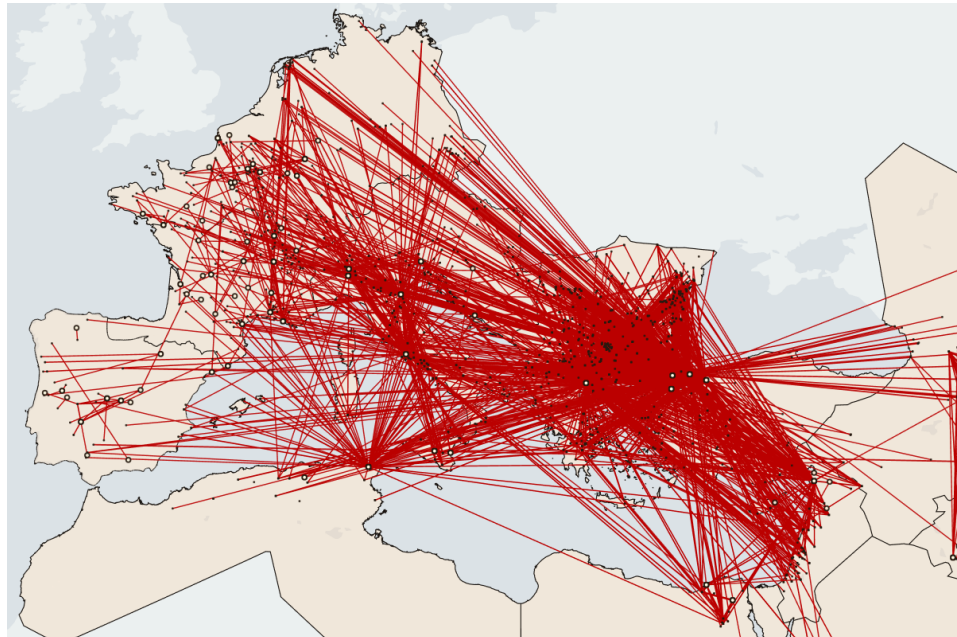
Notes: The dependent variable is the log distance between the mint location and the location of the hoard. The independent variable is the log age of the coin at the date of the tpq of the hoard (where the age is defined as the difference between the midpoint of the minting interval and the maximum of the endpoints of the minting intervals). In the rare cases where this age is zero (the youngest coin in the hoard is dated to a precise year) we set the log age to zero. Mints are identified as all Nomisma or FLAME-recorded entities that have been geocoded to the same $0.1^\circ \times 0.1^\circ$ cell. Columns (4) and (5) exclude FLAME finds that are tagged as not being hoards.

The coefficient of coin age is positive and significant, even when including mint × mint time fixed effects to control for the average distance travelled and age of coins of a particular mint and issue. This suggests that older coins are used on average for more transactions, with each transaction taking them further away from their mint origin. Our structural model is designed to disentangle the many transactions of old coins from the few transactions of young coins.

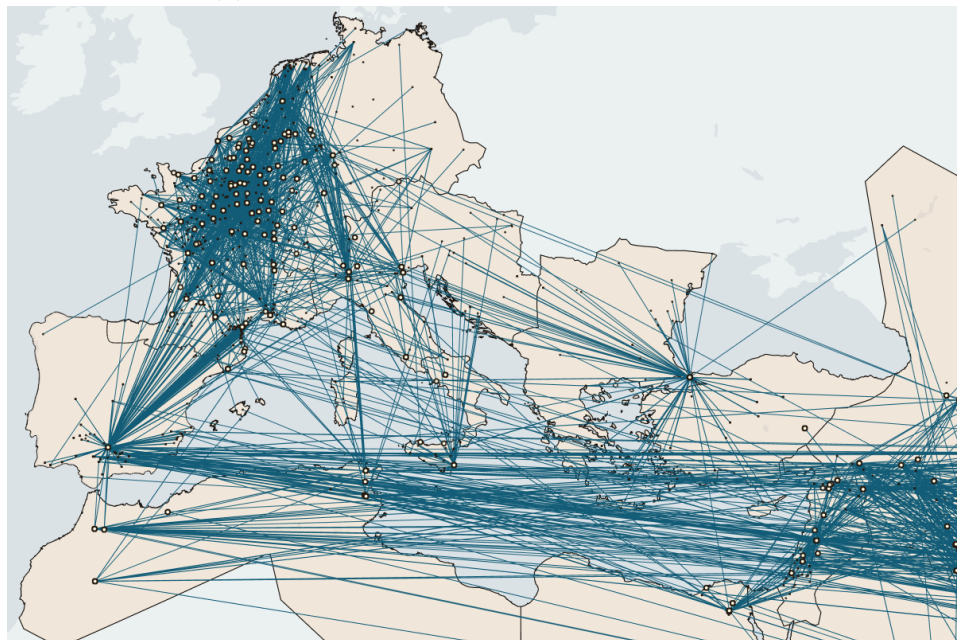
ratio between 1:10 and 1:16 (Bolin, 1953). With this value metric, gold represents 80% of the resulting value in our data. Since the price of copper/bronze fluctuates heavily during Late Antiquity (see Banaji, 2016, Ch. 5) and copper denominations frequently traded at values different from their intrinsic value based on their metal content, we only use silver and gold coins. We also note that FLAME does not record weights of coins, resulting in only approximate calculations.

²³To further investigate the informativeness of coins for trade flows, Appendix figure A.2 compares the distance elasticity from coin flows with distance elasticities obtained from flows of Roman Terra Sigillata ceramics, the only tradable good from Antiquity on which substantial amounts of data are available (Flückiger et al., 2022). We find similar but slightly higher distance elasticities for Terra Sigillata, possibly due to coins being more durable and hence being more frequently re-used in exchange (see Section 2.2).

The geography of coin flows changes sharply around the Arab conquests. We show descriptives of the movements of coins during Late Antiquity. Figure 4 illustrates the changes in the flow of coins across the Mediterranean before and after the Arab conquests.



(a) Before the Arab conquests: AD 450-630



(b) After the Arab conquests: AD 713-900

Figure 4: Changes in coin flows in the ancient world

Notes: The figure shows coin flows, indicated by a straight line, between mints and find spots. The sample consists of all coin groups where both the lower end of the mint interval and the tpq of the hoard lie between AD 450 and AD 630 (panel (a)) and AD 713 and AD 900 (panel (b)). Hoards from outside the shaded area are excluded.

Panel (a) shows flows from AD 450 to AD 630. Constantinople, Thessalonica, Rome, Ravenna,

and Carthage are important mints whose coins flow across the entire Mediterranean. Coins from Carthage cross the sea into Europe, and coins from Rome and Constantinople cross into Africa and the Middle East. Panel (b) shows that the patterns of coin flows change abruptly after 713, when the Arabs conquer the eastern Mediterranean coast (up to and including Antioch), the southern Mediterranean coast, and most of the Iberian peninsula. Most coins flow east to west within the Islamic Caliphate, within the Arab heartlands of Syria, Mesopotamia, and Egypt, and within the Frankish lands of northern Europe. The coin flows emanating from the remaining Byzantine mints in Constantinople, Syracuse, and Italy are much smaller than in the earlier period.²⁴ Besides a few coins from the mints of Ifriqiya and al-Abbasiyya that end up in the hoards of Ilanz and Steckborn (McCormick, 2001), there are almost no north-south flows across the Mediterranean. Flows that cross the border between Christianity and Islam primarily do so in the West across the Pyrenees (Parvére, 2014, 2018). Appendix figure A.3 and table A.3 present additional evidence that the flow of coins across the Mediterranean dropped after the Arab conquests, and that Islamic coins crossing the sea replace Roman coins. Despite the fact that in some historical sources the Arabs called the Mediterranean the “Sea of the Romans” (*Bahr al-Rūm(ī)*), after the Arab conquests the Mediterranean became, at least when it comes to coin flows, an Arab dominated sea.²⁵

While only descriptive, figure 4 suggests that the Arab conquest induced a substantial change in the economic geography of the ancient world, in the middle of our sample period. The structural model in the next section is designed to quantify those changes.

2 Model and estimation

We now introduce a quantitative model of trade, money, and the diffusion of coins. This model forms the basis for the estimation of trade costs, mint outputs, and technology, from which we can quantify the importance of political changes for the economic geography of the ancient world.

This model hinges on two key assumptions. First, we assume that coins are used for transactions. This assumption is natural in a heavily monetized ancient world (Henry, 1967; Bessard, 2020). It is plausible: using alternative means to finance transactions would require complex financial contracts. It is also necessary for our analysis: if coins are not used to clear gross bilateral trades, then data on coin flows would not contain any information on bilateral trade flows. Second,

²⁴The changes in the magnitude and location of Byzantine coin production has been the topic of a large literature. Kazhdan (1954) was the first to argue for a decline of Byzantine cities in the 8th and 9th century based on archaeological evidence. Several authors (including Kazhdan, Zavagno, 2022, and Pennas, 1996) relate these changes to Arab military pressure. Grierson (1973) notes that the eastern mints of Nicomedia, Cyzicus, Thessalonica, Cyprus, as well as Catania, were closed in 629-630, before the Arab conquests, and production was relocated to Constantinople. Nevertheless, a number of provincial mints, including Syracuse, Ravenna, and Rome, remained active until at least the mid-8th century (in the case of Syracuse until 878 when it fell to the Aghlabids).

²⁵Paraphrasing Pirenne (1939). We take the Arab conquests as a proximate cause for these changes, and do not attempt to explain why the Arabs were successful. The commonly held view is that the Byzantine-Sasanian war of 602–628 exhausted the forces of both empires and paved the way for Arab military success (Foss, 1975).

we assume that coins are fungible. This assumption is natural with coins valued for their precious metal content, and is supported by historical evidence on the wide circulation of foreign-origin coins (Bates, 1991; McCormick, 2001).

2.1 Model

Set up. There are N locations, denoted by a subscript. Time is discrete, denoted in square brackets. Each time period is decomposed into three sub-periods: beginning, middle, and end.

At the end of period $t - 1$, location n sets aside $S_n[t]$ coins for consumption and saving at t .

At the beginning of period t , an exogenous fraction $\lambda_n[t]$ of the coins in this stock $S_n[t]$ ceases to circulate, either lost or melted into fresh new coins.²⁶ In addition, some locations own a mint which exogenously generates fresh new coins if it is active in period t , $M_n[t] \geq 0$.

In the middle of period t , $L_n[t]$ identical workers save a fraction $s_n[t]$ of their coins, and spend the rest on consumption, $X_n[t]$. Importantly, expenditures contain spending on all goods, possibly including capital goods. What we label saving, $s_n[t]$, solely captures saving into nominal financial assets (coins), not investment into physical capital. Workers face the following budget constraint,

$$X_n[t] = (1 - s_n[t]) \left((1 - \lambda_n[t]) S_n[t] + M_n[t] \right), \text{ with } s_n[t] \geq 0, \quad (2)$$

where we assume workers cannot borrow ($s_n[t] \geq 0$). This is a ‘coin-in-advance’ economy where consumption is financed by available coins, and not by promised future income.²⁷

At the end of period t , workers earn a competitive wage $w_n[t]$ selling goods in exchange for $w_n[t] L_n[t]$ worth of coins. The stock of coins set aside for the subsequent period evolves recursively,

$$S_n[t+1] = (1 - \lambda_n[t]) S_n[t] + M_n[t] + w_n[t] L_n[t] - X_n[t]. \quad (3)$$

Trade. Within each period trade is shaped by comparative advantages as in Eaton and Kortum (2002). Consumers in n spend a fraction $\pi_{ni}[t]$ of their expenditures on imports from i , $X_{ni}[t]$,

$$\pi_{ni}[t] = \frac{X_{ni}[t]}{X_n[t]} = \frac{T_i[t] (w_i[t] d_{ni}[t])^{-\theta}}{\sum_k T_k[t] (w_k[t] d_{nk}[t])^{-\theta}} \quad (4)$$

²⁶We think of λ primarily as coins melted into bullion for their precious metal content, possibly as a seigniorage tax to be re-minted into fresh new coins. A very small fraction of λ is literally lost, buried into a hoard and forgotten. Some of those lost coins will eventually be found by archaeologists and become part of our dataset.

²⁷If this assumption were relaxed, workers in one location would send their income (coins) to pay for consumption on goods from another location; those coins would become the income of workers in those locations, which they would send to other locations, etc, all within the same period. Coins would travel infinitely many times within each period and data on coin holdings would contain no information on trade. Similarly, if coins were used only to clear bilateral imbalances, data on coins would contain information on net trade but not on gross trade flows.

Inter-temporal allocations. Workers have log-utility over real consumption,

$$U_n[t] = \mathbb{E}_t \left[\sum_{\tau \geq t} \beta^{\tau-t} \ln \left(\frac{X_n[\tau]}{p_n[\tau]} \right) \right], \text{ with } p_n[t] = \gamma \left(\sum_k T_k[t] (w_k[t] d_{nk}[t])^{-\theta} \right)^{-1/\theta}.$$

β is the discount rate and $p_n[t]$ the ideal price index in n at t as in Eaton and Kortum (2002). Each location chooses a sequence of coins stocks to maximize utility, given wages, and subject to the no borrowing constraint (2), the budget constraint (3), the optimal within-period allocation across imports (4), and a transversality condition which prevents holding coins forever,

$$\begin{aligned} & \max_{\{S_n[\tau]\}_{\tau \geq t}} \mathbb{E}_t \left[\sum_{\tau \geq t} \beta^{\tau-t} \ln \left(\frac{(1 - \lambda_n[\tau]) S_n[\tau] + M_n[\tau] + w_n[\tau] L_n[\tau] - S_n[\tau+1]}{\gamma \left(\sum_k T_k[\tau] (w_k[\tau] d_{nk}[\tau])^{-\theta} \right)^{-1/\theta}} \right) \right] \\ & \text{s.t. } S_n[\tau+1] \geq w_n[\tau] L_n[\tau], \forall (\tau \geq t), \text{ and } \lim_{\tau \rightarrow \infty} \beta^\tau \frac{S_n[\tau+1]}{X_n[\tau]} = 0. \end{aligned} \quad (5)$$

In this model, saving ($s_n[\tau] > 0 \Leftrightarrow S_n[\tau+1] > w_n[\tau] L_n[\tau]$) is used for consumption smoothing.

Equilibrium. Wages are determined by market clearing each period, given the trade equilibrium, $\pi_{ni}[t]$ from equation (4), and the coin stock policy function, $S_n[t]$ from equation (5),

$$w_i[t] L_i[t] = \sum_n \pi_{ni}[t] \left((1 - \lambda_n[t]) S_n[t] + M_n[t] + w_n[t] L_n[t] - S_n[t+1] \right), \forall (i, t). \quad (6)$$

In a useful benchmark where agents save little to none, $s_n[t] \approx 0$, expenditures on the right hand side simplify into $X_n[t] = (1 - \lambda_n[t]) w_n[t-1] L_n[t-1] + M_n[t]$.

Steady state equilibrium. We use the following steady state when simulating counterfactual equilibria in section 3. All aggregate variables are constant, in particular $w_n[t] L_n[t] = w_n L_n$ and $M_n[t] = M_n, \forall (n, t)$. If agents correctly anticipate they are in a steady state, there is no consumption smoothing motive for saving, $s_n = 0$ and $X_n = (1 - \lambda_n) w_n L_n + M_n$. If agents incorrectly anticipate shocks and save for precautionary motives, the same equality between expenditure and income (inclusive of minting) holds to a first order, $X_n = \frac{1-s_n}{1-s_n+\lambda_n s_n} ((1 - \lambda_n) w_n L_n + M_n)$ with $\frac{1-s_n}{1-s_n+\lambda_n s_n} \approx 1$.²⁸ Equilibrium wages jointly clear markets,

$$w_i L_i = \sum_n \pi_{ni} \left((1 - \lambda_n) w_n L_n + M_n \right), \text{ and } \pi_{ni} = \frac{T_i (w_i d_{ni})^{-\theta}}{\sum_k T_k (w_k d_{nk})^{-\theta}}, \quad (7)$$

²⁸We estimate $\lambda = 1.7\%$ p.a. (section 2.3), and Scheidel (2015) calculates $s = 1.5\%$ for Roman times.

such that the aggregate stock of coins in circulation is constant, $\sum_n M_n = \sum_n \lambda_n w_n L_n$.²⁹

2.2 Dynamic accumulation in coin hoards

Our aim is to match the quantities in our model to our data on ancient coins, which contains information on mint/hoard locations and dates. To do so, we explicitly follow the movements of coins of different vintages, minted in different locations, as they travel through the trade network.

We denote by $S_{mi}[t, \tau]$ the number of coins minted in location m at time t which are part of the coin stock of location i at time τ , with $S_i[\tau] = \sum_{m=1}^N \sum_{t \leq \tau} S_{mi}[t, \tau]$. Coins start their ‘coin life’ when they are minted, so $S_{mm}[t, t] = M_m[t]$. Subsequently, they circulate across locations as they are used for transactions or saved. $S_{mi}(t, \tau)$ evolves recursively,

$$S_{mi}[t, \tau + 1] = \sum_{n=1}^N (1 - s_n[\tau]) (1 - \lambda_n[\tau]) S_{mn}[t, \tau] \pi_{ni}[\tau] + s_i[\tau] (1 - \lambda_i[\tau]) S_{mi}[t, \tau], \forall (\tau \geq t). \quad (8)$$

At time τ , each location n has a stock of coins set aside. A fraction $(1 - s_n[\tau])$ is spent on goods (non-saved). Of those coins, $(1 - \lambda_n[\tau]) S_{mn}[t, \tau]$ were minted in location m at time t . Consumers in n send a fraction $\pi_{ni}[\tau]$ of their non-saved coins to i to pay for imported goods. We assume that coins are fungible so that buyers draw from their coin stock at random, and $(1 - s_n[\tau]) (1 - \lambda_n[\tau]) S_{mn}[t, \tau] \pi_{ni}[\tau]$ coins minted in location m at time t move from n to i at time τ in expectation. Summing across all (coin) origins we derive the first term (sum) in equation (8). In addition, a fraction $s_i[\tau]$ of coins is saved locally and remains in region i , the second term in equation (8). We can express the dynamic evolution of the composition of coin stocks in a compact matrix form and solve it forward,

$$\begin{aligned} \mathbf{S}[t, t] &= \mathbf{M}[t], \text{ and } \mathbf{S}[t, \tau + 1] = \mathbf{S}[t, \tau] \left((\mathbf{I} - \boldsymbol{\lambda}[\tau]) \tilde{\mathbf{\Pi}}[\tau] \right), \forall \tau > t, \\ &\text{with } \tilde{\mathbf{\Pi}}[\tau] \equiv (\mathbf{I} - \mathbf{s}[\tau]) \mathbf{\Pi}[\tau] + \mathbf{s}[\tau], \\ &\Rightarrow \mathbf{S}[t, T] = \mathbf{M}[t] \left(\prod_{\tau=t}^{T-1} (\mathbf{I} - \boldsymbol{\lambda}[\tau]) \tilde{\mathbf{\Pi}}[\tau] \right) \forall T \geq t. \end{aligned} \quad (9)$$

$\mathbf{S}[t, T]$ is the square $N \times N$ matrix of coin stocks with $(n, i)^{th}$ element $S_{ni}[t, T]$. $\mathbf{M}[t]$ is a diagonal $N \times N$ matrix of minting with n^{th} element $M_n[\tau]$. \mathbf{I} is the $N \times N$ identity matrix and $\boldsymbol{\lambda}[\tau]$ is a diagonal $N \times N$ matrix of coin loss with n^{th} element $\lambda_n[\tau]$. $\tilde{\mathbf{\Pi}}[\tau]$ is the square $N \times N$ matrix,

²⁹We do not impose any constraint on using arbitrarily small coin denominations: if aggregate minting, $\sum_n M_n$, increases (decreases), wages denominated in coins will increase (decrease), leading to inflation (deflation).

Note that this model is analogous to Dekle et al. (2007), where some locations run a trade deficit and some a trade surplus. The trade deficit of location n , equal to the net creation of coins, is $D_n \equiv X_n - w_n L_n = M_n - \lambda_n w_n L_n$. Any non-mint location runs a trade surplus ($D_n < 0$), and a mint location runs a trade deficit if minting is large enough, with at least one mint location running a trade deficit.

which governs bilateral coin flows. This ‘augmented’ trade matrix $\tilde{\boldsymbol{\Pi}}[\tau]$ is a function of $\mathbf{s}[\tau]$, the diagonal $N \times N$ matrix of net saving rates with n^{th} element $s_n[\tau]$, and $\boldsymbol{\Pi}[\tau]$, the trade matrix with $(n, i)^{th}$ element $\pi_{ni}[\tau]$, the classical [Eaton and Kortum \(2002\)](#) trade share from equation (4).

Equation (9) forms the basis of our estimation. Before describing our estimation strategy, we isolate two original features of our model, which helps gain intuition on how we can extract information about trade from coins and clarifies the distinctions between data on coins and trade.

Coin as a medium of exchange versus a store of value. The stock of coins \mathbf{S} in equation (9) diffuses across locations not according to the trade matrix $\boldsymbol{\Pi}$, but to the ‘augmented’ trade matrix $\tilde{\boldsymbol{\Pi}}$. Both matrices have almost the same structure, with one distinction: coins, unlike goods, have an additional tendency to stay locally, because they are also used as a store of value for saving. To make this distinction explicit, we decompose the ‘augmented’ trade share $\tilde{\pi}_{ni}$ into three multiplicative terms: a buyer term, $\tilde{\alpha}_n$, a seller term, $\tilde{\beta}_i$, and a bilateral term $\tilde{\delta}_{ni}$,

$$\begin{aligned}\tilde{\pi}_{ni}[\tau] &= \tilde{\alpha}_n[\tau] \tilde{\beta}_i[\tau] \tilde{\delta}_{ni}[\tau], \\ \tilde{\alpha}_n[\tau] &= \frac{1}{\sum_k \tilde{\beta}_k[\tau] \tilde{\delta}_{nk}[\tau]}, \\ \tilde{\beta}_i[\tau] &= T_i[\tau] (w_i[\tau])^{-\theta}, \\ \tilde{\delta}_{ni}[\tau] &= \frac{(d_{ni}[\tau])^{-\theta}}{(d_{nn}[\tau])^{-\theta}} \times \begin{cases} 1 & \text{if } n = i, \\ (1 - s_n[\tau]/\tilde{\pi}_{nn}[\tau]) & \text{if } n \neq i. \end{cases}\end{aligned}\tag{10}$$

The classical [Eaton and Kortum \(2002\)](#) trade matrix $\boldsymbol{\Pi}[\tau]$ has almost the exact same structure: $\pi_{ni}[\tau] = \alpha_n[\tau] \beta_i[\tau] \delta_{ni}[\tau]$, with buyer and seller terms $\alpha_n[\tau] = 1 / \sum_k \beta_k[\tau] \delta_{nk}[\tau]$ and $\beta_i[\tau] = T_i[\tau] (w_i[\tau])^{-\theta}$, and bilateral term $\delta_{ni}[\tau] = (d_{ni}[\tau])^{-\theta} / (d_{nn}[\tau])^{-\theta}$. In the absence of saving, $s_n = 0$, both matrices are identical. But if $s_n > 0$ the home bias for coins flows is magnified compared to the home bias in trade flows, i.e. the gap between the (high) within-location flows versus the (low) between-location flows increases. In practice this distinction is of little consequence, as the ancient saving rate into coins was likely very low: the savings rate of 1.5% that [Scheidel \(2020\)](#) calculates for Roman times is likely an upper bound for Late Antiquity, where property rights were weaker and conflict was widespread.

Equation (10) shows that coin and trade flows have the same gravity structure, and only differ by a multiplicative constant, so coin flows and the saving rate are sufficient to recover trade flows.

Coin stocks versus coin flows. The second key distinction between coin and trade flows is that coins do not travel just once: they may be used for multiple transactions throughout their stochastic lifespan. This is made explicit by the product of ‘augmented’ trade matrices in equation (9). Our structural estimation unpacks the different elements of the product of matrices in equation (9), leveraging the overlapping yet distinct information contained in ‘young’ coins

—which have only traveled through a few iterations of the ‘augmented’ trade matrix— and in ‘old’ coins —which have traveled through many iterations of the ‘augmented’ trade matrix.

A naive estimation that would wrongly ignore the dynamic nature of coin flows, simply combine all coins of different ages, and run a gravity regression on coin shares would not identify the parameters of the ‘augmented’ trade matrix. This can be most easily seen in a stationary version of our model, though the result extends to non-stationary cases. In a stationary equilibrium with no net saving, $\mathbf{s}[\tau] = 0, \forall \tau$, the trade matrix and ‘augmented’ trade matrix are identical, $\tilde{\boldsymbol{\Pi}} = \boldsymbol{\Pi}$, and the dynamics of coin stocks in equation (9) simplify into

$$\mathbf{S}[t, t+a] = \mathbf{S}[a] = \mathbf{M}((\mathbf{I} - \boldsymbol{\lambda}) \boldsymbol{\Pi})^a, \forall (t, a). \quad (11)$$

In this stationary steady state, only age, a , matters. Combining coins of different ages, we get

$$\sum_{a=0}^A \mathbf{S}[a] = \mathbf{M} \left(\sum_{a=0}^A ((\mathbf{I} - \boldsymbol{\lambda}) \boldsymbol{\Pi})^a \right) \underset{A \rightarrow +\infty}{=} \mathbf{M}(\mathbf{I} - (\mathbf{I} - \boldsymbol{\lambda}) \boldsymbol{\Pi})^{-1}. \quad (12)$$

The share of coins from different mint origins (\mathbf{M}) in different locations depends not on the trade matrix $\boldsymbol{\Pi}$, but on the Leontief inverse of the trade matrix discounted by $(\mathbf{I} - \boldsymbol{\lambda})$: $(\mathbf{I} - (\mathbf{I} - \boldsymbol{\lambda}) \boldsymbol{\Pi})^{-1}$. The reason is simple: newly minted coins percolate through the trade network, just as value added shocks percolate through the input-output network in the work of Wassily Leontief (Leontief, 1941, 1944). The intensity with which coins flow from one location to another depends on bilateral trade shares, just as the intensity with which one upstream sector affects the production of a downstream sectors depends on bilateral input shares. The same coin will travel multiple times through the trade network (until hit by a Poisson death shock λ), just as value added travels multiple times through the input-output network. However, unlike in conventional static models of input-output linkages, coins take time to percolate through the system, as inputs do in Liu and Tsyvinski (2024).

Figure 5 illustrates the potential bias from wrongly interpreting coin stocks as coin flows. Within the first period of their life, coin flows mirror trade flows ($\boldsymbol{\Pi}$ in figure 5). The same trade elasticity θ governs both coin and trade flows, $S_{ni}[t, t+1] \propto \pi_{ni} \propto (d_{ni})^{-\theta}$. In the second period of their life, coins have traveled twice through the trade network ($\boldsymbol{\Pi}^2$ in figure 5). Trade costs have a weaker impact over short distances as coins have traveled longer, and have started diffusing within nearby destinations. The trade elasticity falls below θ . As coins age, their flows gradually escape the negative effect of trade costs; coins diffuse through the trade network and converge towards a uniform distribution.³⁰ The trade elasticity falls towards zero (see the flattening slopes of $\boldsymbol{\Pi}, \boldsymbol{\Pi}^2, \dots, \boldsymbol{\Pi}^{100}$ in figure 5). A naive estimation using coins of all ages combined, i.e. wrongly interpreting the Leontief inverse $(\mathbf{I} - (\mathbf{I} - \boldsymbol{\lambda}) \boldsymbol{\Pi})^{-1}$ as if it were the trade matrix $\boldsymbol{\Pi}$, would infer incorrect parameters. In our numerical example, if we assume that trade costs depend on travel

³⁰Our model of gradual diffusion of coins through a trade network is intimately related to the model of diffusion of information through a trade network in Chaney (2018).

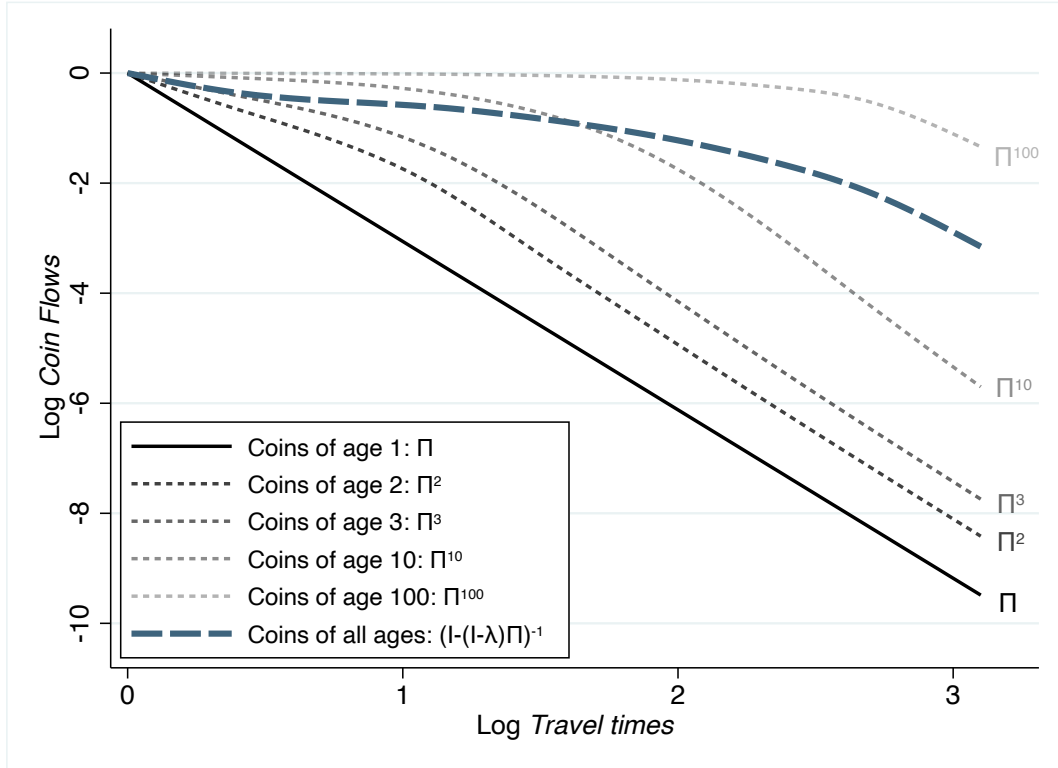


Figure 5: Flows of coins of different ages

Notes: This figure presents a numerical illustration of the flow of coins of different ages as a function of trade costs. We use equations (11) and (12), and the trade model (4) to simulate an economy with 50 locations around a regular polygon, with same technology $T_n = T, \forall n$, a trade elasticity $\theta = 4$, and an annual coin loss rate $\lambda = 0.017$. Locations are symmetric so wages are equalized and trade shares simplify to $\pi_{ni} = \alpha(d_{ni})^{-\theta}$ with $\alpha = 1/\sum_k(d_{nk})^{-\theta}$. We parameterize $(d_{ni})^{-\theta} = (\text{TravelTimes}_{ni})^{-\zeta}$ with $\zeta = 3.06$ (see our structural estimation in section 3). Log travel times are on the x-axis; and log flows of coins of different ages on the y-axis ($\ln S_{ni}[t, t+a]$) for age a). To ease comparisons, we normalize the largest log flows and smallest log travel times to zero, so all curves start at $(0,0)$. ‘Naively’ treating the flows of coins of all ages combined as trade flows, i.e. treating the Leontief inverse $(I - (I - \lambda)\Pi)^{-1}$ as if it were the trade matrix Π , gives a misspecified trade times elasticity of 1.17, substantially below the true $\zeta = 3.06$.

times, $(d_{ni})^{-\theta} = (\text{TravelTimes}_{ni})^{-\zeta}$, with a true elasticity $\zeta = 3.06$, we would wrongly estimate a travel times elasticity of 1.17. This corresponds approximately to the discrepancy between our reduced form estimate combining coins of all ages (1.138 in table 1) and our upcoming structural estimate (3.06 in section 3).³¹ Appendix figure A.4 shows reduced form evidence suggestive of this phenomenon: across separate gravity regressions (as in table 1) for different vintages of coins, the reduced form travel time elasticity falls towards zero as we move from younger to older coins.

Equation (11) and figure 5 illustrate how to combine information on coins of different ages to recover trade flows. If we had perfect data on coin stocks, we could directly recover trade flows from the distribution of age 1 coins, discarding all other information. Unfortunately, our data is sparse. Information on those youngest coins is insufficient, and we need to combine it with information on coins of different vintages. For instance, if no coins are minted in location n at time t , we simply cannot observe them flowing out of n at t . Instead, we can use coins minted at time $t-1, t-2$, etc, that are still in circulation at time t to recover trade flows to n at t .

³¹Figure 5 is not a structural exercise. Our numerical example is a stylized example, with symmetric locations around a regular polygon at a steady state. It is meant to build intuition, not to resemble the real ancient world.

2.3 Mapping the model to the data

To map the model to the data, we need to define the empirical counterparts to time periods, t , locations, n , the coin loss rate, λ , and we parameterize trade costs as a function of observables.

Definition of time periods. We aggregate mint and hoard dates (tpq) to 20-year intervals.

Definition of locations. We partition the world into $N = 13$ regions. In the Islamic world they correspond to regions associated with graph nodes in al-Turayyā (Romanov and Seydi, 2022). In the Roman world they are based partly on Roman provincial borders, and partly on 9th-century political borders (see appendix C for details). To facilitate the identification of the parameters, we choose a level of aggregation such that each region has some minting and hoarding activity before and after the conquests. Figure 6 maps the partition of the ancient world into 13 regions.



Figure 6: Region Definitions

Notes: Regions are based on Roman provincial boundaries and Medieval kingdom boundaries within non-Islamic Europe, and al-Turayyā regions within the maximum extent of the Umayyad caliphate. See appendix C for details.

Assumption: constant loss rate. With a constant loss rate, any collection of coins minted at time t will gradually disappear from the monetary system as those coins are (randomly) ‘lost’ at a rate λ . At time $t + 1$ only a fraction $(1 - \lambda)$ remains, at time $t + 2$ a fraction $(1 - \lambda)^2$, etc. The

same exponential decay holds for any starting date t , and it holds for the random sample found by archaeologists. We aggregate all the coins in our dataset, and express the density of coins of age a as $f(a) \propto (1 - \lambda)^a$, corresponding to figure 3b. Taking logs, we estimate λ by OLS,

$$\ln f(a) = \text{constant} + \ln(1 - \lambda) \times a + \varepsilon(a). \quad (13)$$

We estimate a coin loss rate of 1.7% per year, or 30% per 20-year interval, $\hat{\lambda}_{\text{20-year}} = 0.301$.³²

Parameterization of trade costs. We assume that bilateral trade costs properly scaled by the trade elasticity θ solely depend on (directed) bilateral travel times, TravelTime_{ni} , and on a possible proportional penalty incurred when crossing political and religious boundaries, $\forall(n \neq i, t)$,

$$\ln((d_{ni}[t])^{-\theta}) = \gamma_0 - \zeta \ln(\text{TravelTime}_{ni}) - \kappa_1 \text{PoliticalBorder}_{ni}[t] - \kappa_2 \text{ReligiousBorder}_{ni}[t]. \quad (14)$$

We normalize $d_{nn}[t] = 1, \forall n, t$, as in Eaton and Kortum (2002). $\text{PoliticalBorder}_{ni}[t]$ is a dummy equal to 1 if regions n and i are separated by a political border in period t . $\text{ReligiousBorder}_{ni}[t]$ is a dummy equal to 1 if in period t one region, n or i , is in the Islamic world and the other is not. γ_0 is a scaling constant which adjusts travel time units, and governs the home bias in trade.³³ From our ‘augmented’ trade model, which describes coin flows driven both by transactions (trade) and saving, we derive the bilateral determinants of coin flows, the $\tilde{\delta}_{ni}[t]$ ’s in equation (10), $\forall(n \neq i, t)$,

$$\ln(\tilde{\delta}_{ni}[t]) = \tilde{\gamma}_0 - \zeta \ln(\text{TravelTime}_{ni}) - \kappa_1 \text{PoliticalBorder}_{ni}[t] - \kappa_2 \text{ReligiousBorder}_{ni}[t], \quad (15)$$

and $\tilde{\delta}_{nn}[t] = 1, \forall(n, t)$. The bilateral determinants of external trade flows, $(d_{ni}[t])^{-\theta}$, and coin flows, $\tilde{\delta}_{ni}[t]$, only differ by a multiplicative scalar, $e^{\tilde{\gamma}_0 - \gamma_0}$, due to saving.

Given estimates for within region coin flows, $\tilde{\pi}_{nn}[t]$, this scalar maps into the saving rates,

$$s_n[t] = \tilde{\pi}_{nn}[t] (1 - e^{\tilde{\gamma}_0 - \gamma_0}). \quad (16)$$

$\tilde{\pi}_{nn}[t]$ controls the home bias in coins, and $(1 - e^{\tilde{\gamma}_0 - \gamma_0})$ adjusts for the discrepancy (due to saving $s_n[t]$) between the home bias in coins (governed by $\tilde{\gamma}_0$) and the home bias in trade (governed by γ_0). In the absence of direct evidence on ancient trade, we cannot directly estimate γ_0 . Instead, we choose γ_0 to match the average ancient saving rate into nominal assets of 1.5% (Scheidel, 2020).

³²See appendix table A.4 for the formal estimation results.

³³Our parameterization for trade costs is potentially inconsistent with the assumption of arbitrage trade because we compute optimal travel routes once and for all, without taking into account the additional costs associated with potentially multiple border crossings. In practice, this does not happen: we manually verify that the estimated costs in equation (14) cannot be lowered by taking a longer route avoiding unnecessary border crossings.

Travel times. To compute (optimal) travel times given the transportation network and technology we use two geo-spatial models constructed by historians to provide quantitative estimates of (shortest) distances, trade routes, and trade costs. The first is the Orbis (Scheidel, 2015), a directed graph of cities and trade routes of the Roman world (i.e. from Britannia in the north-west to Egypt, Palestine, and Syria in the south-east) along with a calibrated model of trade costs, in monetary units and units of time, along the edges to allow for the calculation of shortest paths. The second is al-Turayyā (Romanov and Seydi, 2022), a digitalization of the Atlas of the Islamic World of Cornu (1983), which, similarly, contains the coordinates of cities and trading posts connected by trade routes, but without estimates of travel times. We combine the nodes of al-Turayyā and Orbis and extend Scheidel (2015)'s methodology from Orbis to calculate travel times for the Islamic world (see appendix C for details). Figure 7 shows the combined graph. We validate the resulting travel times by comparing them to those reported by the 10th-century Arab geographer Al-Muqaddasī (1994) (see appendix figure A.5).

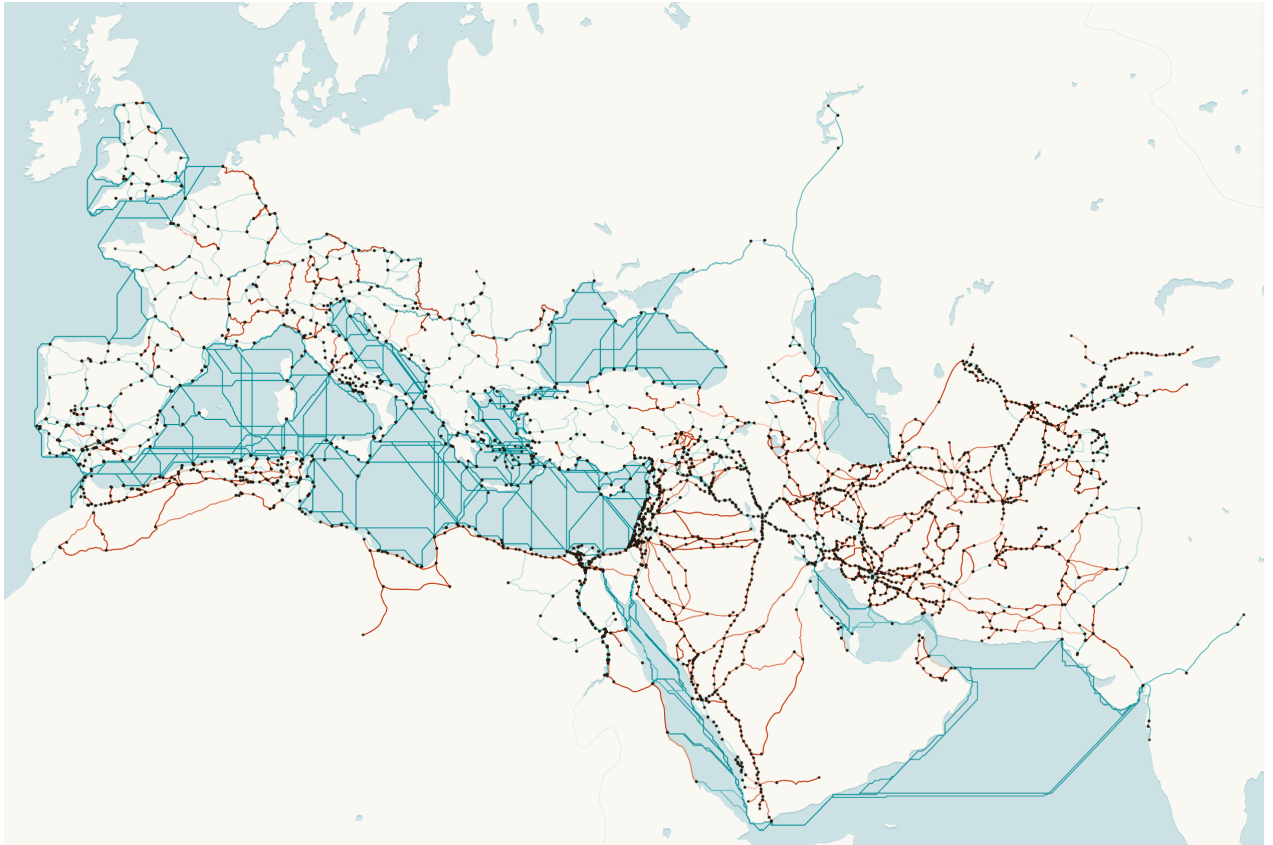


Figure 7: The combined geospatial model

Notes: The figure shows the combined geospatial models from Orbis and al-Turayyā. Edges in blue (red) indicate faster (slower) speeds.

For each region, we calculate the weighted average of mint locations (with the shares of each location in total coin output as weights) and project it to the closest vertex on the road network graph. The shortest travel time between n and i is our time-invariant measure of $TravelTime_{ni}$.

Political and religious borders. We construct political border and religious border dummies by coding the start and end years of the presence of political entities across regions. We set $PoliticalBorder_{ni}[t]$ to one if the set of political entities that occupy at least some part of the regions n and i for some part of the 20-year time interval is completely disjoint. $ReligiousBorder_{ni}[t]$ captures the border between the emerging religion of Islam and the rest of the world. We use two alternative specifications for the religious border effect. The first (simple) specification is a dummy equal to one if all political entities in region n are Islamic and none in i are, or vice versa. The second (detailed) specification distinguishes the eastern, western, and Mediterranean borders of Islam; the eastern land border is between the Byzantine heartlands and the Caliphate regions east of Egypt, the western land border is between al-Andalus and Aquitaine or Francia/Germania, and the Mediterranean maritime border is between all other region pairs.

Coin hoard data generating process. We assume that our hoard dataset \mathbf{H} is a random sample from the stocks of coins in each region and period. We group all coin hoards within a region and period, with $H_h[T]$ the total number of coins found in region h and buried at time T (tpq), which we decompose into coin types, with $H_{m,h}[t,T]$ the number of coins minted in m at time t within that hoard. Our random sampling assumption means that the expected share of coins of different types within a hoard is equal to the share of coins of different types within a coin stock in our model (9). Formally, we assume

$$\mathbb{E} \left[\frac{H_{m,h}[t,T]}{H_h[T]} \right] = \frac{S_{m,h}[t,T]}{S_h[T]}. \quad (17)$$

As we discuss in section 1, we recognize that the probability that a coin ends up in our dataset may vary systematically between regions and periods, depending on whether coins were lost and deposited in the ground, found by archaeologists, and documented by experts. By using only information on the composition of coins *within* hoards, we condition on those events being realized (lost, found, documented), and we purge any variation in the probability of those events.

2.4 Estimation

We estimate the structural parameters of our model by maximum likelihood. Given our assumption of random sampling in equation (17), the probability of observing $(\dots, H_{m,h}[t,T], \dots)_{m,t}$ coins minted in different regions (m 's) at different times (t 's) among the total of $H_h[T]$ coins within a hoard buried in region h at time (tpq) T is multinomial, and depends on coin stocks,

$$\Pr(\dots, H_{m,h}[t,T], \dots) = \frac{H_h[T]!}{\prod_{m',t'} H_{m',h}[t',T]!} \prod_{m,t} \left(\frac{S_{m,h}[t,T]}{S_h[T]} \right)^{H_{m,h}[t,T]}.$$

It depends on the model parameters through the predicted share of coin types, $S_{m,h}[t, T]/S_h[T]$. Assuming a constant loss rate λ (13), the stocks of coins evolve recursively as in equation (9):

$$\mathbf{S}[t, T] = \mathbf{M}[t] \left(\prod_{\tau=t}^{T-1} (1 - \lambda) \tilde{\boldsymbol{\Pi}}[\tau] \right) \forall(T \geq t).$$

We decompose the elements of the coin flow matrix ('augmented' trade matrix) $\tilde{\boldsymbol{\Pi}}[\tau]$ into seller ($\tilde{\beta}_i$) and bilateral terms ($\tilde{\delta}_{ni}$) according to equation (10):

$$\tilde{\pi}_{ni}[\tau] = \frac{\tilde{\beta}_i[\tau] \tilde{\delta}_{ni}[\tau]}{\sum_k \tilde{\beta}_k[\tau] \tilde{\delta}_{nk}[\tau]}, \forall(n, i, \tau).$$

We parameterize the bilateral component of coin flows in equation (15): $\tilde{\delta}_{nn}[t] = 1, \forall(n, t)$, and

$$\ln(\tilde{\delta}_{ni}[t]) = \tilde{\gamma}_0 - \zeta \ln(TravelTime_{ni}) - \kappa_1 PoliticalBorder_{ni}[t] - \kappa_2 ReligiousBorder_{ni}[t], \\ \forall(n \neq i, t).$$

The vector Θ collects all parameters: time-varying minting output $M_n[t]$, time-varying seller terms $\tilde{\beta}_n[t]$, and the parameters governing saving and trade costs, $\tilde{\gamma}_0$, ζ , κ_1 , and κ_2 ,

$$\Theta = \left((\dots, M_n[t], \dots)_{n,t}, (\dots, \tilde{\beta}_n[t], \dots)_{n,t}, \tilde{\gamma}_0, \zeta, \kappa_1, \kappa_2 \right).$$

As we target coin shares within hoards, we can never recover the total number of coins minted over 320-950. We normalize mint output $M_{n_0}[t_0] = 100$ for an arbitrary region n_0 (northern Italy) and period t_0 (320-340). Similarly, only *relative* origin terms matter for coin flow shares, so we normalize $\tilde{\beta}_{n_0}[t] = 100, \forall t$, for region n_0 (northern Italy).

We estimate $\hat{\Theta}$ by maximizing the log-likelihood of observing a sample of coin hoards \mathbf{H} ,

$$\hat{\Theta} = \arg \max_{\Theta} \sum_{h,T} \sum_{m,t} H_{mh}[t, T] \left(\ln S_{mh}[t, T](\Theta) - \ln \sum_{m',t'} S_{m'h}[t', T](\Theta) \right). \quad (18)$$

Given those structural estimates, we recover the parameter γ_0 governing bilateral trade costs (possibly distinct from the parameter $\tilde{\gamma}_0$ governing bilateral coin flows in the presence of saving), using equation (16) and an average net ancient saving rate into coins of 1.5% (Scheidel, 2020),

$$\gamma_0 \text{ s.t. } (1 - e^{\tilde{\gamma}_0 - \gamma_0}) \mathbb{E}_{n,t} \left[\tilde{\pi}_{nn}[t] \right] = 0.015. \quad (19)$$

With those estimates, we can compute all equilibrium variables, including real consumption.

3 Trade and the end of antiquity

3.1 Parameter estimates

Ancient trade costs. Table 3 shows the estimates of the parameters governing ancient trade costs. We consider two specifications for the religious border effect: either a single parameter governing the cost of crossing from Islamic to non-Islamic regions (columns 1 and 3), or different costs of crossing the religious border overland in the east (in and out of Byzantium), in the west (in and out of al-Andalus), or over the Mediterranean in and out of its non-Islamic northern shore (columns 2 and 4). In addition, we use two accounting methods: we either use a simple count of coins (columns 1 and 2), or use only gold and silver coins and measure their value, accounting for weight or denomination, and metal content (columns 3 and 4).

Table 3: Determinants of ancient trade costs

	Log Trade Costs			
	(1)	(2)	(3)	(4)
Log Travel Time	3.04 (0.01)	3.06 (0.02)	1.41 (0.04)	1.09 (0.04)
Political Border	0.64 (0.02)	0.47 (0.02)	2.51 (0.05)	3.19 (0.05)
Religious Border	3.85 (0.11)		2.94 (0.16)	
Religious Border: East		1.99 (0.12)		0.12 (0.30)
Religious Border: West		4.69 (0.21)		14.63 (147.22)
Religious Border: Mediterranean		5.20 (0.19)		2.72 (0.19)
Sample	All	All	Gold/Silver	Gold/Silver
Coin Accounting	Number	Number	Value	Value
Estimator	MLE	MLE	MLE	MLE
Observations	4,389	4,389	2,010	2,010

Notes: The table shows the coefficient estimates in the trade cost function, equation (14)). “Political Border” is one if the sets of political entities that occupy at least some part of the regions during the 20-year time period are completely disjoint, and zero otherwise. “Religious Border” is one if all political entities in one region are Islamic and all are non-Islamic in the other region, and zero otherwise. “Religious Border: East” is one iff the religious border dummy is one and the regions are al-Andalus and Aquitaine or Francia/Germania, or vice versa. “Religious Border: West” is one iff the religious border dummy is one and the regions are the Byzantine Heartlands and one of the Caliphate regions east of Egypt, or vice versa. “Religious Border: Mediterranean” is one for all other region pairs where the religious border dummy is one. “Observations” denotes the number of observations (m, h, t, T) in equation (18) where $H_{m,h}[t, T] > 0$, i.e. which enter the loglikelihood.

In our simpler specification (column 1), the travel time elasticity of trade, $\zeta = 3.04$ (s.e. 0.01), is somewhat larger but close to the 2.05-2.89 range of estimates from Flückiger et al. (2022)

using bilateral trade in terra sigillata in ancient Rome and optimal travel times along the Roman transportation network, and to the 1.9 distance elasticity from Barjamovic et al. (2019) using merchant records in Bronze Age Anatolia. This proximity to estimates using actual (though partial) ancient trade data is reassuring, as we do not use any direct information on trade, but only indirect information from coins. Interestingly, ζ is also larger than the 1.1 elasticity estimated in table 1 using the same data on coin hoards. The reason is that in table 1 we use a naive gravity model, combining coins of all ages, and ignore the fact that older coins have a tendency to travel longer distances. Our structural model (9) corrects this mis-specification (see section 2.2).

This travel time elasticity is robust to alternative specifications for the religion border effect, $\zeta = 3.06$ in column 2 versus $\zeta = 3.04$ in column 1. Our estimate is significantly lower (but still of the same sign) when we restrict our sample to gold and silver coins, and measure their relative values, e.g. $\zeta = 1.41$ in column 3 versus $\zeta = 3.04$ in column 1. We conjecture that the stronger reliance of Byzantium on gold, and the exclusion of bronze coins, induces a systematic bias in our estimates.

In our simpler specification (column 1), the political (κ_1) and religious (κ_2) border effects are large, but of the same magnitude as estimates for modern border effects. Arbitrarily assuming a trade elasticity $\theta = 4$ (Simonovska and Waugh, 2014), those correspond to a 17% tax for crossing a political border ($d_{across}/d_{within} = e^{\kappa_1/\theta} = 1.17$), and a 155% tax for crossing a religious border ($d_{across}/d_{within} = e^{\kappa_2/\theta} = 2.55$), similar to the estimated 49% cost of crossing the modern US-Canada border (Anderson and van Wincoop, 2003).³⁴

Changing the specification of the religious border effect, distinguishing the eastern land border, the Mediterranean border, and the western land border (column 2) does not affect our estimate of the political border effect, which remains relatively small (0.64 in column 1 versus 0.47 in column 2). It does however reveal different estimated penalties associated with crossing from Islamic to non-Islamic regions. The religious border effect is strongest for crossing the Mediterranean ($\kappa_2^{Med.} = 5.20$, s.e. 0.19) and for the western border from al-Andalus ($\kappa_2^{West} = 4.61$, s.e. 0.21), and lowest for the eastern border into Byzantium ($\kappa_2^{Med.} = 1.99$, s.e. 0.12).

Columns 3 and 4 drop bronze coins and compute the value shares within hoards for gold and silver coins using their weights or denominations.³⁵ Under this accounting of the coins data, the political border effect is larger ($\kappa_1 = 2.51$ in column 3 versus 0.64 in column 1). The religious border effect instead is smaller ($\kappa_2 = 2.94$ in column 3 versus 3.85 in column 1). We also estimate statistically insignificant eastern and western religious border effects, and a smaller Mediterranean religious border effect ($\kappa_2^{Med.} = 2.72$ in column 4, versus 5.20 in column 2). As for the travel time elasticity, we conjecture that selectively dropping bronze coins biases our estimates.

To conclude, our structural estimation confirms the reduced form evidence in section 1. The

³⁴Anderson and van Wincoop (2003) estimate that trade is $\exp(1.59) \approx 5$ times larger within the US or Canada than between them. For an elasticity $\theta = 4$ it corresponds to a $d_{across}/d_{within} - 1 = e^{1.59/4} - 1 = 49\%$ border tax.

³⁵We assume a constant exchange rate of 12g of silver for 1g of gold for this exercise; see Appendix ?? for details.

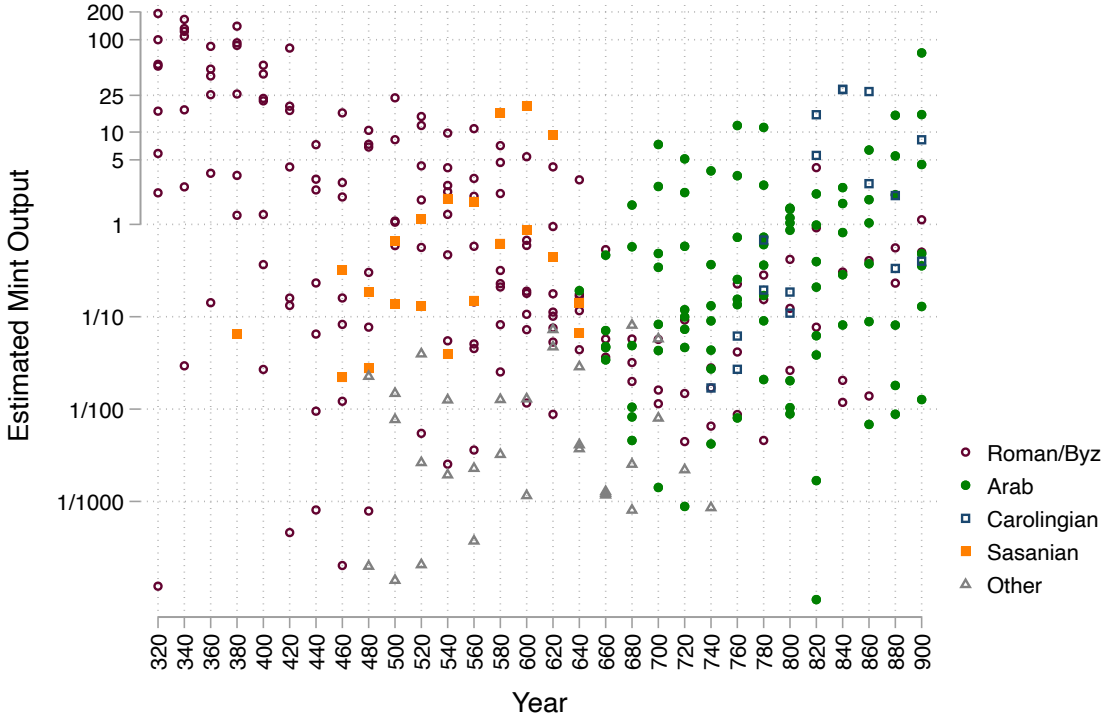


Figure 8: Estimated mint output, AD 320-900

Notes: The figure shows the estimated coin output $M_n[t]$ by time t (horizontal axis) and region n , using specification in column (2) of Table 3, and broken down by the political entities that locations are — at that time — primarily associated with. The units are relative to northern Italy in 320-340, which we normalize to have a mint output of 100.

border between Islamic and non-Islamic regions becomes costlier to cross *after* the birth of Islam.

Minting output. Figure 8 shows estimates of mint output by region and time interval.

Our estimates line up with several patterns described in the numismatic literature: (i) the decline of coin production in the western Mediterranean following the demise of the West Roman Empire in the late 5th century; (ii) the large decline of Byzantine mint output in the ‘Byzantine dark ages’ of the eighth century; (iii) the gradual increase in Arab and Carolingian mint output starting from the late seventh century. It is important to note we are not merely counting coins; we *estimate* minting output from the shares of coins from different mints found across hoards.

3.2 Real consumption in the ancient world

Our full set of estimates further allows us to recover all equilibrium variables in our model.

From the parameters of the trade cost function $(\gamma_0, \kappa_1, \kappa_2)$, data on the determinants of trade (travel times, political and religious borders as in column 2 of table 3), and the seller terms $(\tilde{\beta}_n[t])$, we recover bilateral trade shares $(\pi_{ni}[t])$. Using the goods market clearing condition in equation (6), estimated bilateral trade shares, the coin loss rate (λ), and estimates of minting

output ($M_n[t]$), we recover aggregate regional income ($w_n[t]L_n[t]$). Finally, in the absence of any direct evidence on population, technology, or wages, we assume a simple Malthusian benchmark, $L_n[t] = T_n[t]$, somewhat arbitrarily set the trade elasticity θ to 4 (Simonovska and Waugh, 2014), and we recover population ($L_n[t]$) and technology ($T_n[t]$) from the seller terms ($\tilde{\beta}_n[t]$).³⁶

We can then fully characterize real consumption per capita in any equilibrium, realized or counterfactual, and partition real consumption into three economically meaningful components,

$$\underbrace{\frac{X_n[t]/p_n[t]}{L_n[t]}}_{\text{Real Consumption}} = \underbrace{\gamma^{-1} (\pi_{nn}[t])^{-1/\theta}}_{\text{Openness}} \underbrace{(T_n[t])^{1/\theta}}_{\text{Technology}} \underbrace{\left(1 + \frac{M_n[t] - \lambda w_n[t] L_n[t]}{w_n[t] L_n[t]}\right)}_{\text{Trade Deficit}}. \quad (20)$$

A better technology (higher $T_n^{1/\theta}$) transforms labor into goods more efficiently and improves real consumption. As in Eaton and Kortum (2002) and its generalization in Arkolakis et al. (2012), trade openness (higher $\pi_{nn}^{-1/\theta}$) further increases real consumption, leveraging the gains from trade. As in Dekle et al. (2007), trade deficits financed by net coin creation (higher $X_n/(w_n L_n) = 1 + (M_n - \lambda w_n L_n)/(w_n L_n)$) allow a region to consume more than it produces.³⁷

While ‘openness’ and ‘trade deficit’ are unit-free ratios, technology depends on arbitrary units. We choose those units such that average real consumption is normalized to one each period. Our model informs us on cross-sectional *differences* in real consumption between regions. This is true despite the fact that we only have information on nominal variables (coins); bilateral trade flows reveal real differences in factor prices, which our structural estimation is able to recover. But as any other trade model, our model offers no guidance on the absolute levels of real consumption.

The case of Byzantium and northern Europe. Figure 9 presents the time series of estimated real consumption per capita and its components, for each 20-year period over AD 380-880. We highlight those two regions because they undergo some of the most striking reversals of fortune.³⁸

The heartlands of the Byzantine empire are initially the wealthiest region of the ancient western world, with a real consumption per capita four times larger than the rest of the world. Our estimates suggest that Byzantium is also, by a huge margin, the region that benefits the most from international trade: it imports as much as 70% of its consumption. This reliance on foreign imports is in large part financed by seigniorage from a very large minting output. Around the time of the Arab conquests to its east and south, Byzantium is hit by a triple shock; Byzantine minting collapses until the ‘Byzantine dark ages’ of the eighth century so that Byzantium must increasingly rely on exports to acquire foreign coins, trade drops sharply because of the higher

³⁶We explain in detail how to recover all equilibrium variables from our estimates in the technical appendix.

³⁷The first two components of the decomposition of consumption in equation (20) are the same as in equation (15) on page 1756 in Eaton and Kortum (2002). The last term is the same as in the (all important) unnumbered equation on page 354 in Dekle et al. (2007), where they label trade deficits as D_n . In our model, trade deficits are financed by minting output in excess of coin losses, $D_n = M_n - \lambda w_n L_n$, so that so $1 + D_n/Y_n = 1 + (M_n - \lambda w_n L_n)/(w_n L_n)$.

³⁸See appendix figure A.6 for the time series of all 13 regions.

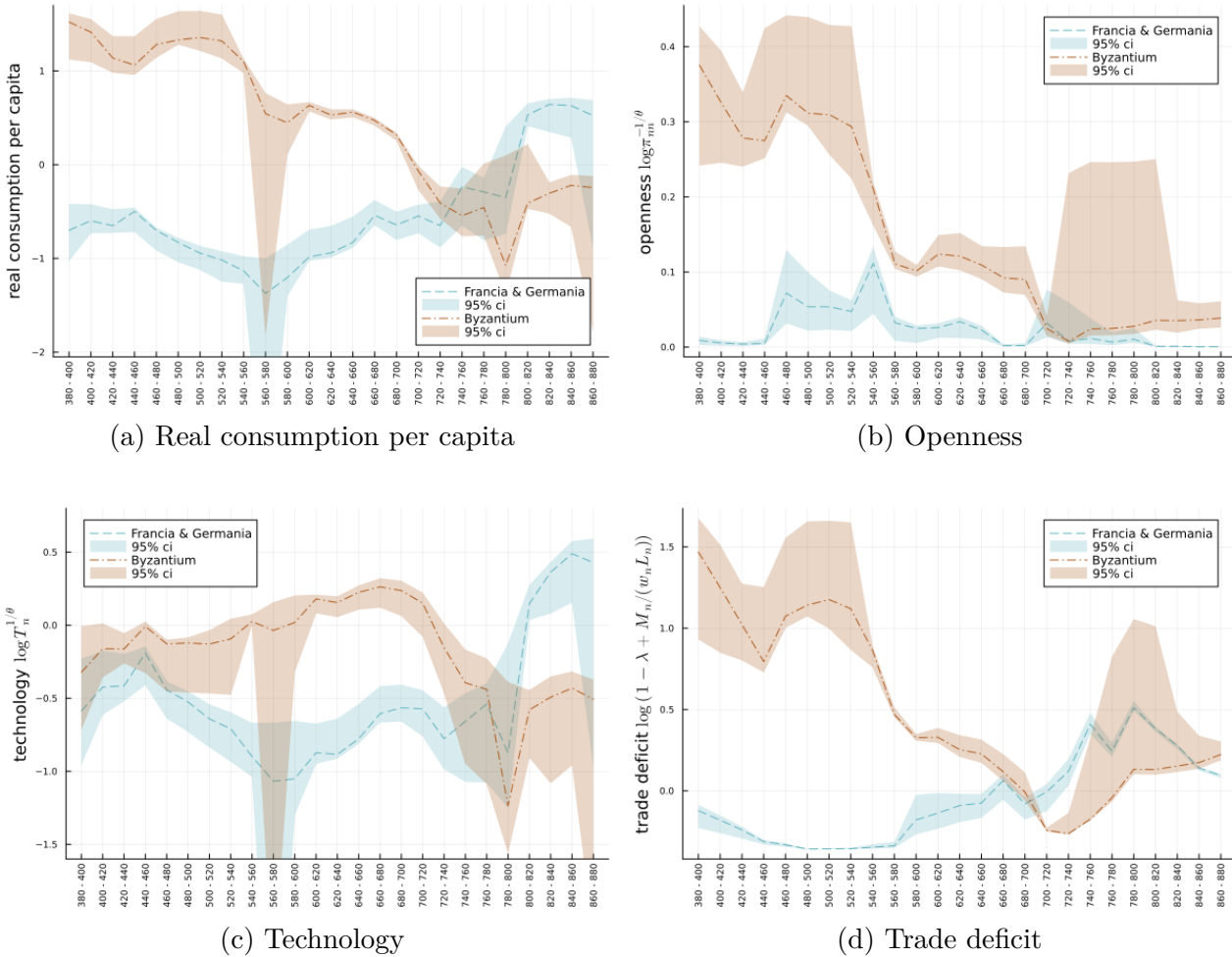


Figure 9: Real consumption per capita AD 380-900: Byzantine Heartlands vs Francia & Germania

Notes: This figure shows the time-series of (logged) real consumption per capita (panel a) from AD 380 to AD 900 for the Byzantine Heartlands and for Francia and Germania, and its partition into ‘openness’ (panel b), ‘technology’ (panel c), and ‘trade deficits’ (panel d) as in equation (20). The technical appendix provides details on the computation of each term, using the dynamic model in equations (4), (6), (10), and the parameter estimates from (18)-(19). Units for technology are chosen such average real consumption per capita equals one for each period. 95% confidence intervals (shaded areas) are computed from fully re-estimating our model on 100 bootstrapped samples from our coin hoard data. Time series for all 13 regions are in appendix figure A.6.

trade barriers into Islamic regions, and technology collapses. Byzantine real consumption is halved following the Arab conquests.

In contrast, the northwest European Frankish lands of Francia and Germania grow from the poorest to one of the wealthiest regions of the ancient world. Given their peripheral position, they trade little, so that variations in trade openness have only a marginal impact on real consumption. Our estimates suggest instead that the growth in real consumption is fueled almost entirely by technological improvements, and to a lesser extent by the very large increase in minting output which allows them to acquire foreign goods with Carolingian silver coins around AD 700.

The time series in figure 9 (and appendix figure A.6) showcase the promise of recovering economically meaningful information from data on ancient coins, but they also reveal that estimates can be imprecise for individual 20-year periods. We turn next to a less granular but also less

noisy description of consumption changes between the first and second halves of our sample, by aggregating across time periods within each half.

The economic geography of the ancient world before and after the Arab conquests. To explore the changes in real consumption from before to after the rise of Islam, we split our sample between AD 460-620, just after the fall of Rome but before the birth of Islam, and AD 700-900, after the Arabs have conquered a territory that stretches from the Indus to the Atlantic. For each period, we average our estimated parameters and solve a full stationary equilibrium using equations (4), (7), (10). We then use equation (20) to compute real consumption per capita and its components for each region and period. The results are presented in table 4 (see appendix table A.5 for additional details). We focus our discussion on a few important regions.

Table 4: Real consumption in the ancient world from AD 460-620 to AD 700-900

	Real consumption		Openness		Technology		Trade Deficit	
	$\Delta \log \left(\frac{X_n/p_n}{L_n} \right)$	(1)	$\Delta \log \left(\pi_{nn}^{-1/\theta} \right)$	(3)	$\Delta \log \left(T_n^{1/\theta} \right)$	(5)	$\Delta \log \left(1 + \frac{M_n - \lambda w_n L_n}{w_n L_n} \right)$	(7)
al-Andalus	0.62	(0.25)	-0.06	(0.04)	0.77	(0.32)	-0.09	(0.18)
Aquitaine and Basque Country	1.28	(0.23)	-0.05	(0.01)	1.22	(0.23)	0.11	(0.06)
Francia and Germania	1.96	(0.24)	-0.05	(0.01)	1.80	(0.26)	0.20	(0.04)
Northern Italy and Balkans	-0.31	(0.24)	-0.08	(0.03)	-0.10	(0.26)	-0.13	(0.10)
Southern Italy	-0.20	(0.34)	0.19	(0.18)	-0.94	(0.37)	0.55	(0.40)
Byzantine Heartlands	-1.56	(0.33)	-0.23	(0.14)	-0.44	(0.41)	-0.89	(0.54)
al-Sham (Greater Syria)	-0.32	(0.27)	-0.04	(0.02)	-0.11	(0.29)	-0.17	(0.11)
Northern Syria and Caucasus	0.22	(0.30)	-0.01	(0.03)	0.15	(0.37)	0.08	(0.12)
al-Iraq, al-Jibal, Khuzistan, Kirman	0.06	(0.27)	-0.00	(0.01)	0.06	(0.29)	-0.00	(0.04)
Eastern Caliphate	0.37	(0.33)	-0.00	(0.00)	0.39	(0.34)	-0.02	(0.04)
Jazirat al-arab and al-Yaman	1.16	(0.34)	-0.01	(0.04)	0.66	(0.45)	0.51	(0.26)
Misr (Egypt)	-0.36	(0.72)	0.09	(0.23)	-0.82	(0.50)	0.37	(0.90)
al-Maghrib	0.28	(0.33)	0.13	(0.07)	-0.49	(0.27)	0.65	(0.30)

Notes: This table shows (log) changes between AD 460-620 and AD 700-900 of real consumption per capita ($(X_n/p_n)/L_n$, column 1), openness ($\pi_{nn}^{-1/\theta}$, column 3), technology ($T_n^{1/\theta}$, column 5), and trade deficits ($1 + (M_n - \lambda w_n L_n)/(w_n L_n)$, column 7), as in equation (20). We solve steady state equilibria for the AD 460-620 and AD 700-900 periods separately, using equations (4), (7), (10), and the parameter estimates from (18)-(19) averaged for each period (see the technical appendix). Units for technology are chosen such that average real consumption per capita equals one for each period. Standard errors, in parentheses in even columns, are computed from re-estimating our model on 100 bootstrapped samples from our coin data. See appendix table A.5 for details on levels.

Byzantine heartlands: the heartlands of the Byzantine empire suffer from the most dramatic drop in relative real consumption, caused by a fall in trade, a large drop in technology, and a collapse in minting output. The fall in Byzantine trade is worth emphasizing; imports fall from 64% to 12% of consumption. While ancient trade decreases in most regions following the Arab conquests, this decrease is milder than for Byzantium, with imports falling on average from 20% to 15% of consumption. This fall is concentrated in regions north of the Mediterranean.

Western and northern Europe: both Islamic (al-Andalus) and non-Islamic (Aquitaine and the

Basque country, and the Frankish lands of Francia and Germania) Western Europe experience the most spectacular relative rise in real consumption. Initially among the poorest regions they grow to become among the wealthiest over the course of a few centuries. This growth is almost entirely fueled by improvements in technology. Regional minting grows substantially, but just enough to keep up with the large increase in aggregate income. Even though trade openness falls due to the newly formed religious border over the Pyrenees and the Mediterranean (imports as a share of consumption fall from around 20% to around 2%), this has only a small impact on real consumption because those regions are not very open to trade before the Arab conquests.

Egypt (Misr): the Arab conquest of Egypt has little impact on real consumption. Although Egypt is partially cut off from trade across the Mediterranean by the Arab conquest, its proximity to central regions of the eastern Caliphate more than compensates this loss. Interestingly, our estimates suggest that Egypt goes from running a small trade surplus under Roman rule, to running a trade deficit under Islamic rule, possibly due to an increased minting of Islamic coins.

Syria (Northern Syria and the Caucasus): as a province of the Byzantine empire, Syria is one of the wealthiest regions before the rise of Islam. Similarly to Egypt, the loss of trade access to Byzantium and Europe is partly compensated by its privileged access to the heart of the eastern Caliphate. Syria also benefits from an improved technology and a larger minting output.

Arabian peninsula (Jazirat al-Arab and al-Yaman): the birthplace of Islam, the Arabian peninsula, initially the poorest region of the ancient world, experiences a sustained growth in real consumption, primarily driven by improved technology and a larger minting output.

We note however that the point estimates for Egypt, Syria, and the Arabian peninsula are imprecise, with wide standard errors (columns 2, 4, 6, and 8 of table 4).

Counterfactual changes. We then leverage our fully specified structural model to explore the causal impact of specific shocks to real consumption changes. They are causal in the sense that we simulate counterfactual equilibria, changing only one set of parameters at a time and keeping all other parameters fixed at their estimated levels. The results are presented in table 5. Column 1 shows (log) real consumption per capita in the estimated AD 460-620 equilibrium. We then compute (log) changes in real consumption between this initial equilibrium and various counterfactual equilibria. In column 3 we turn on the religious border to its 700-900 AD level, keeping all other parameters unchanged. In column 5, we only change technology to its 700-900 AD level. And in column 7, we only change minting output to its AD 700-900 level.

The increase in trade costs associated with crossing the border in and out of Islam has an asymmetric impact on real consumption (column 1). Non-Islamic regions see a large fall in trade, which contributes to substantial reductions in real consumption. The most severely hit region is Byzantium (50% drop in real consumption), the region that benefits the most from access to trade before the Arab conquests. In a counterfactual equilibrium where Byzantine trade to the south and east is severed by the religious border, Byzantium suffers not just from a large drop

Table 5: Counterfactual changes in real consumption per capita after AD 700

	Log consumption		Counterfactual log consumption change if:					
	All parameters AD 460-620		Religious border AD 700-900		Technology AD 700-900		Minting AD 700-900	
	(1)	(2)	(3)	(4)	(5)	(6)	(7)	(8)
al-Andalus	-0.70	(0.10)	0.09	(0.02)	0.55	(0.10)	1.57	(0.31)
Aquitaine and Basque Country	-1.04	(0.08)	-0.15	(0.03)	0.99	(0.09)	3.93	(0.30)
Francia and Germania	-1.55	(0.09)	-0.07	(0.02)	1.68	(0.11)	6.17	(0.47)
Northern Italy and Balkans	0.07	(0.04)	-0.24	(0.05)	-0.24	(0.08)	-0.21	(0.07)
Southern Italy	-0.25	(0.06)	-0.11	(0.02)	-0.60	(0.13)	-0.03	(0.02)
Byzantine Heartlands	1.22	(0.11)	-0.69	(0.08)	-0.57	(0.13)	-1.41	(0.19)
al-Sham (Greater Syria)	0.30	(0.04)	0.04	(0.01)	-0.18	(0.10)	-0.22	(0.08)
Northern Syria and Caucasus	-0.34	(0.11)	0.02	(0.02)	0.15	(0.22)	0.19	(0.19)
al-Iraq, al-Jibal, Khuzistan, Kirman	0.28	(0.08)	0.01	(0.00)	0.03	(0.08)	0.03	(0.06)
Eastern Caliphate	-0.44	(0.08)	0.01	(0.00)	0.38	(0.16)	0.34	(0.26)
Jazirat al-arab and al-Yaman	-1.80	(0.18)	0.26	(0.09)	0.66	(0.40)	2.71	(0.84)
Misr (Egypt)	0.32	(0.07)	0.02	(0.00)	-0.71	(0.24)	-0.09	(0.02)
al-Maghrib	0.12	(0.06)	0.01	(0.00)	-0.46	(0.17)	-0.05	(0.06)

Notes: This table shows levels of (log) real consumption per capita in AD 460-620 (column 1), and (log) changes in real consumption per capita in counterfactual equilibria where we set the religious border to its AD 700-900 level while keeping all other parameters to their AD 460-620 levels (column 3), technology to its AD 700-900 level (column 5), or minting to its AD 700-900 level (column 7). For column 1, we solve for a steady state equilibrium using the AD 460-620 average of parameters estimated from (18)-(19), and use equations (4), (7), (10), and (20) to recover real consumption. For columns 2-4, we set parameters to their counterfactual levels (technology T' , population L' , trade costs d' , and minting M'), solve for endogenous wages as a fixed point (Alvarez and Lucas, 2007) using the trade equilibrium and market clearing conditions in equation (7), and use equation (20) to compute real consumption (see the technical appendix for details). Standard errors, in parentheses in even columns, are computed from re-estimating our model on 100 bootstrapped samples from our coin data.

in trade openness, but also from a sharp reduction in the contribution of trade deficits to real consumption; the massive Byzantine minting output in AD 460-620 can no longer buy foreign imports, and contributes instead to inflation within Byzantium. Other European regions also experience a sharp reduction in consumption (15% drop), as those relatively poor regions benefit from trading with more developed regions south and east of the Mediterranean before the Arab conquests. In contrast, Islamic regions are almost unaffected by the reduced access to trade.

Changes in technology (column 5) and minting (column 7) induce more heterogeneous changes. Western and northern Europe (including Islamic Spain) would have benefited from large technological improvements. Given their relatively small initial size, a counterfactual increase in minting to post-Arab conquests levels would also have allowed those regions to finance large trade deficits, contributing to large gains in real consumption. Byzantine real consumption would have dropped if technology moved to its post Arab conquests level for all regions. Interestingly, this is not just because Byzantine technology itself deteriorates; under the pre-Arab conquests trade costs, Byzantium loses export market shares to competitors from northwestern European and Middle Eastern regions who benefit from improved technology. On the other hand, the collapse of minting

output during the ‘Byzantine dark ages’ would have prevented Byzantium from acquiring foreign wares using seigniorage-financed trade deficits, and would have severely hurt real consumption.

3.3 Urbanization and trade in ancient Europe

We conclude by confronting our estimates for changes in real consumption to realized changes in urbanization in Europe. While our model does not feature any explicit notion of urbanization, we conjecture that a higher real consumption per capita allows to sustain a larger urban population. This exercise is illustrative, meant to verify that our estimates for real consumption derived solely from information on coin flows are in line with independent evidence on economic growth.

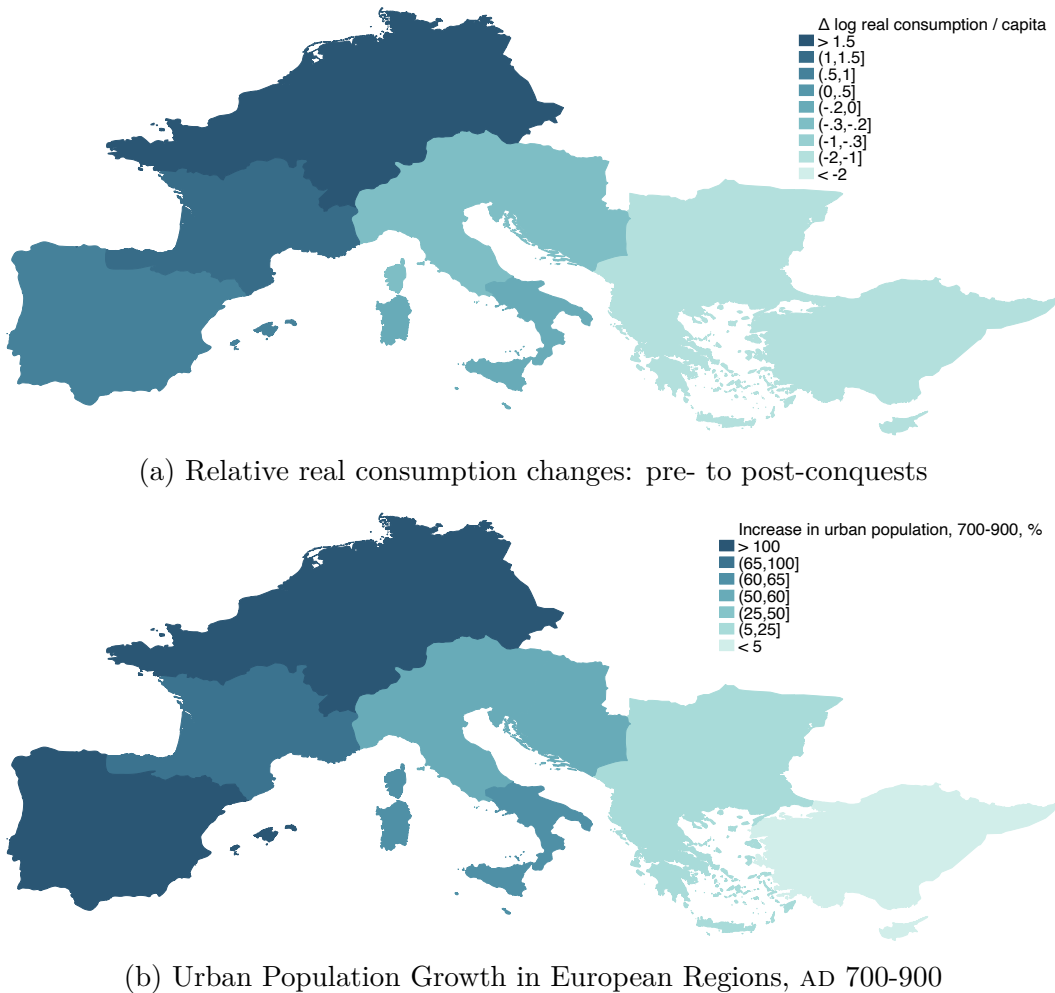


Figure 10: Real consumption and urbanization

Notes: Panel (a) shows the relative real consumption change from the pre-conquest period to the post-conquest period, column 1 of Table 4. Panel (b) shows the percentage growth of the urban population between AD 700 and AD 900. City size data from [Buringh \(2021\)](#), except for Byzantine Anatolia, which is not covered. We construct measures of urban decline in Anatolia (calculations available upon request) based on the shrinking surface area of cities described in [Brändes \(1989\)](#). The resulting figure of a 10% decline in urban population over this time interval seems to be a conservative estimate in light of the fact that many coastal cities saw large amounts of destruction and depopulation as a consequence of Arab raids.

Figure 10 shows our estimates for changes in real consumption per capita (top panel) together

with the patterns of urban population growth between AD 700 and AD 900 in the regions north of the Mediterranean, aggregated from city size data (bottom panel).³⁹ Comparing both maps suggests that our estimates for real consumption are qualitatively in line with independent evidence on urbanization. Our estimated drop in real consumption in the heartlands of the Byzantine empire, and substantial increase in western and northern Europe are in line with the decline in urban population in Asia Minor and Cyprus, low urban growth in Greece, Thracia, and Dacia, medium urban growth in the Balkans, Italy, and Aquitaine, and strong urban growth in Iberia and Francia/Germania.

Conclusion

In this paper we study the patterns of change in economic geography around the Mediterranean during Late Antiquity through the lens of coin flows. We propose a dynamic model of trade where agents use coins to make transactions, so that coins gradually diffuse over space and time in proportion to trade flows. We estimate this model using numismatic data on ancient coins. We are then able to use these parameters to recover granular time series for relative real consumption per capita from the fifth to the tenth century. Our estimates for changes in real consumption are consistent with observed measures of relative urbanization across European regions.

Our evidence from coin finds indicate that trade flows declined following the Arab conquests. This can be explained by a newly formed trade barrier between the emerging Arab Caliphate and the Christian West. These changes in trade patterns are in line with the claims of a trade disruption in the Mediterranean by Pirenne (1939). Pirenne, however, believed that these disruptions in trade flows also led to a vast reduction in economic activity and exchange within the Frankish lands. While our estimates reveal that Francia and Germania did experience a 15% drop in trade as a share of consumption, this cannot have had any meaningful impact on the Frankish economy because pre-conquest trade shares were already low. Our estimates suggest instead that the Frankish economy enjoyed net welfare gains from running trade deficits financed by seigniorage revenues, and strong increases in relative productivity, which far outweigh any reductions in foreign market access. In contrast the Byzantine Empire experienced the largest declines in economic activity in the seventh century, being faced with a triple shock of a lowered access to trade, reductions in relative productivity, and a drop in seigniorage revenues. Any view that attributes most of the changing economic geography of Late Antiquity to the Arab conquests would need to establish their role in driving the changes in relative productivity and in mint output.

³⁹While estimates of city sizes from this period are naturally imprecise, the broad patterns that emerge in panel (b) of Figure 10 are in line with the consensus view of increased urbanization in northwestern Europe and stagnation in the Eastern Mediterranean.

TECHNICAL APPENDIX

Recovering real consumption. We explain here how to recover all equilibrium variables from our structural estimation. Throughout, we approximate the savings rate into coins to zero (informed by the low saving rate in the Roman period of 1.5% computed by Scheidel, 2020), and we arbitrarily set the trade elasticity to $\theta = 4$ (Simonovska and Waugh, 2014).

step 1. Parameters. Our structural estimation (18)-(19) delivers the following parameters: seller terms $\tilde{\beta}_i[t]$, bilateral trade costs $d_{ni}^{-\theta}[t]$, minting outputs $M_i[t]$, and the coin loss rate λ .

Note: It is important to stress two important normalizations in our estimation. First, minting is identified only up to a (single) scaling constant, so we normalize $M_{n_0}[t_0] = 1$ for reference region n_0 and period t_0 . Second, the seller terms enter the numerator and denominator of trade shares each period, they are therefore only identified up to a scaling factor each period, so we are free to normalize them each period.

step 2. Trade shares are recovered from the seller and bilateral terms using equations (4) and (10),

$$\pi_{ni}[t] = \underbrace{\frac{\tilde{\beta}_i[t]\delta_{ni}[t]}{\sum_k \tilde{\beta}_k[t]\delta_{nk}[t]}}_{\text{step 1}}, \forall(n, i, t)$$

Note: Those are *estimated* trade shares, as we do not observe actual trade. As in Eaton et al. (2013), they are also *predicted* trade shares, strictly between 0 and 1, even if realized trade shares may equal 0 or 1. And they are invariant to any normalization of $\tilde{\beta}_i[t]$.

step 3. Aggregate nominal incomes are solved for using the dynamic market clearing conditions, given trade shares, minting, and the coin loss rate. Given that markets clear dynamically, we need to make an assumption for the period $t_0 - 1$ *before* our sample starts. Absent any guidance, we simply assume that aggregate incomes for period $t_0 - 1$ are the same as for period t_0 . We need to solve for one (single) system of linear equations for initial period t_0 , and we then recursively solve for incomes in all subsequent periods $t > t_0$:

(a) We solve (once) for incomes in period t_0 from the system of linear equations (7),

$$w_i L_i[t_0] = \sum_n \underbrace{\pi_{ni}[t_0]}_{\text{step 2}} \left(\underbrace{(1 - \lambda)}_{\text{step 1}} w_n L_n[t_0] + \underbrace{M_n[t_0]}_{\text{step 1}} \right), \forall i$$

(b) We then solve recursively for incomes in all subsequent periods using equation (6),

$$w_i L_i[t+1] = \sum_n \underbrace{\pi_{ni}[t+1]}_{\text{step 2}} \left(\underbrace{(1 - \lambda)}_{\text{step 1}} \underbrace{w_n L_n[t]}_{\text{step 3}} + \underbrace{M_n[t+1]}_{\text{step 1}} \right), \forall i, t > t_0$$

Note: Our estimates for nominal incomes inherit our minting normalization.

- step 4.** Effective labor supply (technology-augmented) is recovered by combining aggregate income and seller terms, assuming a specific value for the trade elasticity θ , and using equation (10),

$$\begin{aligned}\tilde{\beta}_i &= T_i[t] w_i^{-\theta}[t] \\ L_i T_i^{1/\theta}[t] &= \underbrace{w_i L_i[t]}_{\text{step 3}} \underbrace{\tilde{\beta}_i^{1/\theta}[t]}_{\text{step 1}}\end{aligned}$$

Note: our estimation does not allow us to identify *absolute* levels of effective labor supply, only *relative* levels within period; $L_i T_i^{1/\theta}[t]$ inherits the normalizations on $\tilde{\beta}_i[t]$ and $M_i[t]$.

- step 5.** Technology. Using the assumption $L_i[t] = T_i[t]$, we separate technology from labor supply,

$$T_i^{1/\theta}[t] = \underbrace{\left(L_i T_i^{1/\theta}[t] \right)^{\frac{1}{1+\theta}}}_{\text{step 4}}.$$

- step 6.** Real consumption per capita. We are finally in a position to recover real consumption, both aggregate and per capita, using the normalization $d_{nn} = 1$ as in Eaton and Kortum (2002),

$$\begin{aligned}\frac{X_n}{p_n} &= \frac{(1-\lambda) w_n L_n + M_n}{\gamma \left(\sum_k T_k (w_k d_{nk})^{-\theta} \right)^{-1/\theta}} = \gamma^{-1} \left(\frac{T_n (w_n)^{-\theta}}{\sum_k T_k (w_k d_{nk})^{-\theta}} \right)^{-1/\theta} \frac{(1-\lambda) w_n L_n + M_n}{\left(T_n (w_n)^{-\theta} \right)^{-1/\theta}} \\ &= \underbrace{\gamma^{-1} (\pi_{nn})^{-1/\theta}}_{\text{step 2}} \underbrace{\left(L_n T_n^{1/\theta} \right)}_{\text{step 4}} \underbrace{\left(1 + \frac{M_n - \lambda w_n L_n}{w_n L_n} \right)}_{\text{steps 1 and 3}}, \text{ and} \\ \frac{X_n/p_n}{L_n} &= \underbrace{\gamma^{-1} (\pi_{nn})^{-1/\theta}}_{\text{step 2}} \underbrace{(T_n)^{1/\theta}}_{\text{step 5}} \underbrace{\left(1 + \frac{M_n - \lambda w_n L_n}{w_n L_n} \right)}_{\text{steps 1 and 3 Trade Deficit}}.\end{aligned}$$

Note: Our normalizations for the seller terms and for minting do not affect the ‘openness’ and ‘trade deficit’ terms, as both are unit-free ratios. They do however affect our measure of technology (**step 4**), so real consumption is only defined in *relative* terms within each period.⁴⁰ We choose units for technology such that $\mathbb{E}_t [(X_n[t]/p_n[t])/L_n[t]] = 1, \forall t$.

Given the inherent sparsity of our ancient coin hoard data, our time series estimates for seller terms and minting are noisy. In order to smooth out some of this noise, we use a simple mov-

⁴⁰If we re-scale $\tilde{\beta}_n[t], \forall t$, by an arbitrary positive multiplicative constant $(\kappa[t])^{\theta(1+\theta)}$, then we must re-scale technology and population by $(\kappa[t])^\theta$, aggregate consumption by $(\kappa[t])^{1+\theta}$, and real consumption per capita by $\kappa[t]$.

ing average. Formally, for any period $t \in [380, 880]$,⁴¹ we use $\frac{1}{5} \sum_{\tau=t-2}^{t+2} \tilde{\beta}_i[\tau]$ instead of $\tilde{\beta}_i[t]$, and $\frac{1}{5} \sum_{\tau=t-2}^{t+2} M_i[\tau]$ instead of $M_i[t]$. Our estimates for bilateral trade costs suffer less from this estimation noise and are not transformed.

To compute a steady state equilibrium, we follow the same procedure but use only step 3(a).

Computing real consumption across counterfactuals. We compute counterfactual *steady state* equilibria from the trade equilibrium and market clearing (7) as in Alvarez and Lucas (2007),

$$\pi_{ni} = \frac{T_i(w_i)^{-\theta}(d_{ni})^{-\theta}}{\sum_k T_k(w_k)^{-\theta}(d_{nk})^{-\theta}} \text{ and } w_i L_i = \sum_n \pi_{ni} ((1 - \lambda)w_n L_n + M_n). \quad (\text{equation (7) reminded})$$

For any choice of population L' , technology T' , trade costs d' , and minting M' , we solve for equilibrium wages w' using an iterative algorithm, imposing the trade equilibrium and market clearing conditions: for any (n)th starting guess $w^{(n)}$ for wages, we impose the trade equilibrium,

$$\pi_{ni}^{(n)} = \frac{T'_i(w_i^{(n)})^{-\theta}(d'_{ni})^{-\theta}}{\sum_k T'_k(w_k^{(n)})^{-\theta}(d'_{nk})^{-\theta}},$$

and update our guess for wages to $w_i^{(n+1)}$ by solving the *linear* system of market clearing conditions,

$$w_i^{(n+1)} L'_i = \sum_n \pi_{ni}^{(n)} ((1 - \lambda)w_n^{(n+1)} L'_n + M'_n).$$

We iterate this mapping until convergence to find equilibrium wages w' . We can then readily compute counterfactual real consumption and its constituent parts using equation (20).

References

- AHLFELDT, G. M., S. J. REDDING, D. M. STURM, AND N. WOLF (2015): “The Economics of Density: Evidence From the Berlin Wall,” *Econometrica*, 83, 2127–2189.
- AL-MUQADDASI (1994): *Ahsan al-taqāṣīm fi ma’arfat al-aqalīm* (*The Best Divisions for Knowledge of the Regions*), Garnet Publishing (transl. B.A. Collins).
- AL ’USH, A.-F. (1972): *The silver hoard of Damascus: Sasanian, Arab-Sasanian, Khuwarizmian, and Umayyad kept in the National Museum of Damascus*, Damascus: Direction General of Antiquities and Museums.
- ALVAREZ, F. AND R. E. LUCAS (2007): “General equilibrium analysis of the Eaton–Kortum model of international trade,” *Journal of Monetary Economics*, 54, 1726–1768.
- ANDERSON, J. E. AND E. VAN WINCOOP (2003): “Gravity with Gravitas: A Solution to the Border Puzzle,” *American Economic Review*, 93, 170–192.

⁴¹To construct our moving averages we omit the first few and last periods, imprecisely estimated because there are too few overlapping generations of coins at the bounds of our sample period.

- ARKOLAKIS, C., A. COSTINOT, AND A. RODRÍGUEZ-CLARE (2012): “New Trade Models, Same Old Gains?” *American Economic Review*, 102, 94–130.
- ASHTOR, E. (1970): “Quelques observations d’un orientaliste sur la thèse de Pirenne,” *Journal of the Economic and Social History of the Orient*, 13, 166–194.
- BANAJI, J. (2016): *Exploring the Economy of Late Antiquity: Selected Essays*, Cambridge University Press.
- BARJAMOVIC, G., T. CHANEY, K. COŞAR, AND A. HORTAÇSU (2019): “Trade, merchants, and the lost cities of the bronze age,” *The Quarterly Journal of Economics*, 134, 1455–1503.
- BATES, M. (1991): “Coins and money in the Arabic Papyri,” *Documents de l’Islam Medieval*, 43–643.
- BESSARD, F. (2020): “Money Supply and Currency,” in *Caliphs and Merchants: Cities and Economies of Power in the Near East (700-950)*, Oxford University Press.
- BOLIN, S. (1953): “Mohammed, Charlemagne and Ruric,” *Scandinavian Economic History Review*, 1, 5–39.
- BRANDES, W. (1989): *Die Städte Kleinasiens im 7. und 8. Jahrhundert*, De Gruyter.
- BURINGH, E. (2021): “The population of European cities from 700 to 2000: Social and economic history,” *Research Data Journal for the Humanities and Social Sciences*, 6, 1–18.
- CHANEY, T. (2018): “The Gravity Equation in International Trade: An Explanation,” *Journal of Political Economy*, 126, 150–177.
- CORNU, G. (1983): *Atlas du monde Arabo-Islamique à l’époque classique: IX.-X. siècles*, Brill.
- COUPLAND, S. (2014): “The use of coin in the Carolingian Empire in the ninth century,” *Early Medieval Monetary History: Studies in Memory of Mark Blackburn*, Farnham, 257–93.
- DEKLE, R., J. EATON, AND S. KORTUM (2007): “Unbalanced Trade,” *American Economic Review, Papers and Proceedings*, 97, 351–355.
- DONALDSON, D. (2018): “Railroads of the Raj: Estimating the impact of transportation infrastructure,” *American Economic Review*, 108, 899–934.
- DONALDSON, D. AND R. HORNBECK (2016): “Railroads and American economic growth: A “market access” approach,” *The Quarterly Journal of Economics*, 131, 799–858.
- EATON, J. AND S. KORTUM (2002): “Technology, Geography, and Trade,” *Econometrica*, 70, 1741–1779.
- EATON, J., S. KORTUM, AND S. SOTELO (2013): *International Trade: Linking Micro and Macro*, Cambridge University Press, 329–370, Econometric Society Monographs.
- FINDLAY, R. AND K. H. O’ROURKE (2009): *Power and Plenty: Trade, War, and the World Economy in the Second Millennium*, Princeton University Press.

- FLAME (2023a): “Biases in FLAME’s data,” <https://coinage.princeton.edu/biases-in-flames-data/>.
- (2023b): “Framing the Late Antique and early Medieval Economy,” <https://coinage.princeton.edu/>, accessed: 2023-07-01.
- FLÜCKIGER, M., E. HORNUNG, M. LARCH, M. LUDWIG, AND A. MEES (2022): “Roman transport network connectivity and economic integration,” *The Review of Economic Studies*, 89, 774–810.
- FOGEL, R. W. (1964): *Railroads and American economic growth*, Johns Hopkins Press Baltimore.
- FOSS, C. (1975): “The Persians in Asia Minor and the end of Antiquity,” *The English Historical Review*, 90, 721–747.
- GIBBON, E. (1789): *The history of the decline and fall of the Roman Empire*, vol. I-VI, London: Strahan & Cadell.
- GRIERSON, P. (1959): “Commerce in the Dark Ages: a critique of the evidence,” *Transactions of the Royal Historical Society*, 9, 123–140.
- (1973): *Catalogue of the Byzantine Coins in the Dumbarton Oaks Collection and in the Whittemore Collection, 3: Leo III to Nicephorus III, 717-1081*, Dumbarton Oaks.
- HENRY, M. K. F. G. (1967): “Carolingian Coinage,” Tech. rep., The American Numismatic Society.
- HODGES, R. AND D. WHITEHOUSE (1983): *Mohammed, Charlemagne & the origins of Europe: archaeology and the Pirenne thesis*, Cornell University Press.
- HORNBECK, R. AND M. ROTEMBERG (forthcoming): “Growth Off the Rails: Aggregate Productivity Growth in Distorted Economies,” *Journal of Political Economy*.
- IZDEBSKI, A., G. KOLOCH, T. SŁOCZYŃSKI, AND M. TYCNER (2016): “On the use of paleontological data in economic history: new methods and an application to agricultural output in Central Europe, 0–2000 AD,” *Explorations in Economic History*, 59, 17–39.
- JUHÁSZ, R. (2018): “Temporary protection and technology adoption: Evidence from the napoleonic blockade,” *American Economic Review*, 108, 3339–3376.
- KAZHDAN, A. (1954): “Vizantijskie goroda v VII-IX vv,” *Sovetskaja arkheologija*, 21, 164–188.
- KERSHAW, J., S. W. MERKEL, P. D’IMPORZANO, AND R. NAISMITH (2024): “Byzantine plate and Frankish mines: the provenance of silver in north-west European coinage during the Long Eighth Century (c. 660–820),” *Antiquity*, 98, 502–517.
- LEONTIEF, W. W. (1941): *The Structure of the American Economy, 1919–1929*, Cambridge, MA: Harvard University Press.
- (1944): “Output, Employment, Consumption, and Investment,” *The Quarterly Journal of Economics*, 58, 290–314.

- LIU, E. AND A. TSYVINSKI (2024): “A Dynamic Model of Input–Output Networks,” *The Review of Economic Studies*.
- LOPEZ, R. S. (1943): “Mohammed and Charlemagne: a revision,” *Speculum*, 18, 14–38.
- LOVELUCK, C. P., M. McCORMICK, N. E. SPAULDING, H. CLIFFORD, M. J. HANDLEY, L. HARTMAN, H. HOFFMANN, E. V. KOROTKIKH, A. V. KURBATOV, A. F. MORE, ET AL. (2018): “Alpine ice-core evidence for the transformation of the European monetary system, AD 640–670,” *Antiquity*, 92, 1571–1585.
- MCCONNELL, J. R., A. I. WILSON, A. STOHL, M. M. ARIENZO, N. J. CHELLMAN, S. ECKHARDT, E. M. THOMPSON, A. M. POLLARD, AND J. P. STEFFENSEN (2018): “Lead pollution recorded in Greenland ice indicates European emissions tracked plagues, wars, and imperial expansion during antiquity,” *Proceedings of the National Academy of Sciences*, 115, 5726–5731.
- MCCORMICK, M. (2001): *Origins of the European economy: communications and commerce AD 300-900*, Cambridge University Press.
- MICHAELS, G. AND F. RAUCH (2018): “Resetting the Urban Network: 117–2012,” *The Economic Journal*, 128, 378–412.
- MONTESQUIEU, C. (1734): *Considérations sur les causes de la grandeur des Romains et de leur décadence*.
- MORRISON, C. (2002): “Byzantine money: its production and circulation,” *The Economic History of Byzantium*, 3, 909–966.
- NAGY, D. K. (2023): “Hinterlands, City Formation and Growth: Evidence from the U.S. Westward Expansion,” *The Review of Economic Studies*, 90, 3238–3281.
- NAISMITH, R. (2014): “The Social Significance of Monetization in the Early Middle Ages*,” *Past & Present*, 223, 3–39.
- NOONAN, T. S. (1980): “When and how dirhams first reached Russia: a numismatic critique of the Pirenne theory,” *Cahiers du monde russe et soviétique*, 401–469.
- PARVÉRIE, M. (2014): “Corpus des monnaies arabo-musulmanes des VIII et IX siècles découvertes dans le Sud de la France,” *Revista Numismática OMNI*, 79–100.
- (2018): “La circulation des deniers de l’Aquitaine carolingienne en Al-Andalus; un réexamen des trésors ‘Espanya-1, 2 et 3’,” *Bulletin de la Société numismatique de Limousin*, 25, 4–16.
- PASCALI, L. (2017): “The wind of change: Maritime technology, trade, and economic development,” *American Economic Review*, 107, 2821–2854.
- PENNAS, V. (1996): “Life in Byzantine Cities of Peloponnesos: The Numismatic Evidence (8th–12th Century),” in *Mneme Martin Jessop Price*, Hellenic Numismatic Society.
- PEREGRINE, P. N. (2020): “Climate and social change at the start of the Late Antique Little Ice Age,” *The Holocene*, 30, 1643–1648.

- PERSSON, K. G. AND P. SHARP (2015): *An economic history of Europe*, Cambridge University Press.
- PIRENNE, H. (1927): *Medieval Cities: Their Origins and the Revival of Trade*, Princeton University Press.
- (1939): *Mohammed and Charlemagne*, London: G. Allen & Unwin.
- REDDING, S. J. AND D. M. STURM (2008): “The Costs of Remoteness: Evidence from German Division and Reunification,” *American Economic Review*, 98, 1766–97.
- ROMANOV, M. AND M. SEYDI (2022): “al-Thurayyā,” <https://althurayya.github.io/> [Accessed: (1 July 2023)].
- SARAH, G. (2008): “Caractérisation de la composition et de la structure des alliages argent-cuivre par ICP-MS avec prélèvement par ablation laser. Application au monnayage carolingien.” Ph.D. thesis, Université d’Orléans.
- SARAH, G., M. BOMPAIRE, M. MCCORMICK, A. ROVELLI, AND C. GUERROT (2008): “Analyses élémentaires de monnaies de Charlemagne et Louis le Pieux du Cabinet des Médailles: l’Italie carolingienne et Venise,” *Revue numismatique*, 164, 355–406.
- SCHEIDEL, W. (2015): “ORBIS: The Stanford geospatial network model of the Roman world,” Tech. rep.
- (2020): “Roman wealth and wealth inequality in comparative perspective,” *Journal of Roman Archaeology*, 33, 341–353.
- SHATZMILLER, M. (2018): “At the origins of Middle Eastern trade, 700-1000 AD: An application of the gravity theory of trade,” in *Economic integration and social change in the Islamic world system*, ed. by H. Kennedy and F. Bessard, 800–1000.
- SIMONOVSKA, I. AND M. E. WAUGH (2014): “The elasticity of trade: Estimates and evidence,” *Journal of International Economics*, 92, 34–50.
- VOLTAIRE (1756): *Essai sur les mœurs et l'esprit des nations*, Geneva: Frères Cramer.
- WICKHAM, C. (2006): *Framing the early middle ages: Europe and the Mediterranean, 400-800*, Oxford University Press.
- ZAVAGNO, L. (2022): “A Lost World That Never Died,” *Dumbarton Oaks Papers*, 76, 281–310.

Online Appendix for

Trade and the End of Antiquity

by Johannes Boehm and Thomas Chaney

A Additional results	1
A.1 Comparing hoards with circulation hoards of Banaji (2016)	1
A.2 Comparing coin flows to the flows of West Roman Terra Sigillata.	1
A.3 Within-empire coin redistribution before entering circulation?	1
A.4 Arab conquests and the Mediterranean.	1
A.5 Coin stocks versus coin flows, a numerical exploration.	2
A.6 Estimation of λ	2
A.7 Validating the geospatial model.	2
A.8 Changes in real consumption in the ancient world.	2
A.9 Tables and figures	3
B Coin hoard data	14
B.1 Hand-collected data	14
B.2 FLAME	15
B.3 Locating mints	16
B.4 Political entities and the geography of hoards and mints	16
B.5 Tables and references	19
C Mapping the Data to the Model	46
C.1 Constructing regions	46
C.2 Defining the coin sample for the structural analysis	46
C.3 Constructing the geospatial model	47
C.4 Technical details on operations in spherical geometry	52
C.5 Other utilities	55
C.6 Tables and references	57

A Additional results

A.1 Comparing hoards with circulation hoards of Banaji (2016).

To support the argument that the coins in our hoards are broadly reflective of coin circulation during Late Antiquity, we compare the age distribution of the hoards in our data with a sample of Byzantine circulation hoards described by Banaji (2016), Chapter 6. These are twelve hoards containing between 12 and 751 Byzantine solidi. Figure A.1 shows the average fraction of coins in each 10-year age bin in these hoards, alongside the distribution of coin ages in Figure 3b, showing a similar age profile. Banaji (2016) also reports that on average 44% of the coins in these hoards are older than 33 years at time of deposit; in our data the corresponding share (for hoards with more than ten coins) is 38%.

A.2 Comparing coin flows to the flows of West Roman Terra Sigillata.

Figure A.2 compares the relationship between distance and coin flows in our data with the relationship between distance and flows of Terra Sigillata in the data of Flückiger et al. (2022) using binned scatterplots.¹ The distance elasticity is similar but slightly lower for coins, which is potentially due to the fact that naive gravity regressions using coin stocks will exhibit a distance elasticity that is biased towards zero (see Section 2).

A.3 Within-empire coin redistribution before entering circulation?

One potential explanation for why coins flow in particular within empires (i.e. the observed border effect) is that coins could be redistributed across different mints first before they enter circulation. If that were the case, the precise place of minting of a coin should not matter beyond the empire in which it has been minted. Table A.2 investigates this by including hoard cell \times empire (that mints the coin) fixed effects in the specification of equation (1), and finds that distance matters almost to the same degree as in the baseline specification. It is therefore unlikely that a lot of redistribution within an empire happens before coins enter circulation.

A.4 Arab conquests and the Mediterranean.

Figure A.3 shows the number of coins crossing the Mediterranean, and their composition. The time of the Arab conquests, indicated by two dashed vertical lines, corresponds to a decline of north-south flows (almost entirely flows of Roman/Byzantine coins), and an increase in east-west flows. The new flows along both axes are almost entirely made of Islamic coins.

We employ a set of descriptive regressions to further decompose these changes. We estimate by PPML

$$\text{count}_{mhpt} = \exp(a_{mh} + a_{mp} + b_1 \text{Mediterranean}_{mh} \times \text{After}_t + b_2 \text{Mediterranean}_{mh} \times \text{After}_t \times \text{Islamic}_p + u_{mhpt}). \quad (\text{A.1})$$

We aggregate all hoard (h) and mint (m) locations to $1^\circ \times 1^\circ$ cells, separately for each time period (t), and note for each coin which one of fourteen aggregate political blocks p had issued it.² Count _{$mhpt$} is the number of coins issued in cell m under empire/dynasty p and found in a cell h , both within time period t . Mediterranean _{mh} is a dummy that is one if the geodetic line between cells m and h intersects the Mediterranean; After _{t} is a dummy equal to one if t is between 713 and 900, and zero if between 400 and 630; Islamic _{p} is one if the coin is of Islamic issue (any dynasty); a_{mh} and a_{mp} denote mint cell \times hoard cell and mint-cell \times dynasty/empire fixed effects, respectively. The objective is to investigate whether the Mediterranean acts differentially as a barrier to coin flows after the Arab conquests, and if so, for coins of which issue. Table A.3 presents the results. We drop all mint cell \times empire/dynasty combinations that did not produce coins. Column (1) shows a negative coefficient on the interaction of the Mediterranean and post-conquest dummies, so that after the Arab conquests coin flows declined in

¹Comparing the pairwise flows of objects in the two datasets directly does not make sense since Terra Sigillata are produced in locations that are very different from coin mints (see Figure 4 in their paper).

²These political blocks are: Eastern Roman Empire, Western Roman Empire, Roman Empire (pre-division), Sasanians, Umayyads, Spanish Umayyads, Abbasids, Fatimids, Samanids, Visigoths, Ostrogoths, Vandals, Merovingians, and Carolingians. See Appendix Figure B.1 for a breakdown of these and more aggregate political entities.

cell pairs across the sea. Column (2) shows a positive coefficient on the triple interaction: Islamic coins were facing disproportionately lower barriers on sea routes in the post-conquest world, conditional on origin and destination characteristics. Column (3) contrasts this with Roman/Byzantine coins, which experience disproportionately higher barriers. Column (4) shows similar estimates with hoard cell \times time and mint cell \times time fixed effects, neutralizing potential location-time-specific confounders. All specifications point to the same facts highlighted by Figure 4: there are relatively fewer coins flowing across the Mediterranean in the 8th and 9th century than before; the drop is particularly strong for Roman coins, and the emergence of flows of Islamic coins partly make up for this drop.

A.5 Coin stocks versus coin flows, a numerical exploration.

We describe below the stylized numerical model used to generate figure 5.

Figure A.4 uses our data to empirically explore the hypothesis that gravity regressions with flows of durables over longer horizons bias the distance elasticity towards zero. It shows a coefficient plot of the following regression:

$$\text{count}_{mth\tau} = \exp \left\{ \sum_{\tau' \in T} \beta_{\tau'} \log \text{distance}_{mh} \times 1(t - \tau = \tau') + \alpha_{mt} + \alpha_{h\tau} + \varepsilon_{mth\tau} \right\} \quad (\text{A.2})$$

where $T = \{0, 20, 40, 60, 80, 100\}$ and mint and hoard tpq dates are rounded to 20-year intervals. Coins with longer timespans between mint and hoard tpq dates are omitted. We estimate the coefficients using PPML.

The results confirm that the distance elasticity for coins that have travelled for longer is lower (i.e. closer to zero) than for coins that have travelled for shorter periods. Section 2.2 and Figure 5 provide the intuition for this result.

A.6 Estimation of λ .

To estimate λ , we divide coins by their age of deposit (using the tpq as the date of deposit) into n -year bins (for $n = 10$ and $n = 20$). We calculate the fraction $f^{(n)}(k)$ of coins that are in bin $[k, k+n)$, and estimate the parameter of exponential decay from

$$\log f^{(n)}(k) = \tilde{\lambda}^{(n)} \frac{k}{n} + \varepsilon_k.$$

Table A.4 shows the OLS estimation results using 10-year and 20-year bins. The estimates of λ can be recovered from $\lambda = 1 - \exp(\tilde{\lambda})$, yielding, respectively, $\hat{\lambda}^{10} = .15$ and $\hat{\lambda}^{20} = .301$.

A.7 Validating the geospatial model.

We compare the implied travel times from our geospatial model (section C.3) to those reported by the 10th-century Arab geographer al-Maqdisī in his work *The Best Divisions for the Knowledge of the Regions* (Al-Muqaddasī, 1994).³ Figure A.5 shows the comparison. Our model generates travel times that are slightly larger for shorter distances, and on average similar for longer routes.

A.8 Changes in real consumption in the ancient world.

Table A.5 shows the levels of real consumption per capita and its components before and after the Arab conquests. Figure A.6 plots, for all 13 regions, the time series of real consumption per capita from AD 380 to AD 900, and the components that partition real consumption (openness, technology, and trade deficits).

³ Al-Maqdisī reports cities and (unsystematically) distances (in travel stages, post stages, and *farsakhs*) or travel times (in days, or nights in the desert) between cities in different parts of the Islamic lands. Historians note that it is unlikely that al-Maqdisī did indeed travel to all these regions, and some distances and travel times are unrealistic. We exclude the most egregious outliers.

A.9 Tables and figures

Tables

Appendix Table A.1: Gravity and border effects: # coins vs values of coins

	Dep. var.: # Coins _{mdh}			
	(1)	(2)	(3)	(4)
Log Distance	-1.138*** (0.12)	-1.002*** (0.13)	-0.727*** (0.10)	-0.694*** (0.10)
Political border		-1.945*** (0.62)		-1.541*** (0.41)
Hoard Cell FE	Yes	Yes	Yes	Yes
Mint × Empire Cell FE	Yes	Yes	Yes	Yes
Sample	Intensive and Extensive Margins		Intensive Margin only	
Estimator	PPML	PPML	PPML	PPML
Pseudo- R^2	0.767	0.778	0.737	0.744
Observations	217748	217748	6312	6312

Standard errors in parentheses, clustered at mint cell × empire and hoard cell level.

* $p < 0.10$, ** $p < 0.05$, *** $p < 0.01$

Notes: This table presents variations of equation (1). The dependent variable is the number of coins in a hoard cell h from a mint cell m issued by a political entity p . Columns 1 and 2 reproduce columns 1 and 2 from table 1 (intensive and extensive margins of coin flows combined), while columns 3 and 4 exploits only the intensive margin of coin flows (restricting the sample to $m \times h$ pairs where some coins from mint cell m were found in hoard cell h).

Appendix Table A.2: Do coins get redistributed within empires before entering circulation?

	Dependent variable: # Coins_{mdh}			
	(1)	(2)	(3)	(4)
Log Distance	-0.709** (0.092)	-0.924** (0.17)	-0.669** (0.11)	-0.839** (0.068)
Empire \times Hoard Cell FE	Yes	Yes	Yes	Yes
Mint \times Empire Cell FE		Yes		Yes
Sample			Gold only	Gold only
Estimator	PPML	PPML	PPML	PPML
R^2				
Observations	41443	41443	11367	11348

Standard errors in parentheses, clustered at mint cell \times empire and hoard cell level.

+ $p < 0.10$, * $p < 0.05$, ** $p < 0.01$

Notes: This table presents variations of equation (1). The dependent variable is the number of coins in a hoard cell h from a mint cell m issued by a political entity p . The regression drops all (m, d) combinations that have no emitted coins. Hoard and mint cells are $1^\circ \times 1^\circ$. Observations only include those that remain after dropping singletons and separated observations. Political entities here are categorized into fourteen divisions.

Appendix Table A.3: The Mediterranean Before and After the Conquests

	Dependent variable: Number of Coins			
	(1)	(2)	(3)	(4)
Crossing Mediterranean \times After Conquests	-1.774** (0.46)	-3.141** (0.53)	-0.712 (0.66)	-1.751 (1.24)
Crossing Mediterranean \times After Conquests \times Islamic Coin		7.171** (0.91)	4.835** (0.97)	8.382** (1.15)
Crossing Mediterranean \times After Conquests \times Roman Coin			-3.108** (0.79)	-2.976** (0.71)
Mint Cell \times Empire FE	Yes	Yes	Yes	Yes
Mint Cell \times Hoard Cell FE	Yes	Yes	Yes	Yes
After Conquests FE	Yes	Yes	Yes	
Mint Cell \times After Conquests FE				Yes
Hoard Cell \times After Conquests FE				Yes
Estimator	PPML	PPML	PPML	PPML
Observations	10350	10350	10350	6023

Standard errors in parentheses, clustered at the hoard \times era and mint \times era level.

+ $p < 0.10$, * $p < 0.05$, ** $p < 0.01$

Notes: This table presents various specifications of equation (A.1). The dependent variable is the number of coins in a hoard cell from a mint cell \times dynasty \times era (where era is before vs after the conquests). The regression drops all mint \times dynasty combinations that have zero emitted coins. Hoard and mint cells are $1^\circ \times 1^\circ$. Flows before the conquests are those with mint date after 400 and t_{pq} before 630; flows after the conquests are those with mint date after 713 and t_{pq} before 900. Observation counts only include those that remain after dropping singletons and separated observations. “Crossing Mediterranean” is a dummy that is one if the geodesic line between hoard and mint cell intersects with the Mediterranean. “Islamic Coin” and “Roman Coin” are dummies equal to one if the coin is of Islamic issue (any dynasty) or Roman/Byzantine issue, respectively. “Empires” here are categorized as Sasanian, Roman-Byzantine, Franks, Islamic, Germanic Tribes, and Other Christian.

 Appendix Table A.4: Estimation of λ

	Dependent variable: Log share of coins in bin $[k, k + n]$	
	(1)	(2)
k/n	-0.163** (0.010)	-0.358** (0.032)
Bin size n	10	20
R^2	0.829	0.815
Observations	55	31

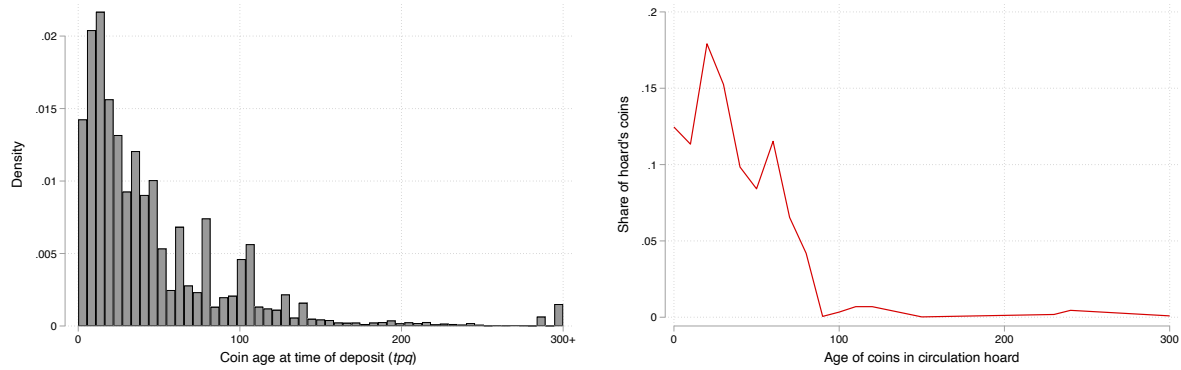
Standard errors in parentheses.

Appendix Table A.5: The components of real consumption, AD 460-620 and AD 700-900

	Consumption $\frac{X_n/p_n}{L_n}$		Import share $1 - \pi_{nn}$		Technology $T_n^{1/\theta}$		Trade deficits $\frac{X_n}{w_n L_n}$	
	460-620 (1)	700-900 (2)	460-620 (3)	700-900 (4)	460-620 (5)	700-900 (6)	460-620 (7)	700-900 (8)
	al-Andalus	0.50 (0.08)	0.93 (0.13)	0.23 (0.08)	0.01 (0.01)	0.47 (0.05)	1.03 (0.15)	0.99 (0.39)
Aquitaine and Basque Country	0.35 (0.03)	1.27 (0.17)	0.22 (0.04)	0.05 (0.02)	0.35 (0.03)	1.20 (0.16)	0.94 (0.06)	1.05 (0.02)
Francia and Germania	0.21 (0.02)	1.49 (0.20)	0.18 (0.04)	0.00 (0.01)	0.25 (0.03)	1.52 (0.20)	0.80 (0.03)	0.98 (0.01)
Northern Italy and Balkans	1.07 (0.05)	0.79 (0.11)	0.31 (0.07)	0.05 (0.04)	0.87 (0.10)	0.79 (0.12)	1.12 (0.11)	0.99 (0.04)
Southern Italy	0.78 (0.04)	0.64 (0.24)	0.41 (0.06)	0.72 (0.23)	0.91 (0.06)	0.35 (0.11)	0.75 (0.04)	1.31 (0.60)
Byzantine Heartlands	3.40 (0.44)	0.71 (1.08)	0.64 (0.06)	0.12 (0.13)	0.96 (0.10)	0.62 (0.12)	2.73 (0.68)	1.11 (19.33)
al-Sham (Greater Syria)	1.34 (0.05)	0.97 (0.15)	0.17 (0.08)	0.02 (0.02)	1.36 (0.16)	1.22 (0.19)	0.94 (0.10)	0.80 (0.04)
Northern Syria and Caucasus	0.71 (0.07)	0.89 (0.15)	0.08 (0.05)	0.04 (0.09)	0.93 (0.13)	1.08 (0.23)	0.75 (0.04)	0.81 (0.12)
al-Iraq, al-Jibal, Khuzistan, Kirman	1.32 (0.09)	1.40 (0.21)	0.08 (0.02)	0.07 (0.03)	1.20 (0.09)	1.27 (0.20)	1.08 (0.02)	1.08 (0.04)
Eastern Caliphate	0.64 (0.05)	0.93 (0.18)	0.02 (0.01)	0.00 (0.00)	0.63 (0.07)	0.93 (0.18)	1.02 (0.03)	1.00 (0.01)
Jazirat al-arab and al-Yaman	0.17 (0.03)	0.53 (0.11)	0.17 (0.07)	0.15 (0.12)	0.23 (0.04)	0.44 (0.23)	0.70 (0.00)	1.16 (0.30)
Misr (Egypt)	1.38 (0.09)	0.96 (1.29)	0.04 (0.03)	0.32 (0.29)	1.74 (0.13)	0.77 (0.24)	0.78 (0.02)	1.13 (3.42)
al-Maghrib	1.12 (0.06)	1.49 (0.36)	0.09 (0.02)	0.45 (0.17)	1.16 (0.04)	0.71 (0.14)	0.95 (0.04)	1.82 (0.58)
<i>Average</i>	1.00 (0.00)	1.00 (0.00)	0.20 (0.02)	0.15 (0.02)	0.85 (0.05)	0.92 (0.13)	1.04 (0.08)	1.09 (1.50)

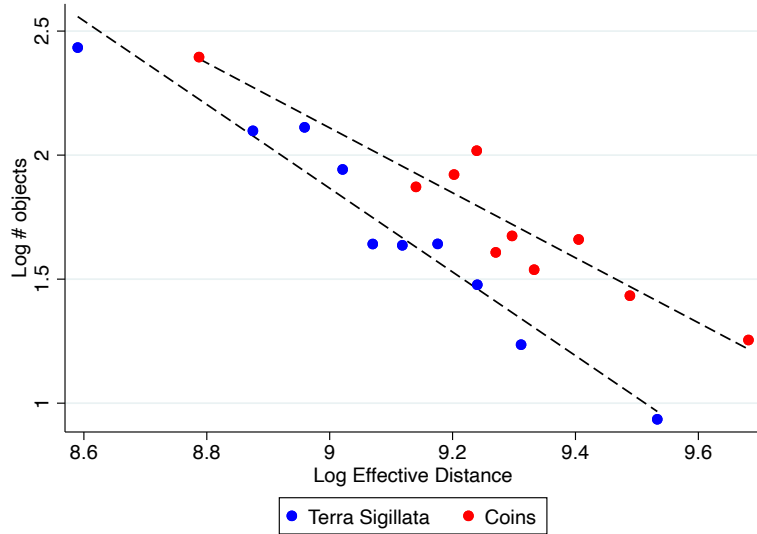
Notes: This table shows the levels (not logs) of all equilibrium variables we use to compute changes in real capita and its components in table 4. Columns 1 and 2 show real consumption per capita normalized to one on average within each period ($(X_n/p_n)/L_n$), for AD 460-620 and AD 700-900 respectively. Columns 3 and 4 show a measure of trade openness, imports as a share of consumption ($1 - \pi_{nn}$), for AD 460-620 and AD 700-900. Columns 5 and 6 show technology ($T_n^{1/\theta}$) for AD 460-620 and AD 700-900. And columns 7 and 8 show trade deficits, i.e. consumption relative to income ($\frac{X_n}{w_n L_n}$) for AD 460-620 and AD 700-900. Standard errors (in parentheses under each point estimate) are computed from re-estimating our model on 100 bootstrapped samples from our coin data.

Figures



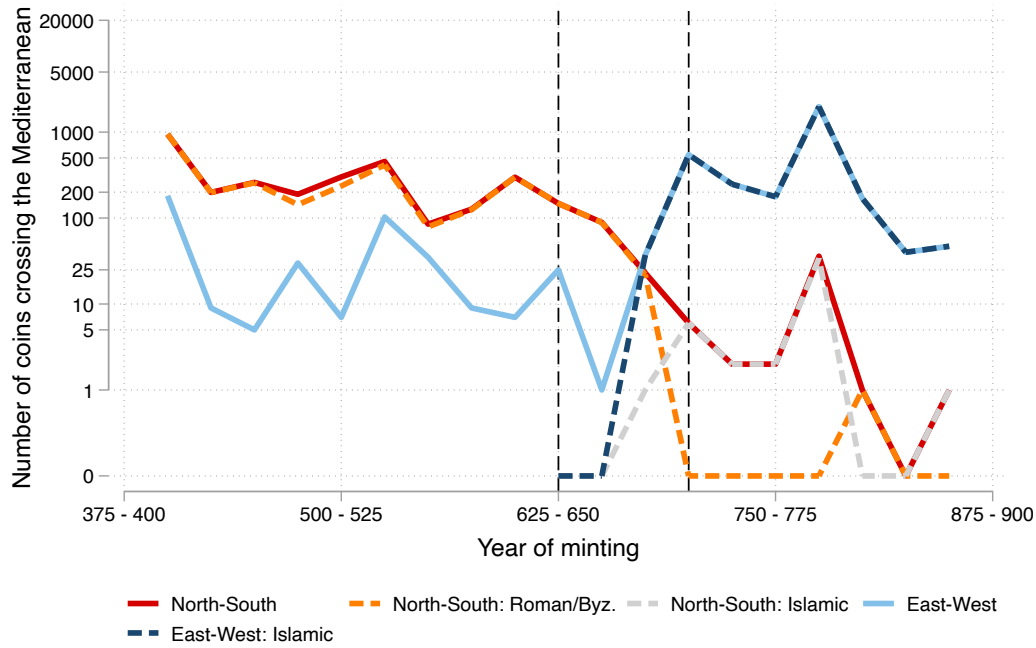
Appendix Figure A.1: Comparison with Circulation Hoards in [Banaji \(2016\)](#)

Notes: The left panel reproduces Figure 3b. The right panel shows the average share of coins in each 10-year age bin in the circulation hoards of [Banaji \(2016\)](#), Chapter 6, who reports the issuing emperors (but not mint dates) of the coins in these hoards. We draw mint dates uniformly from the ruling years of these emperors.



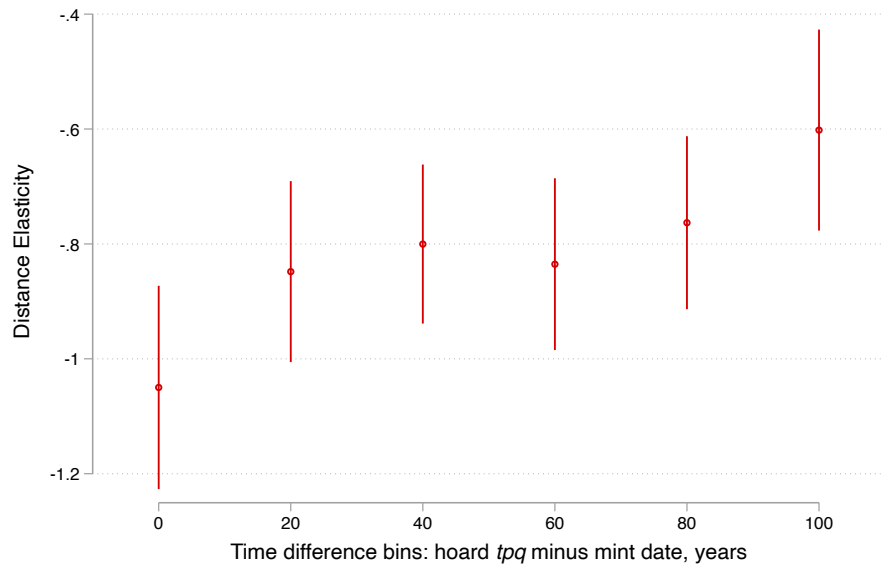
Appendix Figure A.2: Comparison with flows of West Roman Terra Sigillata ([Flückiger et al., 2022](#))

Notes: The figure shows a binscatter of the log number of objects flowing (either coins or number of Terra Sigillata) between two 0.5×0.5 degree cells, against the log effective distance between cells. Both are de-meaned by origin and destination location. Cell definitions and effective distances are from [Flückiger et al. \(2022\)](#). The coin data is restricted to hoards with tpq up to 450 and that lie within the aforementioned cells.



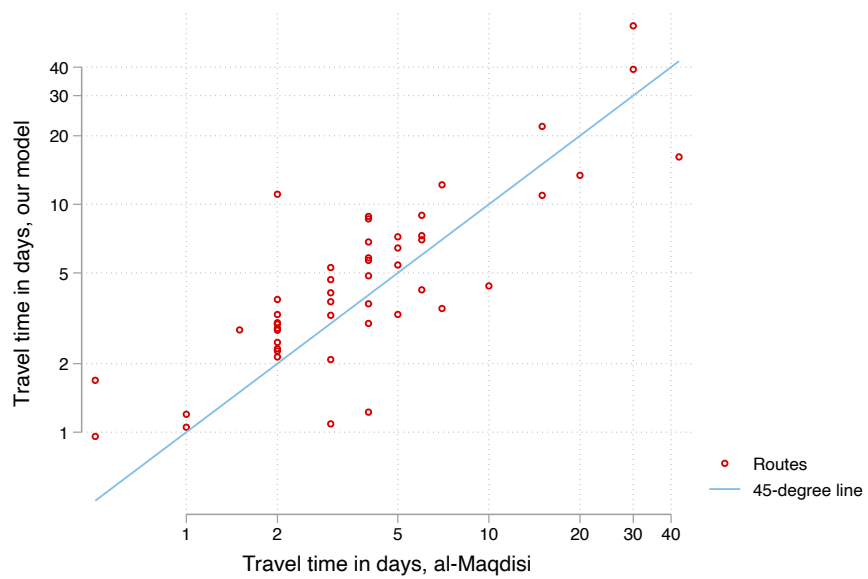
Appendix Figure A.3: Number of coins flowing across the Mediterranean

Notes: The figure shows the number of coins minted in the 25-year interval on the horizontal axis, that are minted on one side of the Mediterranean, and are found on the other. Flows include both directions. The north is defined to go from the Pyrenees to Byzantine Turkey, east from Byzantine Turkey to Egypt, south from Egypt to the Maghreb, and west from Maghreb to Aquitaine. Border regions are included in these definitions, so regions are partly overlapping.



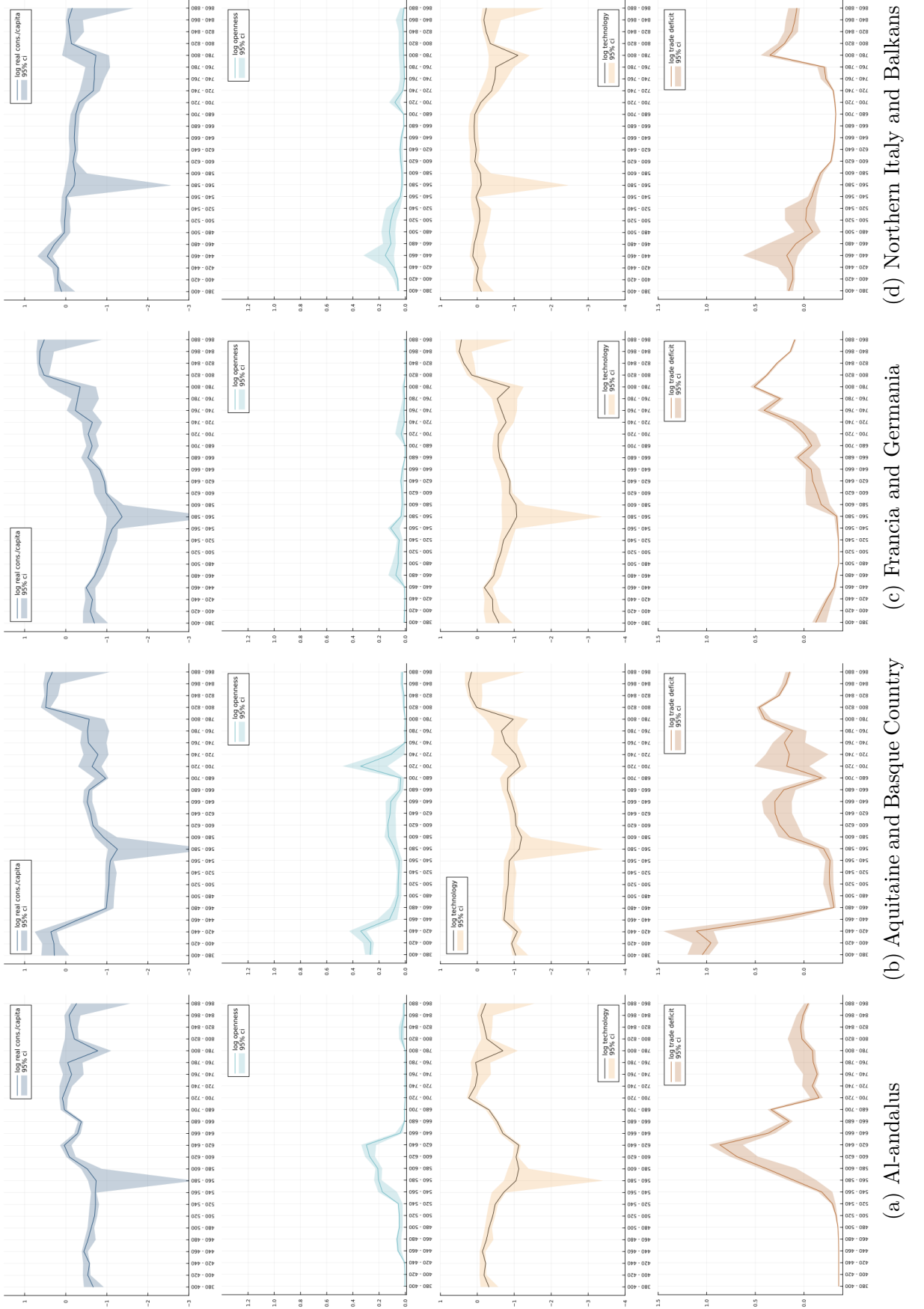
Appendix Figure A.4: The distance elasticity declines as coins age

Notes: The figure shows the distance elasticity estimates when estimating equation (A.2) using PPML.



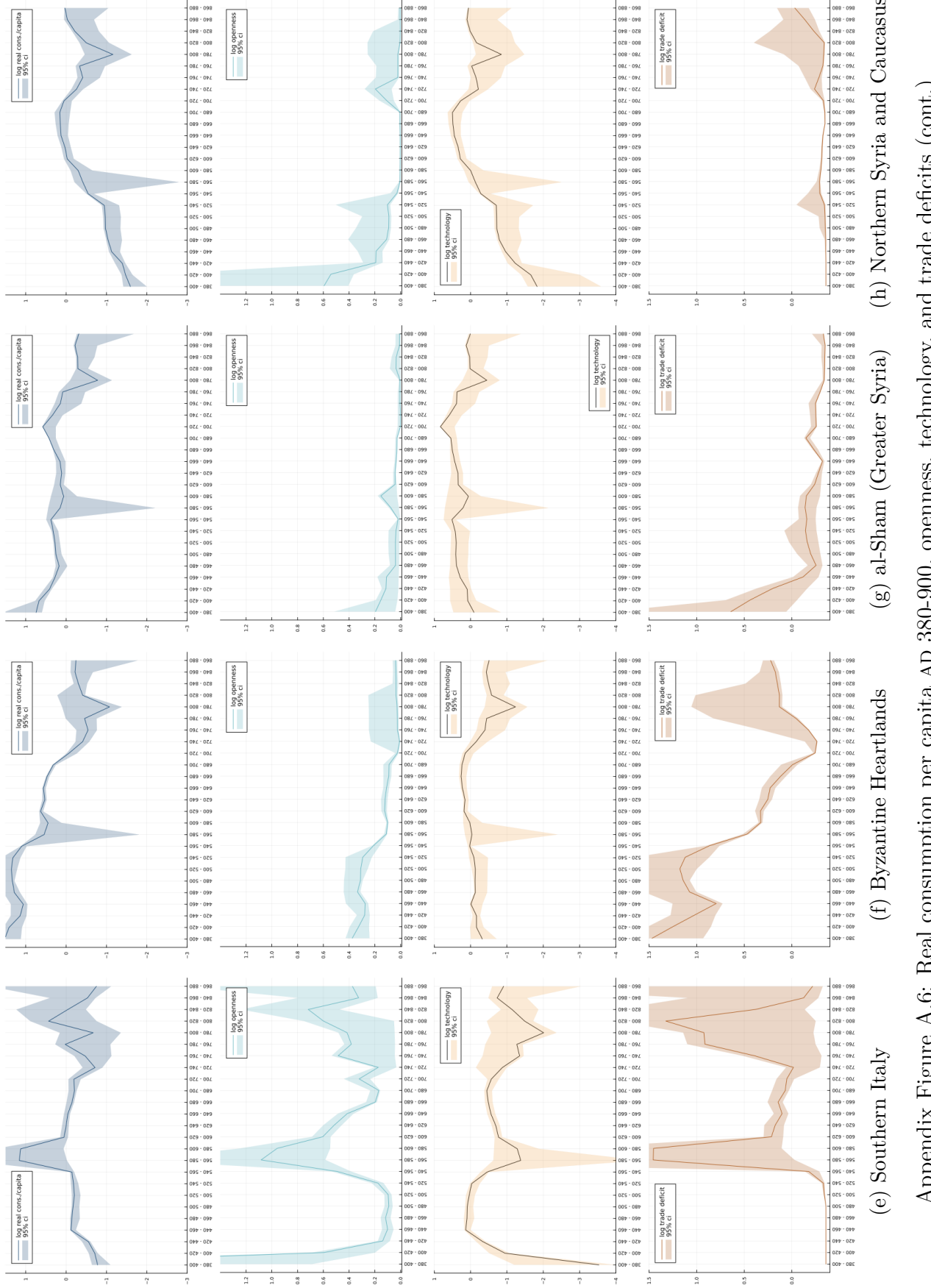
Appendix Figure A.5: Comparison of travel times, geo-spatial model versus Al-Muqaddasī (1994)

Notes: Each dot refers to a city-to-city connection for which Al-Muqaddasī (1994) lists the travel time in days. We exclude desert routes (where he reports travel times in nights or in watering stations, routes with cities cannot be found in al-Thurayya, as well as the route between Tahart and Fes, which he claims can be travelled in three days despite it being a distance of more than 600 kilometers (our model predicts 22 days).

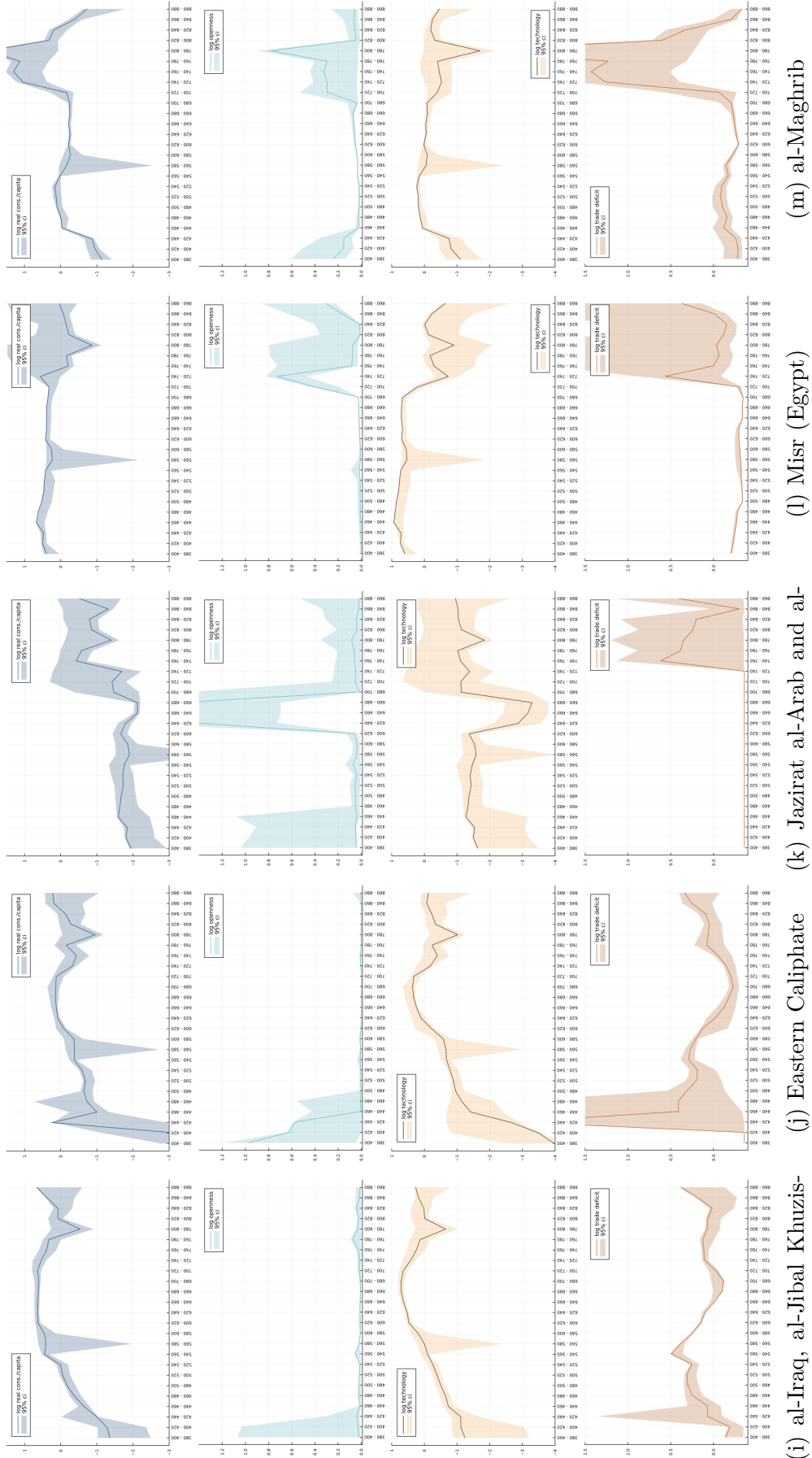


Appendix Figure A.6: Real consumption per capita AD 380-900, openness, technology, and trade deficits

Notes: This figure complements figure 9, showing for all 13 regions the time-series of (logged) real consumption per capita (panel a) from AD 380 to AD 900 for the Byzantine Heartlands and for Francia and Germania, and its partition into ‘openness’ (panel b), ‘technology’ (panel c), and ‘trade deficits’ (panel d) as in equation (20). The technical appendix provides details on the computation of each term, using the dynamic model in equations (4)-(6), (10), and the parameter estimates from (18)-(19). Units for technology are chosen such average real consumption per capita equals one for each period. 95% confidence intervals (shaded areas) are computed from fully re-estimating our model on 100 bootstrapped samples from our coin hoard data. Our estimates are imprecise for some periods because we have too few coins, as evidenced by the spikes of the confidence intervals.



Appendix Figure A.6: Real consumption per capita AD 380-900, openness, technology, and trade deficits (cont.)



Appendix Figure A.6: Real consumption per capita AD 380-900, openness, technology, and trade deficits (cont.)

References

- AL-MUQADDASĪ (1994): *Aḥsan al-taqāṣīm fi maṣarfat al-aqalīm* (*The Best Divisions for Knowledge of the Regions*), Garnet Publishing (transl. B.A. Collins).
- BANAJI, J. (2016): *Exploring the Economy of Late Antiquity: Selected Essays*, Cambridge University Press.
- FLÜCKIGER, M., E. HORNUNG, M. LARCH, M. LUDWIG, AND A. MEES (2022): “Roman transport network connectivity and economic integration,” *The Review of Economic Studies*, 89, 774–810.

B Coin hoard data

Our numismatic data consists of two datasets: first, the set of hoards from the current release of the *Framing the Late Antique and Early Medieval Economy* project (FLAME, 2023). FLAME is a large collaborative effort of historians and numismatists that records data on coin hoards around the Mediterranean and Europe from between AD 325 and AD 725. We use the most recent release (January 2023) which has data on about 1.7m coins belonging to more than 9,000 hoards. Since the temporal and spatial focus of our study does not entirely overlap with that of FLAME, we complement their data by constructing a hand-coded dataset on hoards between AD 700 and AD 900, and hoards with a heavier emphasis on near eastern coins. We describe the hand-collected data and FLAME’s data in turn.

B.1 Hand-collected data

We search the numismatic and archaeological literature for descriptions of coin hoards or coin finds with a *terminus post quem* (= date of the most recent content) of roughly between AD 700 and AD 950, that were discovered in Europe, North Africa, or the Middle East. For the sake of brevity we will refer to a single coin or a collection of coins that was found together in one place as a “hoard” (i.e. unless specifically mentioned, we do not distinguish between single finds, stray finds, mini-hoards, or full hoards). We exclude hoards that largely contain silver that was brought via the Viking route or that clearly have a Viking connection.⁴ We likewise exclude records from excavations, unless they are described as a hoard or constitute a set of coins that were found together in the same location (e.g. in the same room of an excavated building).

An (at least approximate) findspot must be known for a hoard to be of use in our analysis. For each hoard we record the latitude and longitude of its findspot. When the findspot is known only with a low level of precision (e.g. at the country or region level) we code this in a separate dummy variable. Importantly, we do not record coins in museums or collections that have unknown findspots. While we digitize many descriptions of hoards that are incomplete, we omit hoards of which no information on the vast majority of coins has been published.

For each coin (or group of coins with identical properties) in a hoard we record, if documented by the authors of the hoard catalogue:

- The mint where the coin was minted, or believed to have been minted. When a coin is believed to have been an imitation, we note this separately.
- A time interval (consisting of a start year and end year) during which the coin was minted or is believed to have been minted. For some coins, such as most Islamic dirhams, this information is imprinted on the coin. For others, we code this as the shortest time interval during which the coin could have been minted, taking into account the denomination of the coin, the ruler under whose authority it has been issued, as well as his/her dynasty, and other information about coin types (e.g. pre/post-reform coinage). When the coin has been dated through the regnal year of the ruler or in the Islamic calendar, we convert this to Gregorian calendar years.

Beyond the attributes above, we record denomination, material, and issuing rulers and dynasties (mostly with dating of the coins in mind). This information, if known, is typically furnished by the authors of hoard catalogues in the numismatic literature. We do not distinguish between fragments and entire coins.

The geocodes of the hoards and mints are only approximate. We code Nomisma IDs for the mints based on the proximity of the place of minting, not based on the dynasty, e.g. “Sicilliyah” (Sicily) can be also used for non-Islamic issue.

B.1.1 Hoards in the Near East and North Africa

Table B.5 shows the list of hand-coded hoards from the Near East and North Africa, along with references. These hoards consist mainly of Sasanian and/or Islamic coins, and sometimes Byzantine issue. We code approximate

⁴Among the list from Appendix 3 of McCormick (2001), these are the hoards in Britain, Scandinavia, and Schleswig-Holstein (Germany). We also digitized the 10th century Máramaros county hoard (Fomin and Kovács, 1987), but drop it as its content (consisting of many imitations, as well as dirhams from the Samarkand and al-Shash mints) indicate that it was clearly brought in from the east.

mint locations based on the proposals in the literature, typically giving preference to the suggestions of the authors of the original hoards.

A couple of notes on specific hoards:

- We digitize the Umm-Hajarah hoard based on the description by al 'Ush (1972a) but follow Noonan (1980) in treating the isolated Seljuk coin that Al-'Ush dates to 689-690 AH as not belonging to the hoard.
- We digitize Hoge (1997)'s description of a hoard from "North Africa (or Spain?)", and assign Kairouan as approximate location (and note that the precise location of the hoard is immaterial to our exercise). We treat the Safavid dinar that is 650 years younger than the other coins (Hoge: "no doubt added to the other pieces 'in trade'") as extraneous to the hoard.

B.1.2 Islamic hoards in Spain and France

Tables B.6 and B.7 show the hand-digitized hoards from Islamic Spain (al-Andalus) and Islamic coin finds from southern France.

B.1.3 Other Islamic and Byzantine hoards in Europe

We digitize the hoards, mini-hoards, and stray finds from McCormick (2001)'s survey of Arab and Byzantine coins in Europe (Appendix 3) between 668 and 900. We add those to our dataset, except when already covered in our other sources. We update hoard descriptions for which newer catalogues are available.⁵ Finally, we exclude the contested Odoorn/Zuidbarge (1859–60) hoard, as the identity of it as a single hoard is not clear, some of the coins had been converted into jewellery, and the contents are not well described.⁶

B.1.4 Byzantine hoards

The hoards reported in the corpora by Pennas (1991), Füeg (2007), and Nikolaou and Touratsoglou (2019) form the basis of our collection of Byzantine hoards (the corpus on earlier finds by Morrisson et al. (2006) is mostly already incorporated into FLAME). Information on particular regions come from Mirnik (1981) (Balkans), Arslan (2005) (Italy), Kovács (1989) (Hungary), and Wołoszyn (2009) (Central Europe). Hoard catalogues typically refer to collection catalogues (Sabatier, 1862, Wroth, 1908, Grierson, 1968, 1973) which we use to retrieve mint date intervals and likely mints.⁷ We exclude coin finds from running excavations, unless the coins were found as individual parcels in a specific location. Tables B.8 and B.9 show our hand-coded byzantine hoards.

B.1.5 Carolingian hoards

We follow Simon Coupland's *Checklist* (Coupland, 2011a, 2014, 2020) and digitize hoards and finds primarily based on the corpora presented by Völckers (1965), Duplessy (1985), and Haertle (1997), giving priority to more recent descriptions. Tables B.10 to B.14 show details. We follow the mint codings of Louis the Pious' *Christiana religio* coins given by Coupland (2011b). As mentioned above, we exclude the contested Odoorn/Zuidbarge hoard.

B.2 FLAME

FLAME records their data in three different tables: coin finds, coin groups, and mints. In the coin find table each observation is a find that contains one or more coin groups; in the coin group table each observation is a set of coins with common recorded attributes (and linked to the coin find ID), including a mint and an interval for the year of minting. In the mint table each observation is a mint, and the mint name string allows these to be matched to coin groups. Mints and coin finds are geocoded.

⁵A35 (Steckborn): Ilisch (2005), A8 (Cagliari): Saccoccia (2005), who also mentions an Aghlabid semi-dirham of Muhammad I found in Crotone, Sicily. We update A28 (Porto Torres, Sardinia) based on the number and datings reported in Füeg (2007)'s corpus, likewise the dates from A34 (Reno River).

⁶See Coupland (2011a) for a discussion of these issues.

⁷For a large part of the time interval that is not covered by FLAME, Byzantine gold and silver coins are believed to have been exclusively issued at Constantinople (Grierson, 1968).

The records in FLAME thus include a superset of the attributes in the hand-coded data above, except (i) the material of the coin, which we code based on the denomination; (ii) the weight and dimensions of the coins, which are sometimes (but not systematically) coded in the comments. We convert the FLAME data to the same structure as our handcoded data, including the following cleaning steps:

- A small number (6) of coin groups has a start year that's after the end year; we switch those around.
- FLAME contains start and end dates for the coin find itself. For a small number of coin groups the end date of the coin find falls in between the start and end dates of the coin group. This is often the case when very broad ranges have been given for the coin group, and so we truncate the coin group interval at the end date of the find.
- For Sasanian coins, we adhere to the mint codings in FLAME. A number of coins report the mint abbreviation but not the mint, we code and locate them analogously to how we coded them in the hand-coded coins (see below).
- A number of coin groups record a mint string that is not included in FLAME's mint file. We code Nomisma ID's for those mints, wherever possible.
- A large fraction of FLAME coins don't have mints or dates: often large hoards are not recorded by coin (just the total number of coins). Out of 1.7m coins, about 340k have mint and dates.

B.3 Locating mints

For FLAME data, we follow the attribution of mint locations done by the authors of the respective FLAME entries. For hand-collected data, we attempt to map the hand-coded mints to [Nomisma \(2023\)](#) IDs for the mints (`nmo:Mint`). Whenever a geocode for a mint is not available in Nomisma, or whenever the mint is not represented in Nomisma, we hand-code the geocodes. These geocodes should only be regarded as approximate and with a degree of precision required for our particular application in mind. Table B.3 shows the mints we add to Nomisma, along with our codings, and Table B.4 shows the codings for existing Nomisma mints without geocodes.

B.3.1 Sasanian mints

The location of Sasanian mints and the identification of Sasanian mint signatures are contested. We generally follow the reading of the original hoard descriptions, except in situations where these are dated and the literature nowadays prefers different readings. Regarding the approximate location of the mints, we decided to code the approximate location for most signatures following the consensus in the literature; in some cases where the literature only agrees up to the region we chose Nomisma IDs from mints of that region. As with the other codings, the Nomisma IDs should only be seen as approximating the location of the mint, and do not carry any information on dating. Table B.16 summarizes our signature codings with their approximate mint locations.

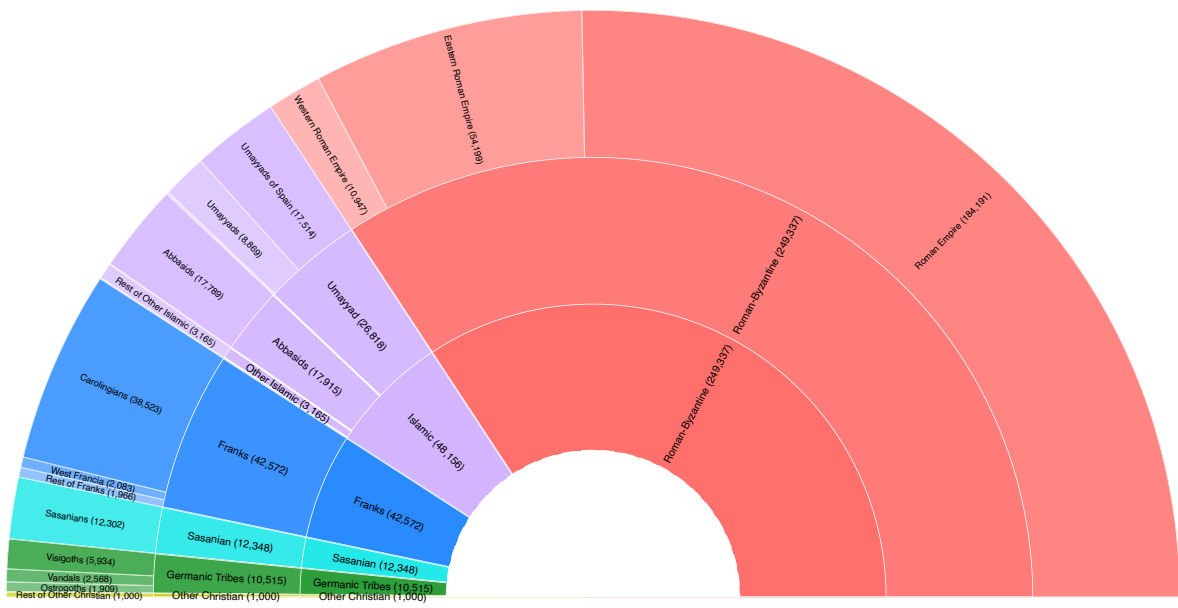
B.4 Political entities and the geography of hoards and mints

B.4.1 Dynasties/Empires

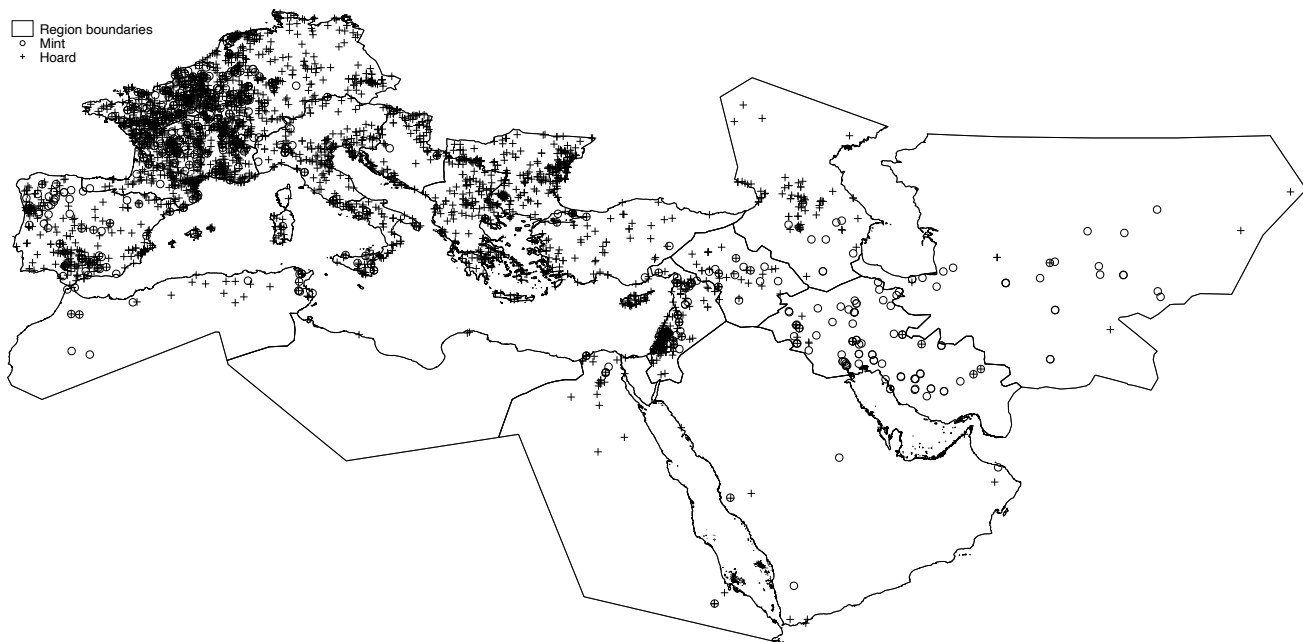
We record dynasties/empires through the `dynastyname` field of FLAME data, and an equivalent field of the hand-coded data. We aggregate these to 10 more aggregate (“level 1”) dynasties/empires, and seven most aggregate (“level 2”) dynasties/empires. Figure B.1 shows the breakdown of recorded dynasties in our final sample.

B.4.2 Location of hoards and mints

Figure B.2 show the location of mints and hoards of our final dataset. Only locations corresponding to coins that were minted after AD 400 are shown. Figure B.3 shows details for western Europe and the eastern Mediterranean.

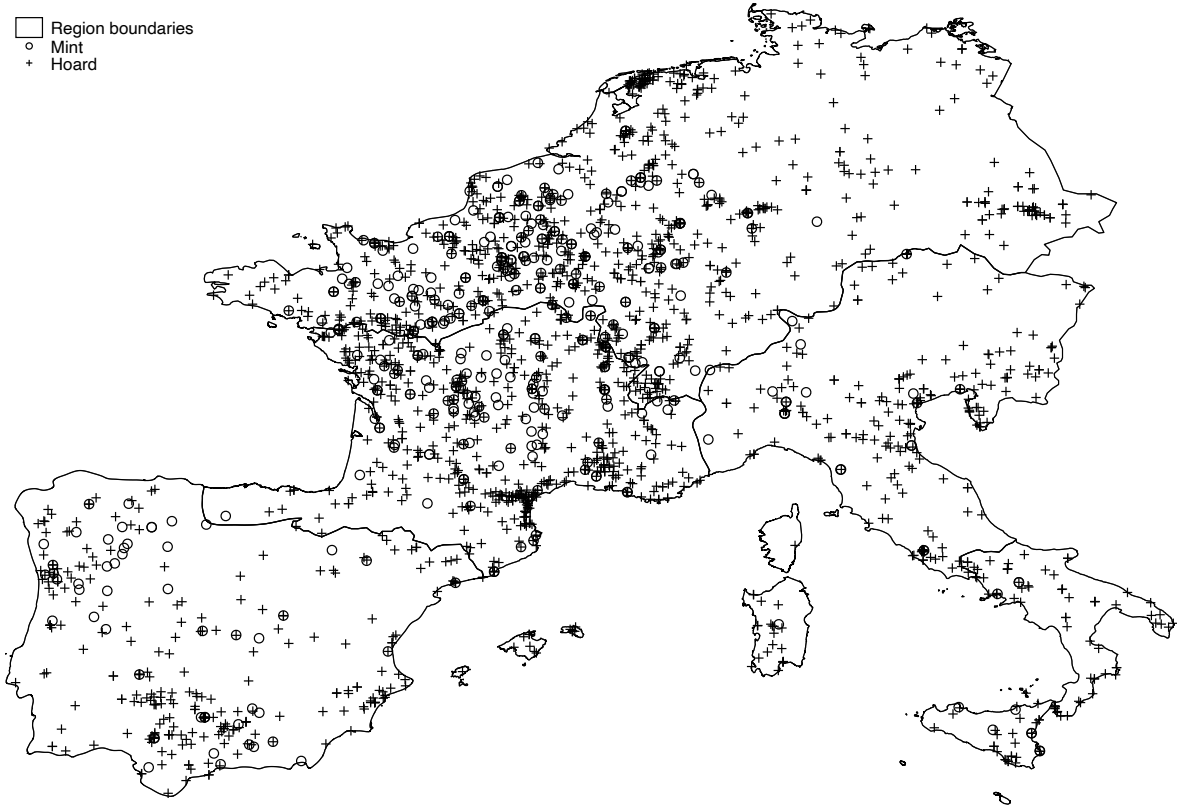


Appendix Figure B.1: Dynasties/Empires

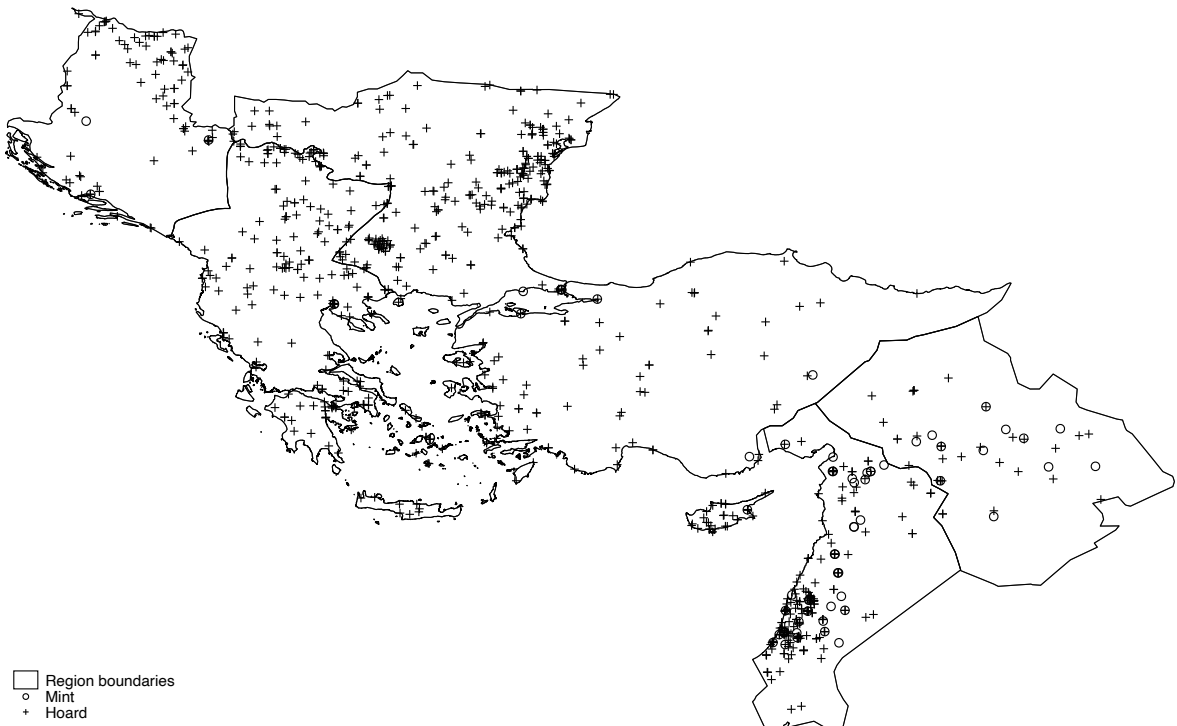


Appendix Figure B.2: Mints and Hoards

□ Region boundaries
○ Mint
+ Hoard



(a) Western Europe



(b) North-eastern Mediterranean

Appendix Figure B.3: Mints and Hoards: Details

Note: Maps show coins minted after AD 400

B.5 Tables and references

Appendix Table B.1: Summary statistics: Coins

	count	mean	sd	min	p10	p50	p90	max
Has mint date interval	494,311	0.85	0.36	0	0	1	1	1
Has mint location	494,311	0.55	0.50	0	0	1	1	1
Has mint location and date interval	494,311	0.55	0.50	0	0	1	1	1
Mint date interval, years	419,008	29.48	41.66	-19	1	20	58	432
Mint date interval, start year	419,008	465.45	186.70	34	306	375	815	949
Mint date interval, end year	419,008	494.93	184.48	79	333	395	840	950
Age at tpq	419,008	59.00	81.54	0	6	29	154	805
Has material	494,311	0.98	0.15	0	1	1	1	1
Coin is gold	494,311	0.07	0.25	0	0	0	0	1
Coin is silver	494,311	0.18	0.38	0	0	0	1	1
Coin is copper/bronze	494,311	0.74	0.44	0	0	1	1	1
Has denomination	494,311	0.99	0.10	0	1	1	1	1
Has some empire/dynasty information	494,311	0.69	0.46	0	0	1	1	1
Geodesic distance mint to hoard, km	273,343	769.74	784.00	0	59	503	1,631	6,302

Notes: Sample consists of all coins from hoards with tpq between 325 and 950. “Age at tpq” is defined as tpq of the hoard minus the midpoint of the mint date interval.

Appendix Table B.2: Summary statistics: Hoards

	count	mean	sd	min	p10	p50	p90	max
Hoard tpq	5,503	590.85	148.14	325	376	578	782	950
Number of coins in hoard	5,503	89.83	823.96	1	1	1	81	43,867
Fraction of coins with mint date interval	5,503	0.98	0.12	0	1	1	1	1
Fraction of coins with mint location	5,503	0.87	0.27	0	0	1	1	1
Fraction of coins with mint date interval and mint location	5,503	0.86	0.28	0	0	1	1	1
Average mint date interval	5,503	23.24	32.66	0	1	11	81	377
Average age of coins at tpq	5,503	25.44	41.76	0	0	10	50	522
Fraction of coins with material	5,503	0.99	0.08	0	1	1	1	1
Fraction of coins that are gold	5,503	0.29	0.45	0	0	0	1	1
Fraction of coins that are silver	5,503	0.15	0.35	0	0	0	1	1
Fraction of coins that are bronze	5,503	0.55	0.49	0	0	1	1	1
Fraction of coins with denomination	5,503	0.99	0.08	0	1	1	1	1
Fraction of coins with empire/dynasty information	5,503	0.80	0.38	0	0	1	1	1
Average distance of coins from mint, km	5,400	684.90	610.64	0	88	533	1,462	6,124

Notes: Sample consists of all coins from hoards with tpq between 325 and 950. “Age at tpq” is defined as tpq of the hoard minus the average coins’ midpoint of the mint date interval.

Mint	id	Location	Latitude	Longitude	Notes
Abarqubadh	abarqubadh		31.28027	47.49266	"This mint was in the district of Khusra-shadh Bahmân (the district of the Tigris) in Irâq, between Wâsit and al-Basra and near the border with Khuzistân." Lloyd (2023)
Adurbadagan al Hashimiyyah	adurbadagan al-hashimiyyah	Ganzak Kufa	37.0123 32.05114	46.2019 44.44017	Sasanian mint (AT) Rare Abbasid mint during al-Mansur's reign, situated close to Kufah (138-146 AH).
al Rahba Arrajan	al-rahba arrajan	Mayadin	35.005 30.65388	40.4235 50.27472	A mint in Syria, on the Euphrates "[Bizamqubadh] was an alternative name for Arrajân in Fars, and also appears to have struck Arab-Sasanian issues." Lloyd (2023)
Hulwan	hulwan		34.465	45.855	"This mint-name is that of a district (astân) in Irâq, which covered an area to the north-east of Baghdad. Le Strange notes that this district was also known as Shâd Firûz - presumably its former Sasanian name. The town of Hulwân itself evidently lay just over the border in Jibâl province, although at this period it appears to have been included with 'Irâq for administrative purposes." Lloyd (2023)
Madinat Elvira Mah al Basrah	madinat_elvira mah-al-basrah	Nihavand, Iran	37.23105 34.18879	-3.70848 48.37046	The archaeological site of Madinat Ilbira. "The term is the Arabic name for Nihavand." (British Museum x107840)
Mah al Kufah	mah-al-kufah	Dinawar, Iran	34.583333	47.43333	"Mah al-Kufah = Dinawar (sometimes incorrectly written Daynawar) in the middle ages was one of the most important towns in Djibal (Media); it is now in ruins. The exact location is 34 degrees 35 minutes Lat. N. and 47 degrees 26 minutes E. Long. (Greenwich)." Lockhart (2012)
Masabadhan	masabadhan		33.52303	46.86539	A district with capital al-Sirawan; the location of al-Sirawan is from Cornu (1983) 's atlas.
Maysan Panjshir Rev-Ardashir	maysan panjshir rev-ardashir	Naysan Panjshir Valley Bushehr	30.8093 35.254095 28.9119	47.5628 69.456014 50.8367	Sasanian mint Maysan (MY) Panjshir Valley, modern-day Afghanistan Sasanian mint (LYW/ LYWARTHST/KWN LY-W/GNC LYW); the location is from FLAME
Roda Sarakhs	roda sarakhs	Sarakhs, Iran	42.26478 36.5449	3.17887 61.1577	A carolingian mint in Rosas, Spain "A town in Khurâsân located roughly midway between Marw and Abrashahr. Sarakhs lay on the eastern bank of the Mashhad river, about forty or fifty miles north of its confluence with the Herât river." Lloyd (2023)
Uman	oman	Oman	23.51234	58.27000	Lloyd (2023) : "Modern Oman on the Persian Gulf."

Appendix Table B.3: Manual mint codings I: new mints

Nomisma ID	Nomisma Note	Latitude	Longitude	Note
al-Abbasiyah	"Earfly Abbasid site in North Africa"	35.62183407	10.18089991	According to Abdul Wahab (2012) , three miles south-east of Kairouan.
al-Furat	"In the district of Shadh Bahman in Iraq, but its exact location unknown. Klat, 16."	30.53269083	47.87593421	Geocodes based on Fig. 11 in Morony (1982) .
al-Madinat Mutawakkiliyah	al- "al-Madinat al-Mutawakkiliyah is just north of Sammara and was built by the Abbasids."	34.2621862	43.85500034	Close to Samarra, Iraq
al-Manadhir	"The name of two districts, with their chief-towns, named Greater Manadhir & Little Manadhir in Khuzistan, Iran"	31.97753445	48.69644554	Lloyd (2023) : "Manâdhîr was a district within the province of Khuzistân, situated between the Dizfûl and Dujayl rivers above their confluence north of Ahwâz. It was apparently divided into two parts named Greater and Little Manâdhîr, each containing a chief town with the same name."
al-Mubarakah (Ab-basid)	"Some place in North Africa"	36.30565739	10.13850323	Unknown location, coding it to modern-day Tunisia
al-Samiyah	"Al-Samiya was in the Shatt al-Arab area of lower Iraq."	30.6617666	47.78548511	Coding to Shatt al-Arab.
Bihqubadh af-Asfal	"Lower Bihqubach (sic) in Iraq on the Euphrates"	31.56718959	45.22725183	Lloyd (2023) : "The three districts of Upper, Middle and Lower Bihqubâdh were located in 'Iraq to the west of the Euphrates. Bihqubâdh is taken from the Persian meaning "the good land of king Qubâdh. Al-Asfal means 'the lower,' and covered the land next to the Euphrates where it entered the Great Swamp." Coordinates based on Fig. 8 of Morony (1982) .
Dastawa Ma'din Bajunays	"South of Qazvin" "Province north of Lake Van"	35.75554989 40.223509	50.08839336 43.8355181	Location very approximate in western Armenia.
Mani	Klat is uncertain of its location although the prefix Mah occurs in older names for Dinavar & Nihevand. Quarter of Jibal. Klat"	34.38582341	47.97904114	Lloyd (2023) puts it either at Mah al Basrah (Nihavand) or Mah al Kufa (Dinavar). Our chosen geocode is halfway between the two.
Nahr Tira	"Exact location on the river or canal of the same name in Khuzistan not know. Klat, p.. 18"	30.8755	49.7131	From FLAME.
Qumis	"A small province which stretches along the foot of the Great Alburz chain of mountains. Klat, p. 17."	35.96088616	54.03571139	Wikipedia "Qumis (region)"
Surraq	"Surraq or DAWRAQ (or Dawraq al-Fors), name of a district (k 'ra; Moqaddasf', pp. 406-07), also known as Sorraq, and of a town that was sometimes its chef-lieu in medieval Islamic times."	30.65094882	48.67463446	Coding to Shadegan, Iran.
Tabaristan	"Tabaristan, also known as Tapuria, was the name of the former historic region in the southern coasts of Caspian Sea roughly in the location of the northern and southern slopes of Elburz range in Iran."	36.5656	53.0588	From FLAME
Tudghah	"Unknown location in Morocco"	31.523	-5.5313	al 'Ush (1982) identifies it with "Todr'a", and cites Renou (1846) (incorrectly as authored by "Lavoix") saying that it was located fourty kilometers west of Sijilmasa, at a river of the same name. That would place it close to Tinghir, Morocco.

Appendix Table B.4: Manual mint codings II: geocoding existing Nomisma mints

Hoard Name	Date	# Coins described	Reference	Location	Latitude	Longitude
Abu Saida	ca. 721	15	Royal Numismatic Society (1975)	Qaryat Abū Ṣaydā as Ṣaghīrah, Iraq	33.924	44.761
Afaq	773-932	1674	Gachet (1993)	Afak, Iraq	32.064	45.247
Afghanistan	86-112 AH	131	Album (1971)	Afghanistan	33.000	66.000
Agrigento	699-828	370	Lagumina (1904)	Agrigento, Italy	37.311	13.577
Al Raqa	698-750	1187	Sears (2000)	Ar Raqqah, Syria	35.953	39.008
Al Wajh		35	Hakiem (1977)	Al Wajh, Saudi Arabia	26.246	36.452
Al-Khobar	tpq 784/85	42	Noonan (1980)	Khobar, Saudi Arabia	26.279	50.208
Amman	AH 79-125	12	Kirkbride (1951)	Amman, Jordan	31.955	35.945
Āmūdā I	tpq 874	646	Ilisch (1990)	‘Āmūdā, Syria	37.104	40.930
Āmūdā II	779-941	643	Ilisch (1990)	‘Āmūdā, Syria	37.104	40.930
Awarta (Nablus I)	602-685	29	Dajani (1951)	‘Awartā, Palestine	32.161	35.284
Bab Tuma	tpq 748	854	Gyselen and Kalus (1983)	Damascus, Syria	33.510	36.291
Babylone, Egypt	157 AH - 241 AH	114	Jungfleisch (1949)	Cairo, Egypt	30.063	31.250
Buseyra	769-943	3108	Al Chomari (2020)	Al Buṣayrah, Syria	35.156	40.427
Capernaum		288	Wilson (1989)	Kfar Nahum, Israel	32.881	35.575
Damascus	548-736	3815	al 'Ush (1972b)	Damascus, Syria	33.510	36.291
Damascus	679-721	546	al 'Ush (1954-1955)	Damascus, Syria	33.510	36.291
Denizbaci	tpq 811	2496	Artuk (1966)	Denizbaci, Turkey	37.139	38.390
Diyarbakir	802-902	224	Ilisch (1979)	Diyarbakir, Turkey	37.914	40.217
En Nebk	tpq 747	102	Royal Numismatic Society (1977)	An Nabk, Syria	34.024	36.728
Gazira	3rd to 9th century	2820	Gyselen and Nègre (1982)	Al Jazīrah, Iraq	36.000	42.000
Godhlaniya		127	American Numismatic Society (2023)	Syrian Arab Republic, Syria	35.000	38.000
Hamah	tpq 950	214	Ilisch (1990)	Hamāh, Syria	35.132	36.758
Huszt		368	Fomin and Kovács (1987)	Khust, Ukraine	48.172	23.298
Iran 1970	tpq 820	668	Noonan (1980)	Islamic Republic of Iran, Iran	32.000	53.000
Isfahan	777-936	582	Lowick (1975)	Isfahan, Iran	32.652	51.675
Jarash		36	Treadwell and Rogan (1994)	Jarash, Jordan	32.281	35.899
Jazira (Illisch)	tpq 886	48	Ilisch (1990)	Al Jazīrah, Iraq	36.000	42.000
Kerman	about 632-651	43	Heidemann et al. (2014)	Kerman, Iran	30.283	57.079
Khdir Elias	tpq 1014	2865	Al-Naqshbandi (1954)	Republic of Iraq, Iraq	33.000	44.000
Khorasan	705-774	196	Hebert (1966)	Mashhad, Iran	36.298	59.606
Khirbat al-Minya	716-734	2	Schneider (1952)	Horbat Minnim, Israel	32.865	35.536
Kufah	tpq 808/09	178	Noonan (1980)	Kufa, Iraq	32.051	44.440
Marv	tpq 815	855	Khodzhanizayev and Treadwell (1998)	Mary, Turkmenistan	37.594	61.830
Near Fez		36	Royal Numismatic Society (1978)	Fès, Morocco	34.033	-5.000
Nippur (Bates)	704-794	76	Bates (1978)	Atṭālā Nafar, Iraq	32.136	45.221
Nippur (Sears)	597-743	97	Sears (1994)	Atṭālā Nafar, Iraq	32.136	45.221
North Africa (Spain?)	tpq 860	87	Hoge (1997)	Kairouan, Tunisia	35.678	10.096
Orif, Nablus	691-742	19	Ma'ayeh (1962)	Urif, Palestine, West Bank	32.159	35.224
Ouenza	789-798	12	Troussel (1942)	Ouenza, Algeria	35.953	8.129
Qamishliyyah	tpq 816	1519	Gyselen and Kalus (1983)	Al Qāmishlī, Syria	37.052	41.231
Ra's al-Khaimah	921-975	43	Lowick and Nisbet (1968)	Ras Al Khaimah City, UAE	25.790	55.943
Sinaw	589-841	948	Lowick (1983)	Sināw, Oman	22.501	58.030
Tabaristan	about 718-760	810	Malek (1996)	Mazandaran Province, Iran	36.250	52.333
Tiflis	ca. 280-330 AH	112	Bartolomei (1857)	Tbilisi, Georgia	41.694	44.834
Umm Hajarah	tpq 808/09	408	al 'Ush (1972a)	Umm Hajarah, Syria	36.195	41.074
Utaifyah	154-193 AH	294	al Bakri (1973)	Baghdad, Iraq	33.341	44.401
Volubilis	tpq 125 AH (742)	232	Eustache (1956)	Oualili, Morocco	34.073	-5.555
Yarubiyah	tpq 815/816	1415	American Numismatic Society (2023)	Al Ya'rubiyyah, Syria	36.811	42.062
Zahu/Zakho	tpq 808-9	3306	Al-Naqshbandi (1949, 1950, 1951, 1952)	Zaxo, Iraq	37.149	42.686

Appendix Table B.5: Near East and North Africa Hoards

Hoard name	Date	# Coins described	Reference	Location	Latitude	Longitude	
Alcaudete	698-734	14	Cano Ávila (1989)	Alcaudete	N 37° 35' 27"	W 4° 4' 56"	
Algeciras	710-727	29	Canto García and Martín Escudero (2009)	Algeciras	N 36° 7' 59"	W 5° 27' 1"	
Alhama	770-876	459	Codera y Zaidín (1892)	Alhama	N 37° 0' 24"	W 3° 59' 22"	
Arrabal Occidental	929-1021	373	Canto García et al. (2020a)	Cordoba	N 37° 53' 29"	W 4° 46' 21"	
Azanuy	699-733	6	Codera y Zaidín (1913)	Azanuy	N 41° 59' 10"	E 0° 18' 58"	
Badajoz	927-1011	99	Prieto (1934)	Badajoz	N 38° 52' 40"	W 6° 58' 14"	
Baena	699-754	160	Martín Escudero (2001)	Baena	N 37° 39' 22"	W 4° 20' 4"	
Barrio de los Olivos Borrachos	941-1004	165	Marcos Pous and Vicent Zaragoza (1992)	Cordoba	N 37° 53' 29"	W 4° 46' 21"	
Benferri	941-958	12	Doménech Belda (1997)	Benferri	N 38° 8' 28"	W 0° 57' 43"	
Bormujos	929-965	11	Cano Ávila (2016)	Bormujos	N 37° 21' 41.9"	W 6° 06' 38.1"	
Calle San Jose	936-950	16	Doménech Belda (1997)	Xàtiva	N 38° 59' 25"	W 0° 31' 6"	
Calle San Pedro	967-1031	19	Canto García and Jabłońska (2019)	Murcia	N 37° 59' 13"	W 1° 7' 48"	
Calle Santa Julia	929-1012	263	Segovia Sopo (2014)	Mérida	N 38° 54' 58"	W 6° 20' 37"	
Campo de la Verdad	775-912	176	Martín and Martín (2006)	Cordoba	N 37° 53' 29"	W 4° 46' 21"	
Carmona	698-753	146	Canto García and Escudero (2012)	Carmona	N 37° 28' 17"	W 5° 38' 46"	
Castillejos de Quintana	933-1010	39	Cravioto (2016)	Castillejos de Quintana	N 36° 46' 58.7"	W 4° 41' 30.9"	
Castro Marim	788-885	53	Rodrigues Marinho (1995)	Castro-Marim	N 37° 13' 14"	W 7° 26' 36"	
Cerro da Villa	831-900	239	Heidemann et al. (2018)	Cerro da Villa	N 37° 4' 48"	W 8° 7' 13"	
Crevillent	770-1269	34	Doménech Belda and Treliš (1990)	Crevillent	N 38° 14' 59"	W 0° 48' 35"	
Cihuela	912-1016	296	Navascués y de Palacios (1961a)	Cihuela	N 41° 24' 26"	W 1° 59' 59"	
Consuegra	835-1010	173	Martín Escudero (2011)	Consuegra	N 39° 27' 44"	W 3° 36' 28"	
Cordoba I	817-1010	25	Navascués y de Palacios (1961b)	Cordoba	N 37° 53' 29"	W 4° 46' 21"	
Cordoba II	933-953	328	Navascués y de Palacios (1958)	Cordoba	N 37° 53' 29"	W 4° 46' 21"	
Cordoba III	933-1021	379	Navascués y de Palacios (1958)	Cordoba	N 37° 53' 29"	W 4° 46' 21"	
Cordoba IV	708-796	119	Canto García (1988)	Cordoba	N 37° 53' 29"	W 4° 46' 21"	
Cova del Randerro	768-835	54	Doménech Belda (1997)	Pedreguer	N 38° 47' 35"	E 0° 2' 2"	
Cuba	932-1010	9	Martín Escudero (2011)	Cuba	N 38° 10' 24"	W 7° 53' 46"	
Domingo Perez	767-865	367	Martín and Martín (2002)	Domingo Pérez	N 37° 29' 45"	W 3° 30' 33"	
Elche	841-1173	316	Doménech Belda (1992)	Elche	N 38° 15' 43"	W 0° 42' 3"	
Electromecanicas I	941-1005	169	Marcos Pous and Vicent Zaragoza (1992)	Cordoba	N 37° 53' 29"	W 4° 46' 21"	
Electromecanicas II	928-1016	102	Marcos Pous and Vicent Zaragoza (1992)	Cordoba	N 37° 53' 29"	W 4° 46' 21"	
El Pedroso	928-1021	144	Cano Ávila and Martín Gómez (2006)	Hacienda Montegil, El Pedroso	N 37° 43' 51.9"	W 5° 51' 39.8"	
El Pedroso III	832-1021	144	Cano Ávila and Gómez (2008)	El Pedroso	N 37° 51' 0"	W 5° 46' 0"	
El Rebollar	810-818	5	Salido Domínguez et al. (2020)	Boalo	N 40° 42' 57"	W 3° 54' 59"	
Finca la Marquesa	941-1036	246	Doménech Belda (1997)	Montilla	N 37° 36' 07.2"	W 4° 37' 11.7"	
Fontanar	941-977	764	Canto García and Martín Escudero (2007)	Cordoba	N 37° 53' 29"	W 4° 46' 21"	
Fuente de Cantos	837-883	15	Segovia Sopo (2006)	Fuente de Cantos	N 38° 15' 0"	W 6° 18' 0"	
Hospital Militar	970-1032	23	Martín Escudero (2003)	Zaragoza	N 41° 39' 21"	W 0° 52' 38"	
Huesca	710-756	100	Martín Escudero (2012)	Huesca region	N 37° 39' 56.1"	W 4° 23' 41.6"	
Izcar	778-886	50	Ariza Armada (1988)	Cortijo de Izcar	N 37° 15' 27"	W 4° 18' 30"	
Iznajar	768-912	1047	Canto García and Marsal Moyano (1988)	Iznajar	Jaen region	N 37° 19' 14"	W 6° 46' 21"
Jaen	711-713	4	González García and Martínez Chico (2017)	Jerez de los Caballeros	N 38° 2' 15"	W 1° 25' 57"	
Jerez de los Caballeros	770-782	277	Canto García (2019)	La Almagra	36°55'13.7"N	4°23'23.7"W	
La Almagra	820-822	7	Museo Arqueológico de Murcia (2014)	Cerro la Fuensanta	N 37°19'17.5"	W 5°13'27.6"	
La Fuensanta	770-812	18	Cravioto and Ayala (1995)	La Lantejuela	N 37° 29' 10"	W 5° 58' 51"	
Lantejuela	773-887	175	Ruiz Asencio (1967)	La Rinconada	N 40° 15' 44"	W 4° 51' 30"	
La Rinconada	770-912	315	Cano Ávila and Martín Gómez (2005)	Gavilanes	N 38° 55' 10"	W 0° 7' 9"	
Las Torres	757-976	18	Martínez Enamorado (2004)	Oliva	N 41° 37' 7"	E 0° 34' 29"	
L'Elca	933-950	31	Doménech Belda (1997)	Lleida	N 37° 39' 32"	W 5° 31' 39"	
Lleida	770-1463	40	Soler Balaguer (1993)	Lora del Rio	N 39° 33' 34"	W 1° 16' 42"	
Lora del Rio	941-1021	165	Pellicer i Bru (1985)	Caudete de las Fuentes			
Los Villares	942-1028	112	Valle (1987)				

Appendix Table B.6: Hoards in al-Andalus, Part I

Hoard name	Date	# Coins described	Reference	Location	Latitude	Longitude
Madinat Iyyuh	711-856	20	Doménech Belda and Gutiérrez Lloret (2006)	El Tolmo de Minateda	N 38° 28' 34"	W 1° 36' 20"
Marroquies Altos	933-1010	270	Asencio (1962)	Jaen	N 37° 46' 9"	W 3° 47' 25"
Marroquies Bajos	941-1015	201	Canto García et al. (1997)	Jaen	N 37° 46' 9"	W 3° 47' 25"
Martos	817-875	24	Canto García (1993)	Cortijo del Mimbre	N 37° 38' 26.0"	W 3° 57' 04.9"
Merida	726-901	60	Rodríguez Palomo and Martín Escudero (2022)	Merida	N 38° 54' 58"	W 6° 20' 37"
Mertola	932-1036	81	Poiares (2000)	Mertola	N 37° 38' 34"	W 7° 39' 40"
Mijas Costa	932-976	533	Ayala Ruiz and Gozalbes Cravioto (1996)	La Cala de Mijas	N 36° 33' 56"	W 4° 40' 11"
Montellano	949-1010	23	Cano Ávila (2014)	Montellano	N 37° 00' 06.1"	W 5° 33' 02.1"
Moraleja	767-854	16	Álvarez (1993)	Moraleja	N 40° 0' 58"	W 6° 41' 51"
Moreria	857-1015	134	Palma García and Segovia Sopo (2007)	Merida	N 38° 54' 58"	W 6° 20' 37"
Niebla	805-884	36	Cano Ávila and Martín Gomez (2011)	Sierra de Alcantara	N 37° 28' 33.8"	W 6° 38' 36.2"
Osuna	954-1022	3	Alfaro Asins (1992)	Osuna	N 37° 14' 15"	W 5° 6' 11"
Parque Cruz conde	852-1021	3341	Canto García et al. (2020b)	Cordoba	N 37° 53' 29"	W 4° 46' 21"
Partida de Atzbares	941-970	26	Doménech Belda (1997)	Atzavares Baix (Elche)	N 38° 15' 43"	W 0° 42' 3"
Pascul de Gayangos	778-1204	159	Marinho (1993)	Algarve		
Pinos Puente	770-816	169	Martín Escudero (2011)	Pinos Puente	N 37° 15' 3"	W 3° 44' 58"
Pozoblanco	948-976	15	Marcos Pous and Vicent Zaragoza (1992)	Pozoblanco	N 38° 22' 44"	W 4° 50' 53"
Priego de Cordoba	770-856	54	Ávila and Pareja (1999)	Priego de Cordoba	N 37° 26' 17"	W 4° 11' 42"
Puebla de Cazalla	770-892	911	Ibrahim and Canto García (1991)	La Puebla de Cazalla	N 37° 13' 17"	W 5° 18' 41"
Puente de Miluze	934-1057	164	Canto García (2001)	Pamplona	N 42° 49' 0"	W 1° 38' 35"
Recopolis	772-785	9	Priego and Enciso (2016)	Recopolis	N 40° 19' 15.1"	W 2° 53' 37.7"
Sagrada Familia	945-1012	316	Marcos Pous and Vicent Zaragoza (1992)	Cordoba	N 37° 53' 29"	W 4° 46' 21"
San Andres de Ordoiz	782-908	167	Uranga (1950)	Estella-Lizarra	N 42° 40' 19"	W 2° 01' 56"
Saqunda	707-930	467	Martín Escudero et al. (2023)	Cordoba	N 37° 53' 29"	W 4° 46' 21"
Sevilla	711-1011	497	Saenz-Diéz (1993)	Sevilla	N 37° 22' 58"	W 5° 58' 23"
Sierra Cazorla	928-1021	237	Pellicer i Bru (1982)	Sierra Cazorla	N 37° 54' 45"	W 2° 58' 34"
Silves	770-875	79	Miles (1960)	Silves	N 37° 11' 21"	W 8° 26' 17"
Sinarcas	942-1037	57	Arroyo Ilera (1989)	Sinarcas	N 39° 44' 0"	W 1° 14' 0"
Solar del Museo Arqueologico	953-1007	16	Marcos Pous and Vicent Zaragoza (1992)	Cordoba	N 37° 53' 29"	W 4° 46' 21"
South France	692-886	204	Parvére (2014, 2019)	South France		
Spain single finds (felus)	699-901	57	Martín Escudero (2012)	Spain		
Tarancon	929-1014	451	Canto García (2014)	Tarancon	N 40° 0' 30"	W 3° 0' 26"
Teatro romano	805-819	25	Segovia Sopo and Jiménez (2011)	Merida	N 38° 54' 58"	W 6° 20' 37"
Tignar	864-913	35	Motos Guirao and Díaz García (1985)	Albolote	N 37° 13' 51"	W 3° 39' 18"
Tijan	976-1021	377	Fontenla Ballesta (1998)	Sierra de Cabrera	N 37° 06' 30.3"	W 1° 55' 49.2"
Trujillo	711-1014	384	Navascués y de Palacios (1957)	Trujillo	N 39° 27' 28"	W 5° 52' 55"
Valencia de Ventoso	933-1006	7	Grañeda Miñón (2021)	Valencia del Ventoso	N 38° 16' 0"	W 6° 28' 0"
Valeria	936-1009	250	Puertas (1982)	Valeria	N 39° 47' 0"	W 2° 9' 0"
Valle de Guadajoz	931-1013	204	Ortega et al. (2006)	Fuentidueña (Baena)	N 37° 43' 42.1"	W 4° 16' 54.3"
Vega Baja	-200-1500	184	Priego (2020)	Toledo	N 39° 51' 29"	W 4° 1' 21"
Vera	941-1024	370	Doménech Belda (1997)	Vera	N 37° 14' 36"	W 1° 51' 32"
Villaviciosa	705-817	1361	Peña Martín and Vega Martín (2007)	Villaviciosa de Cordoba	N 38° 5' 0"	W 5° 1' 0"
Yecla	705-726	5	Codera y Zaidín (1913)	Yecla	N 38° 39' 18"	W 1° 7' 46"
Zafra	789-892	43	Canto García (2019)	Zafra	N 38° 25' 31"	W 6° 25' 2"
Zamora	943-999	10	Cerrato and Esquivel (2019)	Zamora	N 41° 30' 22"	W 5° 44' 40"

Appendix Table B.7: Hoards in al-Andalus, Part II

Hoard Name	Country	Reference	Latitude	Longitude
Ankara 1960?	Turkey	Pennas (1991) 122	39.9388	32.8594
Argos 1983	Greece	Pennas (1991) 8	37.6353	22.7277
Ayies Paraskies/Crete 1962	Greece	Pennas (1991) 59 / Füeg (2007)	35.209	25.2041
Bajagic	Croatia	Mirnik (1981)	43.7581	16.6657
Balchik Stray Find I	Bulgaria	Curta (2005)	43.4119	28.1628
Berezeni	Romania	Oberländer-Târnoveanu (2001) p.67	46.378	28.1523
Bratimir	Bulgaria	Pennas (1991) 90	43.8682	26.7044
But	Italy	Arslan (2005) 2280	46.4768	13.0246
Byala 1954	Bulgaria	Pennas (1991) 73	42.8739	27.8886
Calarasi 1947	Romania	Pennas (1991) 111, Dimian (1957)	44.2029	27.3115
Camarina	Italy	Arslan (2005) 6170	36.8279	14.5241
Camarina ed. 18	Italy	Arslan (2005) 6185	36.8279	14.5241
Camarina ed. 1a	Italy	Arslan (2005) 6181	36.8279	14.5241
Camarina ed. 6	Italy	Arslan (2005) 6182	36.8279	14.5241
Capo Schiso 1950	Italy	Arslan (2005) 6910	37.8244	15.2684
Chryse/Edhessa 1935	Greece	Pennas (1991) 50 / Füeg (2007)	40.81	22.0446
Cleja	Romania	Pennas (1991) 113, Dimian (1957)	46.4019	26.9427
Constanta Stray I	Romania	Dimian (1957)	44.1777	28.6442
Constanta Stray II	Romania	Dimian (1957)	44.1777	28.6442
Corinth 15 May 1934 (South Basilica)	Greece	Pennas (1991) 3	37.9373	22.932
Corinth 1934	Greece	Pennas (1991) 7	37.9373	22.932
Corinth 1965 (Roman Bath)	Greece	Pennas (1991) 1	37.9373	22.932
Corinth 1965 (Roman Bath)	Greece	Pennas (1991) 4 (BCH 90, 1966, 751, 754)	37.9373	22.932
Corinth (St John's monastery)	Greece	Pennas (1991) 9	37.9373	22.932
Didyma (single find)	Turkey	Baldus (2006)	37.3731	27.2639
Drobeta - Turnu Severin	Romania	Oberländer-Târnoveanu (2001) p.68	44.6425	22.6587
Drobeta 1928	Romania	Oberländer-Târnoveanu (2001) p.67	44.6425	22.6587
Dubravice	Croatia	Mirnik (1981)	43.8506	15.9398
Dubrovnik 1982	Croatia	Mosser (1935) p.71 ("Ragusa"), Mirnik (1981) 359	42.6489	18.094
Elazig	Turkey	Füeg (2007)	38.6747	39.2229
Elbistan	Turkey	Füeg (2007)	38.2016	37.1924
Eskisehir	Turkey	Füeg (2007)	39.7743	30.5138
Gabrica	Bulgaria	Sophoulis (2011)	43.5082	26.9736
Govora	Romania	Oberländer-Târnoveanu (2001) p.68	45.0681	24.2302
Hadrianoupolis Acropolis Kimistene	Turkey	Lafli et al. (2016)	40.9231	32.4867
Hadrianoupolis Basilica A	Turkey	Lafli et al. (2016)	40.9231	32.4867
Hadrianoupolis Bath A	Turkey	Lafli et al. (2016)	40.9231	32.4867
Hadrianoupolis Bath B	Turkey	Lafli et al. (2016)	40.9231	32.4867
Hadrianoupolis Building 4	Turkey	Lafli et al. (2016)	40.9231	32.4867
Hadrianoupolis Domus	Turkey	Lafli et al. (2016)	40.9231	32.4867
Hagios Nikolaos, Hydra (Greece)	Greece	Pennas (1996), p. 270	37.3011	23.3967
Iatrus 1962	Bulgaria	Pennas (1991) 77	43.6262	25.587
Iatrus 1975	Bulgaria	Pennas (1991) 75	43.6262	25.587
Ipsala	Turkey	Füeg (2007)	40.9201	26.3828
Istria Stray Finds 869-877	Croatia	Miškć (2002)	45.1439	13.8259
Kavaklı	Turkey	Ünal (2018)	37.755	28.305
Kenchreai 1963	Greece	Pennas (1991) 2	37.8833	22.9873
Kozojedy, Bohemia	Czechia	Profantova (2009)	50.2548	13.8153
Kyme near Aliaga	Croatia	Carroccio, cited by Morrisson (2017)	38.7592	26.9367
Kyulevcha Grave	Bulgaria	Curta (2005)	43.2559	27.111
Lagbe	Turkey	Füeg (2007), Newell (1945)	36.8276	30.4112
Libice, Bohemia	Czechia	Profantova (2009)	50.1285	15.1815
Liopesi (around 1946)	Greece	Pennas (1991) 35 / Vryonis (1971)	37.9545	23.8521
Ljubimets	Bulgaria	Dimian (1957), Sophoulis (2011)	41.8466	26.0781
Luka Krnicka	Croatia	Miškć (2002)	44.9723	14.0171
Macvanska Mitrovica	Serbia	Pennas (1991) 72	44.9655	19.5975
Malthi (Dorion)	Greece	Pennas (1991) 6	37.267	21.8824
Maluk Povorets 1934	Romania	Pennas (1991) 74	43.7133	26.7652
Matera Piazza S. Francesco	Italy	Arslan (2005) 4140	40.6654	16.6087
Medias	Romania	Oberländer-Târnoveanu (2001) p.68, Dimian (1957)	46.1621	24.3567
Melito Porto Salvo	Italy	Arslan (2005) 0450	37.9197	15.7857
Mikulcice	Czechia	Profantova (2009)	48.8167	17.0516
Monemvasia Stray Find	Greece	Pennas (1996), p. 270	36.6876	23.0559
Naxos	Greece	Füeg (2007)	37.0567	25.4638
Nea Syllata/Chalkidiki 1977	Greece	Pennas (1991) 52	40.3275	23.136
Nin	Croatia	Mirnik (1981)	44.2392	15.1791
Odartsı	Bulgaria	Sophoulis (2011)	43.44	27.9616
Osava near Ram	Serbia	Füeg (2007)	44.8006	21.3433
Osvetimany	Czechia	Profantova (2009)	49.0562	17.2496

Appendix Table B.8: Hoards with Byzantine coins, Part I

Hoard Name	Country	Reference	Latitude	Longitude
Oszony, Komarom	Hungary	Oberländer-Târnoveanu (2001) p.68	47.7295	18.1751
Piran	Italy	Arslan (2005) 2808	45.5279	13.5694
Pliska	Bulgaria	Füeg (2007)	43.362	27.1228
Prague, Tynsky dur	Czechia	Profantova (2009)	50.073	14.4286
Rakvice (Breclav)	Czechia	Profantova (2009)	48.8559	16.813
Rasova 1934	Romania	Pennas (1991) 112, Dimian (1957)	44.2403	27.9414
Reggio Calabria	Italy	Arslan (2005) 0670	38.0947	15.6455
Rhodos Stray Find 859	Greece	Kasdagli (2018)	36.436	28.2221
Rhodos V.12 (Kattavia)	Greece	Kasdagli (2018)	35.9534	27.7683
Rome / Tiber	Italy	Morrisson and Barrandon (1988)	41.8882	12.4768
Salamis (South of Amphitheatre, 1964-1974)	Turkey	Füeg (2007)	35.1914	33.8979
Santorini (Thira) 1895-1902	Greece	Pennas (1991) 57	36.4058	25.4588
Sicily (Fagerlie)	Italy	Fagerlie (1974)	37.5732	14.2114
Songurlu / Mosser	Turkey	Füeg (2007) / Mosser (1935)	40.1627	34.3767
Stare Mesto	Czechia	Profantova (2009)	49.0727	17.4463
Stimanga 1955	Greece	Pennas (1991) 5 (BCH 80, 1956, 256)	37.909	22.6989
Streda nad Bodrogom	Slovakia	Profantova (2009)	48.3785	21.758
Syracuse Via G. Di Natale	Italy	Arslan (2005) 7335	37.0724	15.2845
Tegani/Samos 1914	Greece	Pennas (1991) 58	37.6904	26.9417
Telerig Stray Miliaresion	Bulgaria	Curta (2005)	43.8457	27.671
Thessaloniki	Greece	Füeg (2007)	40.652	22.9304
Thessaloniki 1891	Greece	Pennas (1991) 51	40.652	22.9304
Tichilesti	Romania	Dimian (1957)	45.1291	27.9045
Tralleis/Aydin	Turkey	Ünal (2015)	37.8591	27.8335
Trilj	Croatia	Mirnik (1981)	43.6187	16.7241
Unknown Provenance (Turkey) 1987	Turkey	Pennas (1991) 123	39.2963	32.9327
Urluia 1936	Romania	Dimian (1957), Sopoulis (2011)	44.1016	27.9132
Velul lui Trajan	Romania	Pennas (1991) 105	44.1647	28.4621
Velul lui Trajan 1999/2000	Romania	Măncu-Adameșteanu (2016)	44.1647	28.4621
Voila, Romania	Romania	Dimian (1957)	45.818	24.8405
Vukovar - Lijeva Bara	Croatia	Mirnik (1981)	45.3382	19.0079
Yakimovo (Progorelets) 1960	Bulgaria	Pennas (1991) 91	43.6337	23.3621
Yunak	Bulgaria	Pennas (1991) 76	43.0763	27.6109

Appendix Table B.9: Hoards with Byzantine coins, Part II

Hoard Name	Date	Reference	Location	Latitude	Longitude
Aalst	840-855	Bijsterveld et al. (2000)	Aalst	51.39611	5.477
Aalsum	814-855	Morrison and Grunthal (1967)	Aalsum	53.3403	6.00538
Achlum	768-840	Morrison and Grunthal (1967)	Achlum	53.14779	5.48239
Alfocea	943-977	Parvéria (2018)	Alfocea	41.724097	-0.953131
Amerongen	768-877	Coupland (2014)	Amerongen	52.0025	5.46024
Ampurias	768-814	Doménech-Belda et al. (2013)	Ampurias	42.134477	3.111418
Andalusia	814-848	Parvéria (2018)	Andalusia		
Angeac-Champagne	840-877	Duplessy (1985)	Angeac-Champagne	45.60769	-0.29771
Angers I	814-840	Morrison and Grunthal (1967)	Angers	47.4707	-0.55324
Angers II (Saint-Julien)	819-877	Haertle (1997)	Angers	47.4707	-0.55324
Anglure	864-887	Morrison and Grunthal (1967)	Anglure	48.58345	3.81356
ANS find	768-922	Morrison and Grunthal (1967)	France		
Anse I	818-823	Guillemain (1993)	Anse	45.937639	4.717512
Anserall	768-815	Doménech-Belda et al. (2013)	Anserall	42.37829	1.456511
Apremont	793-822	Morrison and Grunthal (1967)	Apremont-sur-Allier	46.906	3.048
Aquitaine	814-887	Coupland (1991)	Aquitaine		
Ardres	888-923	Haertle (1997)	Ardres	50.856432	1.978355
Arras	843-922	Morrison and Grunthal (1967)	Arras	50.29039	2.778414
Ashdon	843-898	Blackburn (1989)	Ashdon	52.05544	0.31373
Aspres-lès-Corps	901-924	Schulze (1984)	Aspres-lès-Corps	44.80162	5.98217
Assebroek	843-877	Morrison and Grunthal (1967)	Assebroek	51.18793	3.27363
Assen	800-911	Morrison and Grunthal (1967)	Assen	52.99421	6.55957
Auxerre	813-877	Haertle (1997)	Auxerre	47.796587	3.570535
Auzeville	814-848	Sarah et al. (2016)	Auzeville	43.5257	1.49342
Avallon	843-877	Coupland (2020)	Avallon	47.488712	3.907758
Avignon	843-887	Morrison and Grunthal (1967)	Avignon	43.95344	4.80601
Bakonyszombathely	898-973	Morrison and Grunthal (1967)	Bakonyszombathely	47.47208	17.96018
Balloo	843-855	Haertle (1997)	Balloo	54.472363	-5.69076
Barbentane	814-840	Morrison and Grunthal (1967)	Barbentane	43.89948	4.74635
Barcelona	814-840	Doménech-Belda et al. (2013)	Barcelona	41.395937	2.174552
Bassenheim	814-876	Coupland (2019)	bassenheim	50.359028	7.462443
Bátorove Kosihy	888-950	Kovács (1989)	Bátorove Kosihy	47.83083	18.41083
Beaumont	843-877	Morrison and Grunthal (1967)	Beaumont (Chalo	48.409016	2.042742
			Saint Mars)		
Bel-Air	768-814	Morrison and Grunthal (1967)	Lausanne	46.57957	6.605807
Bellpuig	887-928	Doménech-Belda et al. (2013)	Bellpuig	41.626531	1.011607
Belvédet	768-840	Morrison and Grunthal (1967)	Belvédet	44.08433	4.36426
Bikbergen	814-855	Cruijssen and der Veen (2015)	Bikbergen	52.287933	5.196186
Bjerndrup	817-924	Coupland (2020)	Bjerndrup	54.93391	9.32867
Blendecques	814-840	Coupland (2020)	Blendecques	50.716982	2.282169
Bligny	814-887	Morrison and Grunthal (1967)	Bligny	48.1725	4.6172
Blois	898-940	Moesgaard (1997)	Blois	47.58696	1.33139
Bondeno	768-814	Morrison and Grunthal (1967)	Bondeno	44.89098	11.41096
Bonnevaux	800-887	Morrison and Grunthal (1967)	Bonnevaux	44.367837	4.030289
Borne	794-813	Coupland (2011a)	Borne	52.30137	6.75779
Bourges	840-877	Morrison and Grunthal (1967)	Bourges	47.08585	2.39293
Bourges	800-887	Coupland (2020)	Bourges	47.08585	2.39293
Bourgneuf	814-888	Morrison and Grunthal (1967)	Bourgneuf	46.167624	-1.022216
Bourgneuf-en-Retz	843-877	Coupland (2010)	Bourgneuf-en-Retz	47.04229	-1.9543
Bray-sur-Seine	840-877	Vandenbossche and Coupland (2012)	Bray-sur-Seine	48.41451	3.24057
Bressuire	814-840	Coupland (1995)	Bressuire	46.84008	-0.49253
Breuvery-sur-Coole	768-813	Dhémin (1989)	Breuvery-sur-Coole	48.86311	4.31164
Brion	814-840	Denais (1908)	Brion	47.4425	-0.1553
Brioux-sur-Boutonne	814-840	Morrison and Grunthal (1967)	Brioux-sur-Boutonne	46.14349	-0.21823
Bruère-Allichamps	814-954	Morrison and Grunthal (1967)	Bruère-Allichamps	46.7695	2.4325
Burgum	843-877	Haertle (1997)	Burgum	53.19527	5.98694
Caden	843-877	Coupland (2020)	Caden	47.630822	-2.287131
Caen	936-954	Coupland (2020)	Caen	49.183512	-0.363489
Calatrava la vieja		Parvéria (2018)	Calatrava la Vieja	39.074099	-3.833274
Campeaux	813-877	Haertle (1997)	Campeaux	48.952844	-0.93197
Carcassonne	768-814	Coupland (2014)	Carcassonne	43.206463	2.363268
Castelsarasin	888-898	Morrison and Grunthal (1967) and Lafaurie (1965)	Castelsarasin	44.039071	1.106969
Catalonia	768-905	Balaguer (1999) and Doménech-Belda et al. (2013)	Calalonia		
Cauroir	843-882	Coupland (2011a)	Cauroir	50.17283	3.30174
Cerdanyola	814-840	Doménech-Belda et al. (2013)	Cerdanyola	41.49201	2.137338
Cerveník	826-950		Cerveník	48.45	17.75

Appendix Table B.10: Carolingian Hoards, Part I

Hoard Name	Date	Reference	Location	Latitude	Longitude
Chaley	936-954	Morrison and Grunthal (1967)	Chaley	45.9552	5.53122
Chalo-Saint-Mars	840-877	Morrison and Grunthal (1967)	Chalo-Saint-Mars	48.4267	2.067
Chalon-sur-Saône I	800-887	Morrison and Grunthal (1967)	Chalon-sur-Saône	46.782132	4.858459
Chalon-sur-Saône II	800-887	Haertle (1997)	Chalon-sur-Saône	46.782132	4.858459
Charente-Maritime	888-898	Coupland (2011a)	Charente-Maritime		
Chartes	923-977	Duplessy (1985)	Chartres	48.446659	1.488596
Chartres II	751-768	Morrison and Grunthal (1967)	Chartres	48.446659	1.488596
Château Roussillon	793-877	Haertle (1997)	Château Roussillon	42.710278	2.946667
Chateauneuf sur Cher	843-954	Morrison and Grunthal (1967)	Chateauneuf sur Cher	46.857333	2.320522
Chaumoux-Marcilly	814-877	Morrison and Grunthal (1967)	Chaumoux-Marcilly	47.12628	2.77884
Chauvigny	843-877	Société des antiquaires de l'Ouest (1982)	Chauvigny	46.56974	0.64345
Chef-Boutonne	800-922	Haertle (1997) and Rondier (1869)	Chef-Boutonne	46.10934	-0.06806
Chester	888-924	Webster et al. (1953)	Chester	53.1903	-2.89437
Chézy-sur-Marne	768-814	Duplessy (1985)	Chézy-sur-Marne	48.989611	3.366294
Choisy-au-Bac	888-898	Haertle (1997)	Choisy-au-Bac	49.44777	2.88097
Ciney Dinant	898-922	Coupland (2020)	Ciney	50.286773	5.098966
Clermont Ferrand	843-918	Coupland (2020)	Clermont-Ferrand	45.778063	3.083696
Compiègne I	877-882		Compiègne	49.41762	2.82513
Compiègne II	843-882	Morrison and Grunthal (1967)	Compiègne	49.41762	2.82513
Corrèze	843-877	Coupland (2014)	Corrèze		
Cosne d'Allier	814-840	Coupland (2014)	Cosne d'Allier	46.474799	2.830127
Cosne-Cours-sur-Loire II	814-877	Morrison and Grunthal (1967)	Cosne-Cours-sur-Loire	47.40983	2.92425
Cosne-Cours-sur-Loire III	877-840	Haertle (1997)	Cosne-Cours-sur-Loire	47.40983	2.92425
Croydon	814-877	Morrison and Grunthal (1967)	Croydon	51.379287	-0.09975
Csorna	888-947	Kovács (1989)	Csorna	47.6167	17.25
Cuerdale	843-922	Morrison and Grunthal (1967)	Cuerdale	53.7553	-2.638
Dalen	843-976	Morrison and Grunthal (1967)	Dalen	52.69847	6.75641
Dauphiné	814-848	Coupland (2014)	Dauphiné		
Deux-Sèvres	814-877	Société de statistique, sciences, lettres et arts du département des Deux-Sèvres (1882)	Deux-Sèvres		
Dijon	770-780	Bompaire and Depierre (1989)	Dijon	47.3268	5.04619
Dommartin-Lettrée	923-936	Duplessy (1985)	Dommartin-Lettrée	48.7669	4.29933
Dordives	750-950	Coupland (2014)	Dordives	48.144081	2.766333
Dorestad	768-877	Morrison and Grunthal (1967)	Dorestadt	51.97212	5.344769
Drantum	814-840	Haertle (1997)	Drantum	52.81942	8.19537
Eichstetten	911-922	Morrison and Grunthal (1967)	Eichstetten	48.094296	7.745429
Ejstrup	814-840	Coupland (2020)	Ejstrup	55.503525	9.377413
Ekeren	819-877	Haertle (1997)	Ekeren	51.276405	4.417467
Ellikon an der Thur	887-915	Zäch (2001)	Ellikon an der Thur	47.56253	8.82386
Emmen	814-877	Morrison and Grunthal (1967)	Emmen	52.49784	6.23039
Entrammes	814-877	Coupland (2014)	Entrammes	47.999133	-0.716154
Espana 1-4	800-1009	Parvérie (2018)	Calatayud	41.352868	-1.641101
Etampes	843-882	Morrison and Grunthal (1967)	Etampes	48.434768	2.162027
Etréchy	832-877	Morrison and Grunthal (1967)	Etréchy	48.88411	3.94374
Evreux	840-954	Duplessy (1985) and Moesgaard (2003)	Evreux	49.02754	1.15028
Extremadura		Parvérie (2018)	Extremadura		
Eyguières	814-840	Coupland (2020)	Eyguières	43.696133	5.030134
Fécamp	900-999	Duplessy (1985)	Fécamp	49.75765	0.37632
Flacey	814-840	Coupland (2020)	Flacey	48.147247	1.349598
Flanders	814-877	Coupland (2020)	Flanders		
Florange		Duplessy (1985) and Simmer (2000)	Florange	49.32743	6.12273
Foissy-lès-Vézelay	864-877	Duplessy (1985)	Foissy-lès-Vézelay	47.43637	3.76447
Fontaines	814-877	Duplessy (1985)	Fontaines	46.85083	4.773055
Frankfurt	814-840	Morrison and Grunthal (1967)	Frankfurt am Main	50.11208	8.68341
Freiburg im Breisgau	898-922	Morrison and Grunthal (1967)	Freiburg im Breisgau	47.99853	7.84965
Fresnes		Duplessy (1985)	Fresnes	48.75043	2.322063
Fridolfing	768-814	Coupland (2020)	Fridolfing	47.998573	12.826917
Frisia	814-855	Morrison and Grunthal (1967)	Grou	53.11035	5.848604
Gannat	800-887	Morrison and Grunthal (1967)	Gelderland	46.10192	3.19692
Gelderland	768-814	Morrison and Grunthal (1967)	Giekau	54.31793	10.50529
Giekau	814-911	Wiechmann (2004)	Glisy	49.8756	2.39788
Glisy	800-922	Morrison and Grunthal (1967)	Gnadendorf	48.61549	16.39885
Gnadendorf	898-905	Daim and Lauermann (2006)	Goutum	53.178037	5.806018
Goutum	814-877	Coupland (2020)	Slagelse	55.3028	11.2647
Grisebjerrgård	898-922		Groningen	53.25713	6.93525
Groningen	814-877	Morrison and Grunthal (1967)	Guardamiglio	45.11055	9.68215
Guardamiglio	843-884	Coupland (2011a)			

Appendix Table B.11: Carolingian Hoards, Part II

Hoard Name	Date	Reference	Location	Latitude	Longitude
Györ I	888-950	Kovács (1989)	Györ	47.69739	17.6527
Györ II	888-951	Kovács (1989)	Györ	47.69739	17.6527
Halimba	902-947	Kovács (1989)	Halimba	47.03345	17.53546
Häljarp	814-840	Morrison and Grunthal (1967)		55.85578	12.910919
Harkirke	843-905	Morrison and Grunthal (1967)	Crosby	53.48919	-3.048081
Harlingen	840-855	Haertle (1997)	Harlingen	53.1735	5.4246
Haute Isle	814-922	Morrison and Grunthal (1967)	Haute Isle	49.083426	1.65697
Haza de Carmen	888-954	Coupland (2020)	Cordoba	37.881495	-4.776125
Hermenches	822-840	Morrison and Grunthal (1967)	Hermenches	46.640456	6.757567
Hoen	814-855	Morrison and Grunthal (1967)	Hoen	60.2204	10.25852
Hole	796-840	Coupland (2020)	Hole	58.897156	6.018229
Holy Family	800-887	Parvéria (2018) and Morrison and Grunthal (1967)	Cordoba	37.888028	-4.7734
Hradec Hilfort	768-814	Coupland (2020)	Hradec-Kralove	50.209703	15.832231
Huriel	800-887	Morrison and Grunthal (1967)	Le Moulin-Gargot (Huriel)	46.37468	2.47842
Ibaneta	800-888	Doménech-Belda et al. (2013)	Puerto d'Ibaneta	43.020083	-1.324207
Ibersheim	768-814	Morrison and Grunthal (1967)	Ibersheim	49.72085	8.40065
Ilanz I	843-905	Morrison and Grunthal (1967)	Ilanz	46.77451	9.20463
Ilanz II	664-814	Bernareggi (1977, 1983), Völckers (1965), McCormick (2001)	Ilanz	46.77451	9.20463
Île Agois	864-877	Johnston (1986)	Île Agois	49.24935	-2.18641
Île-de-France	888-936	Dhémin (2006)	Ile de France		
Imbleville	864-877	Haertle (1997)	Imbleville	49.71539	0.95198
Imphy	751-814	Morrison and Grunthal (1967)	Imphy	46.934537	3.259903
Indre	814-865	Morrison and Grunthal (1967)	Indre		
Indre II	814-848	Coupland (2014)	Indre		
Indre-et-Loire	814-877	Coupland (2011a)	Indre-et-Loire		
Indre-et-Loire II	888-910	Coupland (2011a)	Indre-et-Loire		
Indre-et-Loire III	888-898	Coupland (2020)	Indre-et-Loire		
Isle-Aumont I	814-840	Haertle (1997)	Isle-Aumont	48.21131	4.12459
Isle-Aumont II	864-898	Haertle (1997)	Isle-Aumont	48.21131	4.12459
Issy l'Evêque	843-922	Morrison and Grunthal (1967)	Issy l'Evêque	46.70818	3.9734
Jedomelice	814-840	Coupland (2020)	Jedomelice	50.23411	13.971234
Jelsum	768-814	Morrison and Grunthal (1967)	Jelsum	53.23455	5.783862
Juaye-Mondaye	800-922	Morrison and Grunthal (1967)	Juaye-Mondaye	49.20803	-0.68508
Jura	768-814	Morrison and Grunthal (1967)	Jura		
Karden	814-822	Morrison and Grunthal (1967)	Karden	50.179051	7.299583
Karos-Eperjesszög I	888-915	Révész (1996)	Karos	48.32959	21.73712
Karos-Eperjesszög II	900-911	Gedai (1993)	Karos	48.32959	21.73712
Kättilstorp	814-877	Morrison and Grunthal (1967)	Kättilstorp	58.041694	13.711198
Katwijk I	800-922	Kluge (1993)	Katwijk	52.195273	4.421091
Katwijk II	794-800	Van der Velde (2008)	Katwijk	52.195273	4.421091
Kecel	888-924	Huszár (1955)	Kecel	46.52644	19.24647
Kenézlő	826-950	Huszár (1955)	Kenézlő	48.2	21.53333
Kimsword-Pingjum I	814-877	Morrison and Grunthal (1967)	Kimsword	53.1289	5.4387
Kimsword-Pingjum II	814-878	Morrison and Grunthal (1967)	Kimsword	53.1289	5.4387
Kiskundorozsma-Hosszúhát	826-950	Múzeum Móra Ferenc (2002)	Szeged	46.275	20.06278
Kiskunfélegyháza	881-918	Kovács (1989)	Kiskunfélegyháza	46.71246	19.85279
Koblenz	823-830	Reinhold Fischer Auktionshaus (2010)	Koblenz	50.359618	7.59383
Krinkberg	768-814	Morrison and Grunthal (1967)	Pöschendorf	54.03055	9.472156
La Cornouaille	814-877	Coupland (2020)	La Cornouaille	47.578279	-0.797543
La Couvertoirade	881-898	Coupland (2011a)	La Couvertoirade	43.91127	3.31355
La Roche en Ardenne	750-950	Coupland (2014)	La-Roche-en-Ardenne	50.183528	5.575243
La Tessoualle	814-877	Haertle (1997)	La Tessoualle	47.00535	-0.8494
La Tour-de-Peilz	755-768	Geiser (1990)	La-Tour-de-Peilz	46.45302	6.85686
Ladánybene	888-922	Huszár (1955)	Ladánybene	47.03333	19.45
Lamairé	843-877	Baigl et al. (1995)	Lamairé	46.75707	-0.1263
Lamotte Beuvron	814-877	Coupland (2020)	Lamotte-Beuvron	47.602363	2.025245
Langon	814-877	Morrison and Grunthal (1967)	Langon	44.55389	-0.24833
Langres I	843-922	Morrison and Grunthal (1967)	Langres	47.85816	5.33113
Langres II	864-884	Coupland (2011a)	Langres	47.85816	5.33113
Larino	768-840	De Benedittis and Lafaurie (1998)	Larino	41.7968	14.9128
Lauterach	840-924	Zách and Tabernero (2002)	Lauterach	47.4745	9.730031
Lauzès	814-877	Morrison and Grunthal (1967)	Lauzès	47.4707	-0.55324
Lavelanet	888-898	Coupland (2020)	Lavelanet	42.932652	1.848583
Laxfield	843-877	Morrison and Grunthal (1967)	Laxfield	52.30114	1.36237
Leiderdorp	768-840	Coupland (2020)	Leiderdorp	52.151653	4.529015

Appendix Table B.12: Carolingian Hoards, Part III

Hoard Name	Date	Reference	Location	Latitude	Longitude
Lésigny-sur-Creuse	814-898	Jeanne-Rose (1996)	Lésigny-sur-Creuse	46.84996	0.76421
Levice-Géna	926-950	Minarovicova (2007)	Levice-Géna	48.21639	18.60806
Lillebonne	814-877	Coupland and Moesgaard (2012)	Lillebonne	49.51802	0.53681
Limoux	849-877	Haertle (1997)	Limoux	43.053658	2.217421
Lisówek	848-922	Morrison and Grunthal (1967)	Lisówek	51.9	20.9333
Llanbedrgoch	814-878	Coupland (2020)	Llanbedrgoch	53.300117	-4.236622
Llerida	887-928	Doménech-Belda et al. (2013)	Lleida	41.61879	0.621737
Loire River Bank	814-840	Coupland (2014)	Loire River		
Loiret	843-1027	Duplessy (1985)	Loiret		
Lokeren	843-864	Haertle (1997)	Lokeren	51.10473	3.9865
Longjumeau	843-884	Moesgaard (2010)	Longjumeau	48.69173	2.29005
Loppersum	814-877	Morrison and Grunthal (1967)	Loppersum	53.33276	6.74398
Lucca	947-961	Saccoccia et al. (2004)	Lucca	43.84201	10.51534
Lussac-les-Châteaux	845-848	Haertle (1997)	Lussac-les-Châteaux	46.403093	0.723563
Lutkesaaxum	843-864	Haertle (1997)	Lutkesaaxum	53.364638	6.489072
Luzancy	814-877	Sombart (2008)	Luzancy	48.97205	3.1865
Lyon	751-771	Coupland (2020)	Lyon	45.758973	4.830895
Maine et Loire	751-878	Coupland (2014)	Maine-et-Loire		
Marçay	840-898	Morrison and Grunthal (1967)	Marçay	47.10002	0.21706
Marssum	814-855	Coupland (2011a)	Marssum	53.21056	5.73008
Marsum	814-887	Morrison and Grunthal (1967)	Marsum	53.339476	5.73008
Matha	778-877	Coupland (2014)	Matha	45.867625	-0.321187
Melle I	875-877	Haertle (1997)	Melle	46.221471	-0.147358
Melle II	843-877	Haertle (1997)	Melle	46.221471	-0.147358
Melle IV	823-825	Coupland (2018)	Melle	46.221471	-0.147358
Mercurey	822-877	Duplessy (1985) and Haertle (1997)	Mercurey	46.833364	4.722119
Méréville	814-877	Morrison and Grunthal (1967)	Méréville-Saint-Pierre	48.59069	6.15058
Metz	843-877	Morrison and Grunthal (1967)	Metz	49.11566	6.1732
Meurthe et Moselle	898-922	Coupland (2014)	Meurthe-et-Moselle		
Midlaren	814-877	Morrison and Grunthal (1967), Haertle (1997)	Midlaren	53.1111	6.67616
Midlum	900-961	Morrison and Grunthal (1967)	Midlum	53.18204	5.44716
Mikulčice	887-900	Slovenská akadémia vied. Archeologický ústav (1979)	Mikulčice	48.81667	17.05
Molliens-Vidame	817-877	Haertle (1997)	Molliens-Dreuil	49.8839	2.02
Monchy-au-Bois	840-922	Morrison and Grunthal (1967)	Monchy-au-Bois	50.17999505	2.656698281
Montmain	768-814	Coupland (2020)	Montmain	49.410716	1.252625
Montreux-en-Sologne II	800-922	Morrison and Grunthal (1967)	Montreux-en-Sologne	47.55408	1.72638
Montreux-en-Sologne III	864-898	Morrison and Grunthal (1967)	Montreux-en-Sologne	47.55408	1.72638
Moreria		Parvéria (2018)	Moreria	38.916776	-6.349645
Mourlieu	900-925	Caron (1882)	Mourlieu	46.564931	0.512703
Muizen	822-877	Morrison and Grunthal (1967)	Muizen	51.01056	4.514722
Mullaghboden	814-877	Morrison and Grunthal (1967)	Mullaghboy	54.83536	-5.72671
Muret	814-840	Coupland (2020)	Muret	43.460924	1.327252
Nagyszokoly	926-947	Kovács (1989)	Nagyszokoly	46.72132	18.21182
Nagyvázsony	902-947	Kovács (1989)	Nagyvázsony	46.9835	17.69408
Neufchateau I	800-922	Coupland (2014)	Neufchateau	48.356071	5.692627
Neufchateau II	814-848	Coupland (2014)	Neufchateau	48.356071	5.692627
Neuvy-au-Houlme	814-877	Morrison and Grunthal (1967), Duplessy (1985)	Neuvy-au-Houlme	48.8181	-0.19966
Niederlahnstein	855-869	Coupland (2020)	Niederlahnstein	50.315193	7.598382
Nourray	843-877	Morrison and Grunthal (1967)	Nourray	47.71903	1.06023
Nr.Trier	768-855	Coupland (2014) and Morrison and Grunthal (1967)	Trier	49.755513	6.640075
Odoorn	843-961	Morrison and Grunthal (1967)	Odoorn	52.85033	6.847823
Orléans	814-864	Haertle (1997)	Orléans	47.90143	1.90496
Oudwoude	814-877	Morrison and Grunthal (1967)	Oudwoude	53.27968	6.11413
Palma de Majorque	800-888	Doménech-Belda et al. (2013)	Palma de Majorque	39.570589	2.648991
Paule	843-877	Coupland (2014)	Paule	48.235953	-3.4444348
Pilligerheck	814-877	Petry and Wittenbrink (2021), Coupland (2011b)	Muenstermaifeld	50.20461	7.31152
Pingjum	900-911	Morrison and Grunthal (1967)	Pingjum	53.11519	5.44004
Place Unknown	954-986	Morrison and Grunthal (1967)			
Plessé	875-877	Haertle (1997)	Plessé	47.54109	-1.88812
Poitou Charentes	814-877	Coupland (2020)	Poitou-Charente		
Pommern	887-924	Coupland (2020)	Pommern	50.169368	7.269726
Pont Saint-Pierre	864-877	Coupland (2011a)	Pont-Saint-Pierre	49.33388	1.2745
Postsaal	814-1024	Coupland (2020)	Bavière		
Pouzauges	875-898	Haertle (1997)	Pouzauges	46.7822	-0.8361

Appendix Table B.13: Carolingian Hoards, Part IV

Hoard Name	Date	Reference	Location	Latitude	Longitude
Questembert	814-877	Haertle (1997)	Questembert	47.66097	-2.4521
Raalte	814-877	Coupland (2011a)	Raalte	52.38724	6.27462
Regensburg	843-877	Haertle (1997)	Regensburg	49.016213	12.097468
Rennes	843-922	Morrison and Grunthal (1967)	Rennes	48.10761	-1.68448
Rijs	814-877	Morrison and Grunthal (1967)	Rijs	52.86298	5.49838
Rijswijk	814-840	Coupland (2020)	Rijswijk	52.039942	4.325633
Rochefort	900-911	Coupland (2020)	Rochefort	45.935077	-0.962458
Roches l'Evêque	814-922	Morrison and Grunthal (1967)	Roches l'Evêque	47.7772	0.8922
Roermond	222-877	Haertle (1997), Coupland (2011b), Zuyderwyk and Besteman (2010)	Roermond	51.193179	5.98624
Rome I (Forum)	887-950	Metcalf (1992)	Rome	41.90509	12.46194
Rome II (Vatican)	898-922	Morrison and Grunthal (1967)	Rome	41.90509	12.46194
Rosas	814-840	Doménech-Belda et al. (2013)	Rosas	42.265002	3.178593
Roswinkel	768-882	Morrison and Grunthal (1967)	Roswinkel	52.83787	7.03843
Rotterdam	814-840	Coupland (2020)	Rotterdam	51.919909	4.47544
Saint Bris le Vineux	814-877	Coupland (2020)	Saint-Bris-le-Vineux	47.74291	3.651349
Saint Ponc	884-887	Doménech-Belda et al. (2013)	Saint-Ponç	41.963245	1.603627
Saint Yrieix la Perche	888-898	Coupland (2020)	Saint-Yrieix-la-Perche	45.51359	1.203618
Saint-Brieuc	864-875	Haertle (1997)	Saint-Brieuc	48.5136	-2.7653
Saint-Calais	768-877	Paty (1848)	Saint-Calais	47.9211	0.7439
Saint-Cyr-en-Talmondais	814-877	Morrison and Grunthal (1967)	Saint-Cyr-en-Talmondais	46.4614	-1.3356
Saint-Denis	793-875	Haertle (1997)	Saint-Denis	48.9364	2.3547
Saint-Martin-sur-le-Pré		Coupland (2014)	Saint-Martin-sur-le-Pré	48.9778	4.3394
Saint-Même-le-Tenu	814-877	Coupland (2014)	Saint-Même-le-Tenu	47.020808	-1.794104
Saint-Michel-de-Chavaignes		Haertle (1997)	Saint-Michel-de-Chavaignes	48.018584	0.570918
Saint-Pierre-de-Maillé	814-840	Benoit and Braunstein (1983)	Saint-Pierre-de-Maillé	46.6797	0.8444
Saint-Pierre-des-Fleurs I	823-877	Coupland and Moesgaard (2012)	Saint-Pierre-des-Fleurs	49.2514	0.9667
Saint-Pierre-des-Fleurs II	888-898	Cardon et al. (2008)	Saint-Pierre-des-Fleurs	49.2514	0.9667
Saint-Seine-l'Abbaye		Coupland (2014)	Saint-Seine-l'Abbaye	47.440003	4.788637
Santa Elena	961-966	Doménech-Belda et al. (2013)	Irun	43.337137	-1.786251
Santiago de Compostela	800-888	Doménech-Belda et al. (2013)	Santiago de Compostela	42.880265	-8.543118
Sarlat	814-877	Coupland (2020)	Sarlat-la-Canéda	44.889865	1.216381
Sarzana	768-814	Morrison and Grunthal (1967)	Sarzana	44.11186	9.95886
Saumeray	843-877	Morrison and Grunthal (1967)	Saumeray	48.25027	1.32157
Saumur-Thouars	843-898	Morrison and Grunthal (1967)	Saumur	47.1218	-0.1704
Saverne		Duplessy (1985)	Saverne	48.73947	7.36602
Savigné-sous-le-Lude	843-898	Morrison and Grunthal (1967)	Savigné-sous-le-Lude	47.61845	0.05801
Savigny en Véron	814-877	Coupland (2020)	Savigny-en-Véron	47.205554	0.147106
Seiches sur le Loir	751-814	Coupland (2014)	Seiches-sur-le-Loir	47.578315	0.362977
Séranon	814-840	Coupland (2020)	Séranon	43.772823	6.704362
Sevilla region	888-898	Parvérie (2018)	Sevilla	37.393305	-5.993535
's-Hertogenbosch	814-840	Coupland (2014)	's-Hertogenbosch	51.698578	5.303773
Sigean	768-814	Coupland (2020)	Sigean	43.0287	2.978539
Silverdale	800-898	Coupland (2014)	Silverdale	54.167322	-2.82505
Minor Finds	751-1027	Morrison and Grunthal (1967)			
Søndre Bø	814-883	Morrison and Grunthal (1967)	Søndre Bø	58.11019	6.88224
Strasbourg-Basel	843-954	Morrison and Grunthal (1967)	Strasbourg/Basel	48.171	7.6473
Szabadbattyán	826-950	Huszár (1955)	Szabadbattyán	47.11798	18.3629
Szabadeghyháza	888-924	Kovács (1989)	Szabadeghyháza	47.07845	18.69228
Szedeg-othalom	902-924	Coupland (2014)	Szeged	46.265179	20.140614
Szekszárd	902-947	Huszár (1955)	Szekszárd	46.34779	18.70626
Tarrega	887-928	Doménech-Belda et al. (2013)	Tarrega	41.648564	1.140707
Taizy	864-877	Coupland (2020)	Taizy	49.51967	4.25832
Teloché	864-877	Hucher (1845)	Teloché	47.88987	0.26731
Ter Apel	900-911	Morrison and Grunthal (1967)	Ter Apel	52.878359	7.063981
Ter Heijde	814-840	Coupland (2020)	Ter Heijde	52.02903	4.164265
Terslev	814-966	Morrison and Grunthal (1967)	Terslev	55.37476	11.9693
Thoiry	875-894	Haertle (1997)	Thoiry	48.86519	1.79463
Thouars	822-855	Morrison and Grunthal (1967)	Thouars	46.977604	-0.21579
Tiel	898-922	Coupland (2011a)	Tiel	51.88809	5.43069
Tiszaeszlár I	814-950	Kovács (1989)	Tiszaeszlár	48.05	21.46667
Tiszaeszlár II	926-950	Kovács (1989)	Tiszaeszlár	48.05	21.46667
Tiszanána	888-946	Kovács (1989)	Tiszanána	47.56111	20.52382

Appendix Table B.14: Carolingian Hoards, Part V

Hoard Name	Date	Reference	Location	Latitude	Longitude
Troyes	814-840	Coupland (2014)	Troyes	48.299055	4.077872
Troyes II	843-877	Coupland (2020)	Troyes	48.58345	3.81356
Tuscany	888-973	Ciampoltrini et al. (2001)	Tuscany		
Tytsjerksteradiel	814-855	Coupland (2020)	Burgum	53.195748	5.987155
Tzummarum I	819-855	Haertle (1997)	Tzummarum	53.238297	5.549116
Tzummarum II	855-865	Coupland (2020)	Tzummarum	53.238297	5.549116
Unknown	954-986	Morrison and Grunthal (1967)	France		
Vale of York	898-922	Williams and Ager (2010)	Vale of York	54.20361	-1.36398
Valence	819-840	Haertle (1997)	Valence	44.93347	4.890808
Vallée de la Risle	814-877	Coupland and Moesgaard (2012)	Vale of Risle	49.424	0.725
Vercelli	768-814	Morrison and Grunthal (1967)	Vercelli	45.32255	8.41844
Verdun I	875-877	Haertle (1997)	Verdun	49.15952	5.382316
Verdun II	881-887	Morrison and Grunthal (1967)	Verdun	49.15952	5.382316
Vereb	858-024	Morrison and Grunthal (1967)	Vereb	47.31867	18.61802
Vernon	814-877	Coupland (2020)	Vernon	49.091052	1.483426
Vicq sur Gartempe	814-877	Coupland (2020)	Vicq sur Gartempe	46.721302	0.862012
Vire	843-877	Morrison and Grunthal (1967)	Vire-Normandie	48.83919	-0.89
Vrigny	843-877	Haertle (1997)	Vrigny	48.08167	2.243889
Wagenborgen	814-877	Haertle (1997)	Wagenborgen	53.25713	6.93525
Westerkief I	814-877	Sarfati et al. (1999)	Westerkief	52.89494	4.93322
Westerkief II	814-877	Besteman (2006)	Westerkief	52.89494	4.93322
Wiesbaden-Biebrich	717-814	Morrison and Grunthal (1967)	Wiesbaden-Biebrich	50.050115	8.237668
Wijk bij Duurstede I	793-822	Morrison and Grunthal (1967)	Wijk-Bij-Duurstede	51.971869	5.344562
Wijk bij Duurstede II	752-768	Van Es and Verwers (1980)	Wijk-Bij-Duurstede	51.971869	5.344562
Wijk bij Duurstede III	768-820	Van Es and Verwers (1980)	Wijk-Bij-Duurstede	51.971869	5.344562
Wijk bij Duurstede IV	823-840	Dijkstra (2005)	Wijk-Bij-Duurstede	51.971869	5.344562
Wijk bij Duurstede V	751-768	Coupland (2020)	Wijk-Bij-Duurstede	51.971869	5.344562
Wirdum	814-877	Coupland (2020)	Wirdum	53.149585	5.803308
Worms	814-840	Coupland (2020)	Worms	49.632241	8.36221
Yde	814-877	Morrison and Grunthal (1967)	Yde	53.11143	6.58365
Yonne	814-840	Coupland (2014)	Yonne	47.89753	3.588695
York	751-887	Dolley (1965)	York	53.95333	-1.08342
Yronde	843-877	Morrison and Grunthal (1967)	Yronde	45.6133	3.25481
Zelzate	814-877	Morrison and Grunthal (1967)	Zelzate	51.19753	3.81463
Zetel	768-793	Völckers (1965)	Zetel	53.4146	7.9699
Zillis	888-949	Zäch (2001)	Zillis	46.6355	9.44514
Zuidlaren	875-894	Haertle (1997)	Zuidlaren	53.09231	6.679414

Appendix Table B.15: Carolingian Hoards, Part VI

Signatures	Approx. Nomisma ID	Location	Notes
AHM	hamadhan		
AIRAN, AYLAN	hulwan	Eran-asankar-Kavad	
AM	amol	Amol, Khorasan	
APL, APR	nishapur		
ART, TART	ardashir_khurrah	TART: Tawwaj as dependency of Ardashir Khurra	
AT	adurbadagan		
AU, AW	suq_al-ahwaz	AU is used by Al-Ush, we interpret it as "AW", Hormizd-Ardashir	
AY, AYL	al-sus	Eran-khvarrah-Shapur. AYL: British Museum says "possibly referring to Susa."	
AS	ctesiphon	Following the coding in FLAME.	
BBA	ctesiphon	Court mint, probably at Ctesiphon (Gyselen)	
BCLA, BJRA, DS, DST	al-basrah	Mallon-McCorgray interprets BCLA as al-Basra. Accoring to Schindel (2005) BJRA is al-Basra.	
BISH, BYS, BYSH	bishapur		
BN, BRMKRMAN, DL, DR, GLM,	kirman	Multiple mints that are in Kirman province.	
KL, KLMAN, KLMANLCN, KR,			
KRAMAN H P, KRMAN, KRMAN			
W ST, KRMAN-GY, KRMAN-NAR,			
KRMAN-NAW, NAL, NAR			
D', DA, DAP	darabjird		
DAP	fasa		
GD	jayy		
GU, GW	gorgan	We follow Schindel (2005) in attributing GW to Gorgan (after Yazdegerd I). Gyselen (1977) attributes GU to Gorgan.	
HL	harat		
HWC	jundi_sabur		
LAM, RAM	ramhurmuz		
LD, RD	rayy		
LYW, RIU	rev-ardashir	Bivar (1970) associates RIU with LYW, and confirms Nö's interpretation as Rev-Ardashir	
MA	masabadhan		
MB, MY, PL	maysan		
ML, MR	marw		
NH, NIHJ, NYHC, WH, WYHC	ctesiphon*	NH, WH: Veh-Ardashir. On WYHC, Album (2011) : "A mint in northern Iraq, ostensibly the treasury mint near Ktesiphon prior to the AH50s, and thereafter, for a series dated AH67-73, Arrajan". We follow Album (2011) , Schindel (2005) , and others in attributing it to Ctesiphon before AH50, then Arrajan.	
NHR	nahr_tira		
NIH, WYH	bihqubadh_af-asfal		
NIHJ	arrajan	Almost certainly the same as WYHC.	
NY, NYH	antiocheia_persis	NY: Nihawand. For NYH, Schindel (2005) suggests Nihawand.	
SHI	shiraz		
SK	zaranj, sijistan		
ST	istakhr		
SY	fars_shiraz	Unlocated mint, probably in Fars province (or Kirman, as has sometimes been suggested).	
TPWRSTAN	tabaristan		
YZ, ZR, GZ	yazd		

Appendix Table B.16: Sasanian mint codings

References

- ABDUL WAHAB, H. (2012): “al-Abbāsiyya,” in *Encyclopaedia of Islam*, ed. by P. Bearman, T. Bianquis, C. Bosworth, E. van Donzel, and W. Heinrichs, Brill.
- AL BAKRI, M. D. (1973): “Kanz al-’Utayfiyah al-fiddi,” *al-Maskukat*, 4.
- AL CHOMARI, A. A. (2020): *Le commerce régional et international au Xe siècle en Syrie: D’après le trésor monétaire de Buseyra et d’autres trésors de l’époque*, Archaeopress.
- AL-NAQSHBANDI, N. (1949): “Rare Islamic coins in the Iraq Museum,” *Sumer*, 5, 199–202.
- (1950): “The Zakho Treasure,” *Sumer*, 6, 177–188.
- (1951): “The Zakho Treasure,” *Sumer*, 7, 165–172.
- (1952): “The Zakho Treasure,” *Sumer*, 8, 220–227.
- (1954): “Khidr Elias Treasure,” *Sumer*, 10, 180–196.
- AL ’USH, A.-F. (1954-1955): “Al-Kanz al-dhahabī al-umawī,” *Annales Archeologiques de Syrie*, IV-V, 21–28.
- (1972a): *Kunz umm ḥajarah al-fiddi (Trésor de monnaies d’argent trouvé à Umm Hajarah)*, Damascus.
- (1972b): *The silver hoard of Damascus: Sasanian, Arab-Sasanian, Khuwarizmian, and Umayyad kept in the National Museum of Damascus*, Damascus: Direction General of Antiquities and Museums.
- (1982): *Monnaies Aghlabides, étudiées en relation avec l’histoire des Aghlabides*, Institut Français de Damas.
- ALBUM, S. (1971): “An Umayyad hoard from Afghanistan,” *Museum Notes (American Numismatic Society)*, 17, 241–246.
- (2011): “Checklist of Islamic Coins, 3rd Edition,” .
- ALFARO ASINS, C. (1992): “La colección de moneda hispano-árabe del Museo Arqueológico Nacional de Madrid,” *III Jarique de Numismática hispano-árabe. Actas (Museo Arqueológico Nacional. Madrid, 13-16 diciembre 1990)*, 39–75.
- ÁLVAREZ, M. D. L. Á. P. (1993): “Tesorillo de monedas árabes de Moraleja (Cáceres),” *Alcántara: revista del Seminario de Estudios Cacereños*, 37–44.
- AMERICAN NUMISMATIC SOCIETY (2023): “MANTIS Database,” <https://numismatics.org/collection>, accessed: 2023-07-01.
- ARIZA ARMADA, A. (1988): “Un tesorillo de dirhames de Baena (Cordoba),” *Arqueología Medieval*, 2, 137–140.
- ARROYO ILERA, R. (1989): “Descripción y análisis de las monedas árabes de Sinarcas (Valencia),” in *Actas del VII Congreso Nacional de Numismática, Madrid, Museo Casa de la Moneda*, 467–479.
- ARSLAN, E. A. (2005): “Il Repertorio dei ritrovamenti di moneta altomedievale (489-1002),” .
- ARTUK, I. (1966): *Denizbaci definesi*, Ankara: Türk Tarih Kurumu.
- ASENCIO, J. M. R. (1962): “Tesoro de dirhemes califales hallado en Jaén,” *Boletín del Instituto de Estudios Giennenses*, 109.
- ÁVILA, R. C. AND A. R. H. PAREJA (1999): “Un conjunto monetario andalusí de plata emiral procedente de la Junta de los Ríos (Priego de Córdoba),” *Antiquitas*, 125–136.
- AYALA RUIZ, J. A. AND C. GOZALBES CRAVIOTO (1996): “Un tesorillo califal aparecido en la Cala de Mijas-Costa (Málaga),” *Gaceta Numismática*, 121, 61–76.

- BAIGL, J.-P., A. CLAIRAND, AND O. JEANNE-ROSE (1995): “Trovailles récentes de monnaies carolingiennes dans les Deux-Sèvres: petits trésors et monnaies isolées,” *Bulletin de la Société française de numismatique*, 50, 1152–1154.
- BALAGUER, A. M. (1999): *Història de la moneda dels comtats catalans*, vol. 2, Institut d’Estudis Catalans.
- BALDUS (2006): *Didyma. III. Ergebnisse der Ausgrabungen und Untersuchungen seit dem Jahre 1962. 3. Fundmünzen aus den Jahren 1962-1998*, Deutsches Archäologisches Institut.
- BARTOLOMEI, I. A. (1857): “Description d’une trouvaille de 200 dirhems koufiques, faite aux environs de Tiflis, en 1857,” *Bulletin de l’Académie impériale des sciences de St. Petersburg*, 3.
- BATES, M. L. (1978): “A hoard of dirhams found at Nippur,” *Excavations at Nippur, twelfth season*, 126–138.
- BENOIT, P. AND P. BRAUNSTEIN (1983): *Mines, carrières et métallurgie dans la France médiévale*, Paris: Edition du CNRS.
- BERNAREGGI, E. (1977): “I tremissi longobardi e carolingi del ripostiglio di Ilanz nei Grigioni,” *Quaderni ticinesi di numismatica*, VI.
- (1983): “Carolingian gold coins from the Ilanz hoard,” in *Studies Philip Grierson*, 127–135.
- BESTEMAN, J. (2006): “Westerkliif II, a second Viking silver hoard from the former island of Wieringen; with a contribution by Gert Rispling and Simon Coupland,” *Jaarboek voor Munt-en Penningkunde*, 93, 5–80.
- BIJSTERVELD, A., N. NEUFEGLISE, AND B. VAN DER VEEN (2000): “Een heilige plaats onder de grond. Aalst en zijn middeleeuwse kerk,” *Brabants Heem*, 52, 81–92.
- BIVAR, A. D. H. (1970): “Appendix: The Sasanian Coin from Qumis,” *Journal of the Royal Asiatic Society of Great Britain and Ireland*, 156–158.
- BLACKBURN, M. A. (1989): “The Ashdon (Essex) hoard and the currency of the Southern Danelaw in the late ninth century,” *British Numismatic Journal*, 59, 13–38.
- BOMPAIRE AND DEPIERRE (1989): “le trésor carolingien de dijon, rue du chapeau rouge,” Tech. rep., bulletin de la société française de numismatique.
- CANO ÁVILA, P. (1989): “Algunos dirhemes hallados cerca de Alcaudete (Jaén),” in *VII Congreso Nacional de Numismática: Memoria*, 489–503.
- (2014): “Hallazgo de dírhemes del califato Omeya de Al-andalus en Montellano (Sevilla),” *Revista Numismática OMNI*, 149–164.
- (2016): “Hallazgo de dírhems del Califato omeya de al-Andalus en Bormujos (Sevilla),” in *Patrimonio numismático y museos: actas XV Congreso Nacional de Numismática. Madrid, 28-30 de octubre de 2014*, Museo Casa de la Moneda, 1133–1148.
- CANO ÁVILA, P. AND C. M. GÓMEZ (2008): “Hallazgo de un tesorillo de dírhemes del imamato fatimí y del califato omeya de al-Andalus en El Pedroso (Sevilla). El Pedroso III,” in *Moneda y arqueología: actas XIII Congreso Nacional de Numismática*, Universidad de Cádiz, 799–824.
- CANO ÁVILA, P. AND C. MARTÍN GÓMEZ (2006): “Hallazgo de un tesorillo de dírhemes del califato omeya de al-Andalus en El Pedroso (Sevilla),” in *Actas XII Congreso Nacional de Numismática: Madrid. 25-27 de octubre de 2004*, Real Casa de la Moneda, Fábrica Nacional de Moneda y Timbre, 443–464.
- CANO ÁVILA, P. AND C. I. MARTÍN GÓMEZ (2005): “Tesoro de dirhemes emirales hallado en La Rinconada (Sevilla),” in *XIII Congreso Internacional de Numismática, Madrid, 2003: actas-proceedings-actes*, Ministerio de Cultura, 1553–1566.

- CANO ÁVILA, P. AND C. I. MARTÍN GOMEZ (2011): “Hallazgo de dírhemes del emirato omeya de al-Ándalus en Niebla (Huelva),” in *Ars metallica. Monedas y medallas: Nules-Valencia, 25-27 de octubre de 2010*, Museo Casa de la Moneda, 817–834.
- CANTO GARCÍA, A. (1988): “Tesoro de moneda emiral del siglo II de la Hégira, conservado en el MAn [Museo Arqueológico nacional],” *Actas I Jarique de Estudios Numismáticos Hispano-Árabes, Zaragoza, Institución Fernando el Católico*, 147–162.
- (1993): “Sobre un pequeño hallazgo de moneda emiral en Martos (Jaén),” *Antiquitas*, 63–66.
- (2001): “La moneda hispanoárabe y su circulación por Navarra,” in *La moneda en Navarra: Museo de Navarra, Pamplona: exposición 31 de mayo a 25 de noviembre de 2001*, Fundación Caja Navarra, 73–82.
- (2014): “El tesoro de Tarancón (Cuenca, 1893): nuevos datos e imágenes sobre el mismo,” *Revista Numismática OMNI*, 21–64.
- (2019): “Hallazgos de Moneda Andalusi y Documentacion,” Tech. rep., Universidad Autónoma de Madrid.
- CANTO GARCÍA, A., R. CLAPÉS, AND W. JABŁOŃSKA (2020a): “Un hallazgo de monedas califales en el arrabal occidental de Córdoba.”
- CANTO GARCÍA, A. AND F. M. ESCUDERO (2012): “El tesoro de monedas árabes de Carmona y una rectificación de A. Vives Escudero,” *Cuadernos de Prehistoria y Arqueología de la Universidad Autónoma de Madrid*, 38.
- CANTO GARCÍA, A., G. GARCÍA RUIZ, AND L. RUIZ QUINTANAR (1997): “Hallazgo de monedas califales de Marroquines Bajos (Jaén),” *Arqueología y territorio medieval*, 4, 81–101.
- CANTO GARCÍA, A. AND W. JABŁOŃSKA (2019): “Algunas precisiones sobre el hallazgo de dinares califales de la calle San Pedro (Murcia),” *Tudmir: Revista del Museo Santa Clara, Murcia*, 5–13.
- CANTO GARCÍA, A. AND E. MARSAL MOYANO (1988): “Hallazgo de moneda emiral de Iznájar (Granada),” *Al-Qantara*, 9, 427.
- CANTO GARCÍA, A. AND F. MARTÍN ESCUDERO (2007): “El hallazgo de moneda califal de Fontanar (Córdoba),” *Documenta & Instrumenta*, 129–156.
- (2009): “Hallazgos monetarios islámicos en Algeciras,” *Caetaria: revista bianual de Arqueología*, 125–130.
- CANTO GARCÍA, A., F. MARTÍN ESCUDERO, AND W. JABLONSKA (2020b): *El hallazgo de monedas califales del Parque Cruz Conde (Córdoba)*, Museo Casa de la Moneda.
- CARDON, T., J. C. MOESGAARD, R. PROT, AND P. SCHIESSER (2008): “Le premier trésor monétaire de type viking en France. Denier inédit d’Eudes pour Beauvais,” *Revue numismatique*, 6, 21–40.
- CARON, E. (1882): *Monnaies féodales françaises*, vol. 1, Rollin et Feuardent.
- CERRATO, C. B. AND A. M. ESQUIVEL (2019): “Conjunto de dírhames califales hallado en Zamora: estudio e interpretación,” *Archivo español de arqueología*, 92, 287–306.
- CIAMPOLTRINI, G., E. ABELA, AND S. BIANCHINI (2001): “Lucca: un contesto con monete del X secolo dell’area dell’ex ospedale Galli Tassi,” *Bollettino di Numismatica*, 153–166.
- CODERA Y ZAIDÍN, F. (1892): “Tesoro de monedas árabes, descubierto en Alhama de Granada,” *Boletín de la Real Academia de la Historia*, XX, 442–449.
- (1913): “Monedas árabes orientales encontradas en Aragón,” *Boletín de la Real Academia de la Historia*, LXIII, 552–556.
- CORNU, G. (1983): *Atlas du monde Arabo-Islamique à l'époque classique: IX.-X. siècles*, Brill.

- COUPLAND, S. (1991): “The early coinage of Charles the Bald, 840-864,” *The Numismatic Chronicle* (1966-), 121–158.
- (1995): “Bilan Société Française de Numismatique,” Tech. rep., Société Française de Numismatique.
- (2010): “Le trésor de Bourgneuf-en-Retz et les monnaies de Melle au monogramme d’un roi Charles’,” *Bulletin de la Société française de numismatique*, 65, 190–3.
- (2011a): “A checklist of Carolingian coin hoards 751-987,” *The Numismatic Chronicle*, 171, 203–256.
- (2011b): “The Roermond coins reconsidered,” *Medieval and Modern Matters*, 2, 25–50.
- (2014): “A supplement to the checklist of Carolingian coin hoards, 751-987,” *The Numismatic Chronicle* (1966-), 174, 213–222.
- (2018): “Les monnaies de Melle sous Louis le Pieux’,” *Mine, métal, monnaie, Melle. Les voies de la quantification de l’histoire monétaire du haut Moyen Âge*, 259–278.
- (2019): “Der Karolingschatz von Bassenheim,” Tech. rep., Münzfunde aus Rheinland-Pfalz 36.
- (2020): “A Second Supplement to the Checklist of Carolingian coin hoards, 751-987,” *The Numismatic Chronicle*, 180, 259–289.
- COUPLAND, S. AND J. C. MOESGAARD (2012): “Trésors monétaires peut-être enfouis lors des premiers raids vikings dans la vallée de la Seine’,” *Bulletin de la Société française de numismatique*, 67, 222–229.
- CRAVIOTO, C. G. (2016): “Tesorillo de monedas andalusíes de Castillejos de Quintana (Pizarra, Málaga),” in *Patrimonio numismático y museos: actas XV Congreso Nacional de Numismática. Madrid, 28-30 de octubre de 2014*, Museo Casa de la Moneda, 1353–1360.
- CRAVIOTO, C. G. AND J. A. AYALA (1995): “Un tesorillo de monedas del emirato independiente hallado en el Cerro de la Fuensanta (Antequera-Casabermeja-Colmenar. Málaga),” *Mainake*, 235–242.
- CRUYSHEER, A. AND B. J. V. DER VEEN (2015): “De Karolingische schatvondst Bikbergen 1992,” Tech. rep., De Beeldenaar.
- CURTA, F. (2005): “Byzantium in Dark-Age Greece (the numismatic evidence in its Balkan context),” *Byzantine and Modern Greek Studies*, 29, 113–146.
- DAIM, F. AND E. LAUERMANN (2006): *Das frühungarische Reitergrab von Gnadendorf (Niederösterreich)*, Verlag des Römisch-Germanischen Zentralmuseums.
- DAJANI, A. (1951): “A hoard of Byzantine gold coins from Awarta, Nablus,” *Annual of the Department of Antiquities, Jordan*, 1, 41–43.
- DE BENEDITTIS, G. AND J. LAFaurie (1998): “Trésor de monnaies carolingiennes du VIIIe siècle trouvé à Larino (Italie, Molise),” *Revue Numismatique*, 6, 217–243.
- DENAIS, J. (1908): “Catalogue illustré du musée de Beaufort-en-Vallée,” Tech. rep.
- DHÉNIN, M. (1989): “Le trésor monétaire de Breuvery-sur-Coole (Marne),” *Comptes rendus des séances de l’Académie des Inscriptions et Belles-Lettres*, 133, 811–823.
- DHÉNIN, M. (2006): “Les monnaies carolingiennes d’Arpajon (anciennement Chartres), Essonne,” *Bulletin de la Société Française de Numismatique*, 61, 226–230.
- DIJKSTRA, M. F. P. (2005): “‘Middeleeuwse gulle gaven, greppels en waterputten. De opgraving Wijk bij Duurstede-David van Bourgondieweg?’,” 26.

- DIMIAN, I. (1957): "Cîteva descoperiri monetare bizantine pe teritoriul RPR," *Studii si cercetari de numismatica*, 1, 189–216.
- DOLLEY, M. (1965): "New Light on the Pre-1760 Coney Street (York) Find of Coins of the Duurstede Mint.," *Jaarboek Voor Munt-en Penningkunde*, 52, 1966.
- DOMÉNECH BELDA, C. (1992): "Revisión de un hallazgo de monedas árabes de Elche (Alicante)," .
- (1997): "Circulación monetaria durante el período islámico en el País Valenciano," .
- DOMÉNECH BELDA, C. AND S. GUTIÉRREZ LLORET (2006): "Viejas y nuevas monedas en la ciudad emiral de Madīnat Iyyuh (El Tolmo de Minateda, Hellín, Albacete)," *Al-Qantara*, 27, 337–374.
- DOMÉNECH BELDA, C. AND J. TRELIS (1990): "Hallazgos numismáticos de época islámica en Crevillente (Alicante)," *III Jarique de Numismática Hispano-árabe*.
- DOMÉNECH-BELDA, C. ET AL. (2013): "La circulation de monnaie carolingienne dans la péninsule ibérique. À propos d'un denier de l'atelier de Roda," *Revue Numismatique*, 6, 383–410.
- DUPLESSY, J. (1985): "Les trésors monétaires médiévaux et modernes découverts en France, vol. 1, 751-1223," .
- EUSTACHE, D. (1956): "Monnaies musulmanes trouvées à Volubilis," *Hespérus: Archives berbères et bulletin de l'institut des hautes études-marocaines*, XLIII.
- FAGERLIE, J. M. (1974): "A Byzantine "Sicilian" Hoard," in *Studies George C. Miles*, 175–183.
- FLAME (2023): "Framing the Late Antique and early Medieval Economy," <https://coinage.princeton.edu/>, accessed: 2023-07-01.
- FOMIN, A. V. AND L. KOVÁCS (1987): *The tenth century Máramaros County ("Huszt") dirham hoard*, Magyar Numizmatikai Társulat.
- FONTENLA BALLESTA, S. (1998): "Un tesorillo de plata medieval del Tijan (Turre, Almeria)," Tech. rep., Axarquia 3.
- FÜEG, F. (2007): *Corpus of the Nomismata from Anastasius II to John I in Constantinople, 713-976*, Classical Numismatic Group.
- GACHET, A. (1993): *Présentation d'un trésor monétaire des premiers temps de l'Islam : le trésor d'Afak*.
- GEDAI, I. (1993): "The denars of Luis the Child in a grave find in Hungary," *Numismatiche e antichità classica*, 273–278.
- GEISER, A. (1990): *Un trésor de monnaies de Pépin le Bref trouvé à La Tour-de-Peilz (VD), nécropole du Clos d'Aubonne*, Gazette numismatique suisse.
- GONZÁLEZ GARCÍA, A. AND D. MARTÍNEZ CHICO (2017): "Cuatro hallazgos aislados de dinares epigráficos latinos hispano-musulmanes en Jaén," .
- GRAÑEDA MIÑÓN, P. (2021): "Reexcavando en el Museo Arqueológico Nacional: los tesoros de Valencia del Ventoso (Badajoz) y Osuna (Sevilla)," Tech. rep., XVI Congreso Nacional de Numismática: Tesoros y hallazgos monetarios: protección, estudio y musealización (Barcelona, 28-30 de noviembre de 2018).
- GRIERSON, P. (1968): *Catalogue of the Byzantine Coins in the Dumbarton Oaks Collection and in the Whittemore Collection, 2: Phocas to Theodosius III, 602-717*, Dumbarton Oaks.
- (1973): *Catalogue of the Byzantine Coins in the Dumbarton Oaks Collection and in the Whittemore Collection, 3: Leo III to Nicephorus III, 717-1081*, Dumbarton Oaks.

- GUILLEMAIN, J. (1993): "Deux trouvailles de monnaies médiévales au nord de Lyon," *Bulletin de la Société Française de Numismatique*.
- GYSELEN, R. (1977): "Trésor de monnaies sasanides trouvé à Suse. I. Inventaire," *Cahiers de la Délégation archéologique française en Iran*, 7, 61–74.
- GYSELEN, R. AND L. KALUS (1983): *Deux trésors monétaires des premiers temps de l'Islam*, Bibliothèque Nationale de France, Paris.
- GYSELEN, R. AND A. NÈGRE (1982): "Un trésor de Gazīra (Haute-Mésopotamie): monnaies d'argent sasanides et islamiques enfouies au début du IIIe siècle de l'Hégire/IXe siècle de notre ère," *Revue Numismatique*, 6, 170–205.
- HAERTLE, C. M. (1997): *Karolingische Münzfunde aus dem 9. Jahrhundert*, Böhlau.
- HAKIEM, A. A.-A. D. (1977): "A critical and comparative study of early Arabian coins on the basis of Arabic textual evidence and actual finds," Ph.D. thesis, University of Leeds.
- HEBERT, R. J. (1966): "Notes on an Umayyad hoard from Khurāsān," *Museum Notes (American Numismatic Society)*, 12, 157–163.
- HEIDEMANN, S., J. RIEDERER, AND D. WEBER (2014): "A Hoard from the Time of Yazdgard III in Kirmān," *Iran*, 52, 79–124.
- HEIDEMANN, S., T. SCHIERL, AND F. TEICHNER (2018): "Coins from the seaside. An Emiral silver coin hoard from a harbour settlement on the Cerro de Vila (Vilamoura, Algarve, Portugal)," *Al-Qantara*, 39, 169–224.
- HOGE, R. (1997): "A Parcel of Mainly'Abbāsid Gold Coins," *The Numismatic Chronicle*, 157, 239–247.
- HUCHER, E. F. F. (1845): *Essai sur les monnaies frappées dans le Maine*, de Gallienne.
- HUSZÁR, L. (1955): *Das Münzmaterial in den Funden der Völkerwanderungszeit im mittleren Donaubecken*, Akadémiai Kiadó.
- IBRAHIM, T. B. H. AND A. CANTO GARCÍA (1991): "Hallazgo emiral en Puebla de Cazalla (Sevilla)," *Numisma: revista de Estudios Numismáticos*, 69–86.
- ILISCH, L. (1979): "Ein Dirhamfund des frühen 10. Jahrhunderts aus der Gegend von Diyarbakir," *Münstersche Numismatische Zeitung*.
- (1990): "Whole and fragmented Dirhams in near eatsern hoards," in *Sigtuna papers: proceedings of the Sigtuna symposium on Viking-age coinage, 1-4 june 1989*, ed. by K. Jonsson and B. Malmer, Kungl. Vitterhets Historie och Antikvitets Akademien.
- (2005): "Der Steckborner Schatzfund von 1830 und andere Funde nordafrikanischer Dirhams im Bereich des Karlsreiches," in *Simposio Simone Assemani sulla monetazione islamica*, ed. by G. Gorini, Esedra.
- JEANNE-ROSE, O. (1996): "Troupes isolées de monnaies carolingiennes en Poitou: inventaire provisoire," *Revue numismatique*, 6, 241–283.
- JOHNSTON, P. (1986): *The archaeology of the Channel Islands*, Phillimore.
- JUNGFLEISCH, M. (1949): "La trouvaille du cimetière de Sainte-Barbe à Babylone d'Egypte," *Revue Numismatique*, 11, 165–169.
- KASDAGLI, A.-M. (2018): *Coins in Rhodes: From the monetary reform of Anastasius I until the Ottoman conquest (498 - 1522)*, Archaeopress.
- KHODZHANIYAZOV, T. AND L. TREADWELL (1998): "The Marv hoard of early Islamic dirhams," *Iran*, 36, 85–94.

- KIRKBRIDE, A. (1951): “Recent Finds of Arabic Coins,” *Annual of the Department of Antiquities, Jordan*, 1, 17–19.
- KLUGE, B. (1993): “Fernhandel und Geldwirtschaft: Beiträge zum deutschen Münzwesen in sächsischer und salischer Zeit,” .
- KOVÁCS, L. (1989): *Münzen aus der ungarischen Landnahmezeit: archäologische Untersuchung der arabischen, byzantinischen, westeuropäischen und römischen Münzen aus dem Karpatenbecken des 10. Jahrhunderts*, Akadémiai kiadó.
- LAFAURIE, J. (1965): “Deux trésors monétaires carolingiens: Saumeray (Eure-et-Loir), Rennes (Ille-et-Vilaine),” *Revue Numismatique*, 6, 262–305.
- LAFLI, E., C. LIGHTFOOT, AND M. RITTER (2016): “Byzantine coins from Hadrianoupolis in Paphlagonia,” *Byzantine and Modern Greek Studies*, 40, 187–206.
- LAGUMINA, B. (1904): “Ripostiglio di monete arabe rinvenuto in Grgenti,” *Archivio storico siciliano*, 29.
- LLOYD, S. (2023): “Post-Reform Umayyad Dirhams and their Mint Towns,” <https://www.angelfire.com/ny3/vaguebrit/>, accessed: 2023-07-01.
- LOCKHART, L. (2012): “Dīnawar,” in *Encyclopaedia of Islam*, ed. by P. Bearman, T. Bianquis, C. Bosworth, E. van Donzel, and W. Heinrichs, Brill.
- LOWICK, N. (1975): “An early tenth century hoard from Isfahan,” *The Numismatic Chronicle*, 110–154.
- (1983): “The Sinaw Hoard of Early Islamic Coins,” *The journal of Oman studies*, 6, 199–230.
- LOWICK, N. AND J. NISBET (1968): “A hoard of dirhems from Ra’s al-Khaimah,” *The Numismatic Chronicle*, 231–240.
- MA’AYEH, F. S. (1962): “A Hoard of Omayyad Dinars from Orif,” *Annual of the Department of Antiquities, Jordan*, 6/7, 76–97.
- MALEK, H. M. (1996): “A Hoard Group Of Drachms of the Dābūyid Ispahbads and Early’Abbāsid Governors of Tabaristān,” *The Numismatic Chronicle*, 156, 175–191.
- MĂNUCU-ADAMEȘTEANU, G. (2016): *Monede bizantine descoperite în Dobrogea: monede bizantine descoperite în mediul rural din nordul Dobrogei, Secolele VII-XV*, Muzeul Municipiului București.
- MARCOS POUS, A. AND A. M. VICENT ZARAGOZA (1992): “Los tesorillos de moneda hispano-árabe del Museo Arqueológico de Córdoba,” *III Jarique de Numismática Hispano-Árabe*, 192–215.
- MARINHO, J. R. (1993): “As moedas hispano-muçulmanas da coleção Justino Cumano numa carta de Pascual de Gayangos,” Tech. rep., III Jarique de numismática hispano-arabe.
- MARTÍN, M. V. AND S. P. MARTÍN (2002): “Del hallazgo de dirhames emirales en Domingo Pérez (Iznalloz, Granada),” *Al-Qantara*, 23, 155–192.
- (2006): “Sobre el hallazgo emiral del Campo de la Verdad (Córdoba),” in *Actas XII Congreso Nacional de Numismática: Madrid. 25-27 de octubre de 2004*, Real Casa de la Moneda, Fábrica Nacional de Moneda y Timbre, 403–416.
- MARTÍN ESCUDERO, F. (2001): “El hallazgo omeya de Baena: un tesoro olvidado,” in *IV Jarique de numismática andalusí*, Universidad de Jaén, 81–94.
- (2003): “Sobre el hallazgo de dinares del Hospital Militar de Zaragoza (1858),” in *XI Congreso Nacional de Numismática: actas, Zaragoza, 2002*, Real Casa de la Moneda, Fábrica Nacional de Moneda y Timbre, 257–268.

- (2011): “Las monedas de Al-Andalus: de actividad ilustrada a disciplina científica,” *Las monedas de Al-Andalus*, 1–394.
- (2012): “Monedas que van, monedas que vienen... circulación monetaria en época de cambios,” *De Mahoma a Carlomagno. Los primeros tiempos (siglos vii–ix)*. XXXIX Semana de Estudios Medievales de Estella, 311–350.
- MARTÍN ESCUDERO, F., M. T. CASAL GARCÍA, AND A. CANTO GARCÍA (2023): “Feluses, dírhams y monedas en el arrabal de Šaqunda (Córdoba): análisis y clasificación tipológica.” .
- MARTÍNEZ ENAMORADO, V. (2004): “Frontera de al-Andalus. El Valle del Tiétar en el contexto de la Tagr al-Awsat,” .
- MCCORMICK, M. (2001): *Origins of the European economy: communications and commerce AD 300-900*, Cambridge University Press.
- METCALF, D. M. (1992): „The Rome (forum) hoard of 1883 ,” *British Numismatic Journal*, 62, 63–96.
- MILES, G. C. (1960): “A Hoard of Arab Dirhems from Algarve, Portugal,” *Museum Notes (American Numismatic Society)*, 9, 219–230.
- MINAROVICOVA, E. (2007): “Novoobjavený rímsky denár z hromadného nálezu rímskych mincí z Vyškovieč nad Ipľom, okr. Levice,” Tech. rep., Slovenska Numizmatika.
- MIRNIK, I. A. (1981): *Coin hoards in Yugoslavia*, BAR Publishing.
- MišKEC, A. (2002): *Die Fundmünzen der römischen Zeit in Kroatien. Abt. 18. Istrien*, von Zabern.
- MOESGAARD, J. C. (1997): “A hoard from the Blois region and the proto-feudal coinage of Blois, c. 920/40,” *The Numismatic Chronicle (1966-)*, 157, 196–205.
- (2003): “Le trésor de Saint-Taurin à Evreux (Xe siècle),” *Cahiers Numismatique*, 158, 23–40.
- (2010): “Le “maillon manquant” entre Quentovic et Rouen?” *Bulletin de la Société française de numismatique*, 65, 57–61.
- MORONY, M. G. (1982): “Continuity and Change in the Administrative Geography of Late Sasanian and Early Islamic al-Iraq,” *Iran*, 20, 1–49.
- MORRISON, K. F. AND H. GRUNTHAL (1967): *Carolingian Coinage*, New York: American Numismatic Society.
- MORRISSON, C. (2017): “Coinage in Byzantine Anatolia,” in *The Archaeology of Byzantine Anatolia. From the End of Late Antiquity to the Coming of the Turks*, ed. by P. Niewöhner, Oxford University Press.
- MORRISSON, C. AND J.-N. BARRANDON (1988): “La trouvaille de monnaies d’argent byzantines de Rome (VIIe–VIIIe s.): Analyses et chronologie,” *Revue numismatique*, 6, 149–165.
- MORRISSON, C., V. POPOVIĆ, AND V. IVANIŠEVIĆ (2006): *Les Trésors monétaires byzantins des Balkans et d’Asie Mineure (491-713)*, Lethielleux.
- MOSSER, S. M. (1935): *A bibliography of Byzantine coin hoards*, New York: American Numismatic Society.
- MOTOS GUIRAO, E. AND A. DÍAZ GARCÍA (1985): “Tesorillo árabe de Tígnar,” *Miscelánea de estudios árabes y hebraicos. Sección Árabe-Islam. Vol. 34 (1985)*.
- MUSEO ARQUEOLÓGICO DE MURCIA (2014): “Tesoros. Materia ley y forma. Catalogue of the exhibition December 2014 to April 2015,” Tech. rep., Museo Arqueológico de Murcia.
- MÚZEUM MÓRA FERENC (2002): *Studia archaeologica VIII*, Szeged: Múzeum Móra Ferenc.
- NAVASCUÉS Y DE PALACIOS, J. (1957): “Tesoro hispano-árabe encontrado en Trujillo (Cáceres),” *Numario Hispánico*, 6, 5–28.

- (1958): “Tesorillo de monedas de plata del califato cordobés y fatimíes,” *Numario Hispánico*, 7, 207–210.
- (1961a): “Tesoro de Cihuela (Soria),” *Numario Hispánico*, X, 173–175.
- (1961b): “Tesoro de moneda califal,” *Numario Hispánico*, X, 169–173.
- NIKOLAOU, Y. AND I. TOURATSOGLOU (2019): *The Circulation of Byzantine Coinage in Mainland Greece and the Balkans. The Hoard Evidence: 5th - 15th centuries*, Athens: Friends of the Numismatic Museum.
- NOMISMA (2023): “The Nomisma.org project,” <https://nomisma.org/>, accessed: 2023-07-01.
- NOONAN, T. S. (1980): “When and how dirhams first reached Russia: a numismatic critique of the Pirenne theory,” *Cahiers du monde russe et soviétique*, 401–469.
- OBERLÄNDER-TÂRNOVEANU, E. (2001): “From the Late Antiquity to the Early Middle Ages—the Byzantine Coins in the territories of the Iron Gates of the Danube from the second half of the 6th Century to the first half of the 8th Century,” *Etudes byzantines et post-byzantines*, 4, 29–69.
- ORTEGA, M. R. R., J. B. ESTELLA, R. G. TORRES, AND M. M. M. MARQUÉS (2006): “Estudio de un conjunto monetario de época califal procedente del Valle del Guadajoz (Córdoba),” in *Actas XII Congreso Nacional de Numismática: Madrid. 25-27 de octubre de 2004*, Real Casa de la Moneda, Fábrica Nacional de Moneda y Timbre, 417–441.
- PALMA GARCÍA, F. AND R. SEGOVIA SOPO (2007): “Un tesorillo de moneda islámica aparecido en Morería (Mérida),” Tech. rep., Biblioteca Virtual Miguel de Cervantes.
- PARVÉRIE, M. (2014): “Corpus des monnaies arabo-musulmanes des VIII et IX siècles découvertes dans le Sud de la France,” *Revista Numismática OMNI*, 79–100.
- (2018): “La circulation des deniers de l’Aquitaine carolingienne en Al-Andalus; un réexamen des trésors ‘España-1, 2 et 3’,” *Bulletin de la Société numismatique de Limousin*, 25, 4–16.
- (2019): “Supplément au corpus des monnaies arabomusulmanes découvertes en France,” *Revista Numismática OMNI*, 283–294.
- PATY, E. (1848): “Étude archéologique sur Saint Calais et son canton,” Tech. rep., Bulletin de la Société royale d’agriculture, science et arts de la Sarthe.
- PELLICER I BRU, J. (1982): “Un tresor de dirhems àrabs a SC.-J.” *Acta numismàtica*, 139–166.
- (1985): “El tresoret de moneda àrab LR-P dels anys 331-418 AH,” *Acta numismàtica*, 157–182.
- PEÑA MARTÍN, S. AND M. VEGA MARTÍN (2007): “La amonedación canónica del emirato omeya andalusí antes de Abd-al-Rahman II, según el hallazgo de dirhams de Villiciosa (Córdoba),” .
- PENNAS, V. (1991): “Byzantine Monetary Affairs during the 8th, 9th, 10th and 11th Centuries,” D.phil thesis, University of Oxford.
- (1996): “Life in Byzantine Cities of Peloponnesos: The Numismatic Evidence (8th-12th Century),” in *Mneme Martin Jessop Price*, Hellenic Numismatic Society.
- PETRY, K. AND S. WITTENBRINK (2021): *Der karolingische Münzschatzfund von Pilligerheck (Landkreis Mayen-Koblenz), vergraben nach 855*, Verein der Münzfreunde für Westfalen und Nachbargebiete.
- POIARES, A. (2000): “Diremes califais encontrados ao norte de Mértola,” *Arqueólogo Português*, 201–268.
- PRIEGO, M. C. (2020): “Estratos, vellones,” feluses” y tremises: Estratigrafía y numismática en el yacimiento de la Vega Baja de Toledo (ss. VII-XV dC),” in *El sitio de las cosas: la Alta Edad Media en contexto*, Servicio de Publicaciones, 123–160.

- PRIEGO, M. C. AND L. O. ENCISO (2016): “Dírhams, feluses y contextualización arqueológica en el centro de la Península: nuevos hallazgos de época emiral (s. VIII-IX dC) en Recópolis,” in *Patrimonio numismático y museos: actas XV Congreso Nacional de Numismática. Madrid, 28-30 de octubre de 2014*, Museo Casa de la Moneda, 1097–1114.
- PRIETO, A. (1934): “Tesoro de monedas musulmanas encontrado en Badajoz,” *Al-Andalus*, 2, 299.
- PROFANTOVA, N. (2009): “Byzantine Coins from the 9th-10th century from the Czech Republic,” in *Byzantine Coins in Central Europe between the 5th and 10th century*, ed. by M. Wołoszyn, Polish Academy of Arts and Sciences, Institute of Archaeology.
- PUERTAS, A. F. (1982): “Catálogo de los fondos numismáticos hispanomusulmanes del Museo de Cuenca,” *Cuadernos de la Alhambra*, 115–142.
- REINHOLD FISCHER AUCTIONSHAUS (2010): “Auction 114,” Tech. rep.
- RENOU, E. J. (1846): *Description géographique de l'empire de Maroc*, vol. 8, Imprimerie Royale.
- RODRIGUES MARINHO, J. (1995): “Um Achado de Dirhames do Emirado Ándalus em Castro Marim,” *O Arqueólogo Português IV*, 13–15.
- RODRÍGUEZ PALOMO, D. AND F. MARTÍN ESCUDERO (2022): “Moneda en contexto arqueológico en Mārida (siglos VIII-IX). Estudio e interpretación,” *Arqueología y territorio medieval*, 29.
- RONDIER, R. F. (1869): “Troupailles de monnaies près de Chef-Boutonne,” *Revue de l'Aunis, de la Saintonge et du Poitou*.
- ROYAL NUMISMATIC SOCIETY (1975): *Coin Hoards, Volume 1*, London.
- (1977): *Coin Hoards, Volume 3*, London.
- (1978): *Coin Hoards, Volume 4*, London.
- RUIZ ASENCIO, J. M. (1967): “Tesorillo de dirhemes del Emirato hallado en la Lantejuela,” Tech. rep., nvmisma.
- RÉVÉSZ, L. (1996): “A karosi honfoglalás kori temetők : régészeti adatok a Felső-Tisza-vidék X. századi történetéhez,” Tech. rep.
- SABATIER, J. (1862): *Description générale des monnaies byzantines frappées sous les empereurs d'Orient depuis Arcadius jusqu'à la prise de Constantinople par Mahomet II*, Rollin et Feuardent.
- SACCOCCI, A. (2005): “Ritrovamenti di monete islamiche in Italia continentale e in Sardegna (secc. VII-XVI),” in *Simone Assemani Symposium sulla monetazione islamica. Simone Symposium on Islamic Coinage*, 137–149.
- SACCOCCI, A. ET AL. (2004): “Il ripostiglio dall'area “Galli Tassi” di Lucca e la cronologia delle emissioni pavesi e lucchesi di X secolo,” *Bollettino di Numismatica*, 36, 165–203.
- SAENZ-DIÉZ, J. I. (1993): “Museo municipal de Sevillla : fondos islamicos de la colección Gago,” Tech. rep., III Jarique de numismática hispano-arabe.
- SALIDO DOMÍNGUEZ, J., R.-L. GARCÍA LERGA, R. GÓMEZ OSUNA, E. GARCÍA ARAGÓN, M. BLANCO DOMÍNGUEZ, AND J. BARRIO MARTÍN (2020): “Un nuevo conjunto de monedas emirales del centro peninsular: los dírhams del yacimiento arqueológico de El Rebollar (El Boalo, Madrid),” .
- SARAH, G., V. GENEVIÈVE, AND C. GUERROT (2016): “Le trésor carolingien découvert à Auzeville (Haute-Garonne) en 1878. Étude des monnayages toulousains de Charles le Chauve et de Pépin II d'Aquitaine,” *Revue numismatique*, 6, 417–498.
- SARFATIJ, H., W. J. H. VERWERS, AND P. WOLTERING (1999): *In discussion with the past: Archaeological studies presented to WA van Es*, Foundation for Promoting Archaeology (Stichting Promotie Archeologie).

- SCHINDEL, N. (2005): “Sasanian coinage,” *Encyclopædia Iranica*.
- SCHNEIDER, A. M. (1952): “Hirbet el-Minje am See Genesareth,” *Annales Archéologiques Syriennes*, 2, 23–45.
- SCHULZE, M. (1984): “Das ungarische Kriegergrab von Apres-Lès-Corps. Untersuchungen zu den Ungarneinfällen nach Mittel-, West- und Südeuropa (899–955 n. Chr.) mit einem Exkurs zur Münzchronologie altungarischer Gräber,” *Jahrbuch des Römisch-Germanischen Zentralmuseums Mainz*, 31, 473–514.
- SEARS, S. D. (1994): “A late Umayyad hoard from Nippur,” *The Numismatic Chronicle*, 133–146.
- (2000): “An Abbasid Revolution Hoard from the Western Jazira (al-Raqqa?),” *American Journal of Numismatics*, 12, 171–193.
- SEGOVIA SOPO, R. (2006): “Tesorillo de moneda del Emirato Independiente hallado en Fuente de Cantos y su contextualización en las Guerras de Ibn Marwan contra la corte cordobesa,” in *VI Jornada de Historia de Fuente Cantos: Actas*, Asociación Cultural Lucerna, 145–178.
- (2014): “El tesorillo numismático andalusí de la C/Santa Julia de Mérida (Badajoz): circulación y ocultación monetaria durante la ‘Fitna’ del Califato de Córdoba,” *Cuadernos emeritenses*, 1–396.
- SEGOVIA SOPO, R. AND A. V. JIMÉNEZ (2011): “Un inédito tesorillo de moneda emiral independiente hallado en el Teatro Romano de Mérida,” in *Ars metallica. Monedas y medallas: Nules-Valencia, 25-27 de octubre de 2010*, Museo Casa de la Moneda, 795–816.
- SIMMER, A. (2000): “Le trésor carolingien d’Ebange-Florange,” *Les cahiers lorrains*, 3–18.
- SLOVENSKÁ AKADÉMIA VIED. ARCHEOLOGICKÝ ÚSTAV (1979): *Rapports du IIIe Congrès international d’archéologie slave: Bratislava, 7-14 septembre 1975*, vol. 1, Veda.
- SOCIÉTÉ DE STATISTIQUE, SCIENCES, LETTRES ET ARTS DU DÉPARTEMENT DES DEUX-SÈVRES (1882): “Sur un trésor carlovingien provenant de Brioux,” *Bulletins de la Société de statistique du département des Deux-Sèvres*, V.
- SOCIÉTÉ DES ANTIQUAIRES DE L’OUEST (1982): “Communications,” *Bulletins de la Société des antiquaires de l’Ouest*, 6.
- SOLER BALAGUERO, M. (1993): “Las monedas árabes del gabinete numismático del IEI,” in *III Jarique de numismática hispano-arabe*.
- SOMBART, S. (2008): “Le trésor carolingien de Luzancy (77138), enfoui ou perdu vers 865–870?,” *Bulletin de la Société française de numismatique*, 63, 128–9.
- SOPHOULIS, P. (2011): “Byzantine coin-circulation in early medieval Bulgaria (mid 8th - early 9th c.),” .
- TREADWELL, L. AND E. ROGAN (1994): “An Ottoman report of an Umayyad coin hoard: Jarash, 1898,” *Yarmouk Numismatics*, 6, 20–29.
- TROUSSEL, M. (1942): “Monnaies d’argent (dirhams) idrissites et abbassides trouvées à Ouenza,” *Recueil des notices et mémoires de la Société archéologique de Constantine*, 65, 105–123.
- ÜNAL, C. (2015): “The Tralleis Hoard and the Reflection of the Iconoclastic Idea in Byzantine Coin Iconography,” *American Journal of Numismatics*, 27, 199–205.
- (2018): “Kavaklı Defnesi: II. Constans Dönemine Ait Altın Sikkeler,” *Cedrus*, 6, 465–483.
- URANGA, J. E. (1950): “El hallazgo de” dírhemes” del Emirato en San Andrés de Ordoiz (Estella, Navarra),” *Príncipe de Viana*, 11, 85–101.
- VALLE, A. M. (1987): “El tesoro califal de “Los Villares” (Caudete, Valencia),” *Acta numismática*, 177–196.

- VAN DER VELDE, H. (2008): “Cananefaten en Friezen aan de monding van de Rijn,” *ADC Monografie*, 5, 536.
- VAN ES, W. A. AND W. J. H. VERWERS (1980): *Excavations at Dorestad. 1: The Harbour, Hoogstraat*, Amersfoort: Rijksdienst voor het oudheidkundig bodemonderzoek.
- VANDENBOSSCHE, É. AND S. COUPLAND (2012): “Une trouvaille de deniers carolingiens dans la région de Bray-sur-Seine,” *The Numismatic Chronicle*, 172, 307–321.
- VÖLCKERS, H. H. (1965): *Karolingische Münzfunde der Frühzeit, 751-800: Pippin, Karlmann, Karl der Große, I. und II. Münzperiode*.
- VRYONIS, S. J. (1971): “An Attic Hoard of Byzantine Gold Coins (668–741) from the Thomas Whittemore Collection and the Numismatic Evidence for the Urban History of Byzantium (1963),” in *Byzantium: its internal history and relations*.
- WEBSTER, G., R. DOLLEY, AND G. DUNNING (1953): “A Saxon treasure hoard found at Chester, 1950,” *The Antiquaries Journal*, 33, 22–32.
- WIECHMANN, R. (2004): “Karolingische Denare aus Bardowick–Münzumlauf an der nördlichen Peripherie des Frankenreichs,” in *Delectat et docet. Festschrift zum 100jährigen Bestehen des Vereins der Münzenfreunde in Hamburg*, Hamburg, 13–44.
- WILLIAMS AND AGER (2010): “The Vale of York Hoard,” Tech. rep., British Museum Objects in Focus.
- WILSON, J. (1989): “The gold hoard,” in *Excavations at Capernaum I (1978–1982)*, ed. by V. Tzaferis, Eisenbrauns.
- WOŁOSZYN, M. (2009): *Byzantine Coins in Central Europe between the 5th and 10th century*, Polish Academy of Arts and Sciences, Institute of Archaeology.
- WROTH, W. (1908): *Catalogue of the Imperial Byzantine Coins in the British Museum*, Order of the Trustees, British Museum.
- ZÄCH, B. (2001): *Kanton St. Gallen I: Mittelalterliche und neuzeitliche Münzfunde*, Schweizerische Akademie der Geistes-und Sozialwissenschaften.
- ZÄCH, B. AND J. D. TABERNERO (2002): “Zwei Münzfunde des 9. und 10. Jahrhunderts aus dem Alpenrheintal: Lauterach (1868) und Chur (1997),” *Schweizerische numismatische randschau= Revue suisse de numismatique*, 93–128.
- ZUYDERWYK, J. AND J. BESTEMAN (2010): “The Roermond hoard: a Carolingian mixed silver hoard from the ninth century,” *Medieval and Modern Matters*, 1, 73–154.

C Mapping the Data to the Model

C.1 Constructing regions

To map our data to the model, we need to define which hoard and find locations correspond to which model locations. We define spatial aggregates based on historical political boundaries, geography, and computational feasibility, noting that political boundaries change over time, while our location definition must not. Moreover, administrative boundaries are not available for the same time period for all regions. We proceed in two steps; we first construct region boundaries based on the regions in al-Thurayya (Romanov and Seydi, 2022), covering the maximum extent of the Umayyad caliphate, and then define regions for the remainder of our area of interest.

Constructing regions for the Arab world .We use the `region` tag associated with each Althurayya locations to establish a historical provincial partition of the Arab world.

1. We manually delineate a rough approximation of the Arab world's boundary.
2. We apply spherical voronoi tessellation (see section C.4) to all al-Thurayya locations within this boundary.
3. The resulting polygons are categorized based on the region information associated with each polygon's corresponding location, aligning them with the 22 regions presented in table C.2 (excluding NoRegion).
4. We then take the union of the polygons under the same `region` tag.
5. We intersect the resulting (multi-)polygon with the coastline to remove the portions of the polygon that extended into the sea.
6. The final (multi-)polygon represents the corresponding Arab region.

We also corrected some erroneously labelled region labels⁸.

Constructing regions for the western world .We construct regions in the western world roughly based on administrative boundaries that we retrieve from the *Digital Atlas of the Roman and Medieval Civilizations* (DARMC) hosted at Harvard University, specifically the AD 200 and 303-325 Roman provincial boundaries (which are based on the Barrington Atlas, Talbert, 2000) and the Medieval kingdom boundaries around AD 814, which are an original contribution of DARMC.

We define the boundaries of our region of interest in Europe by taking the union of the AD 200 Roman provincial boundaries with the 814 boundaries of the Frankish empire and the area of the West Slavs. The resulting border is roughly the modern-day German-Polish border, plus Bohemia, but follows otherwise roughly the AD 200 Roman Empire boundary. In the areas covered by al-Thurayya, the border is delineated roughly by the convex hull of the spatial extent of administrative district boundaries.

Aggregating regions. We then merge a number of regions in order to have mints and hoards in all regions (which is important for identification). We merge the realm of Charlemagne with the Frankish lands in Germania; the areas of Byzantine Thracia and Dacia, and combine Sardinia and Corsica. In the east, we combine the administrative districts of the eastern Caliphate where hoard coverage is sparse, the regions of al-Iraq, al-Jibal, Khuzestan, and Kirman; and finally the regions of the Arabian Peninsula.

C.2 Defining the coin sample for the structural analysis

We use the same sample of coins as for the reduced-form analysis in section 1, with the following exceptions:

- We exclude coins where the mint date interval exceeds 150 years.
- We exclude non-hoard coin finds from excavations (because the *tpq* is meaningless).

⁸See [this link](#).

C.3 Constructing the geospatial model

We build our geospatial model by combining two geospatial models constructed by historians to model travel distances and routes. The first one, ORBIS (Scheidel, 2015), is a geospatial model of the Roman world and spans roughly the maximum extent of Roman conquests. The second, Al-Thurayya (Romanov and Seydi, 2022) is a digitization of Cornu (1983)'s atlas of the Islamic world in the 9th and 10th century. Both geospatial models take the form of undirected graphs; in the case of ORBIS this is augmented by measures of travel costs on each edge. ORBIS also contains sea routes; for the Arab world we augment al-Thurayya with a number of known sea routes. For al-Thurayya we also construct bilateral travel distances ourselves.

Vertices. The following links in this document point to the [ORBIS city data](#) and [Althurayya city data](#) we used in our analysis. ORBIS data labels locations as either actual cities or crossroads. Actual cities are denoted by their authentic names, which correspond to those displayed on the ORBIS website. Crossroads are not designated with a name and are labeled using an "x" and are not visible on the ORBIS website. Similarly, Althurayya locations are characterized by more diverse types, including capitals, metropoles, quarters, sites, towns, villages, waters, waystations, and xroads. Note that some of these locations do not have a name in the dataset.

Edges. The edge data for [ORBIS](#) and [Althurayya](#) is accessible via the respective links provided in this document. We employ the Haversine formula to calculate the length of ORBIS edges, assuming a radius of 6371 km for the Earth. The lengths of Althurayya edges are included within the raw dataset.

Merging the graphs. We merge the two graphs by primarily merging vertices shared between them. Some cities hold significance in both the early Islamic world and the Roman world. The challenge of this task is due to differences in location names for the same city within each database. For instance, the city known as Cádiz in Spain is referred to as Gades in ORBIS and Qadis in Althurayya. To address this issue, we implement a preliminary screening process to identify Althurayya locations within a 20km radius of each ORBIS location. We then manually determine whether the location in ORBIS and its counterpart in Althurayya indeed represent the same city. The collection of our refined city pairs and the decisions made can be accessed through the following [link](#).

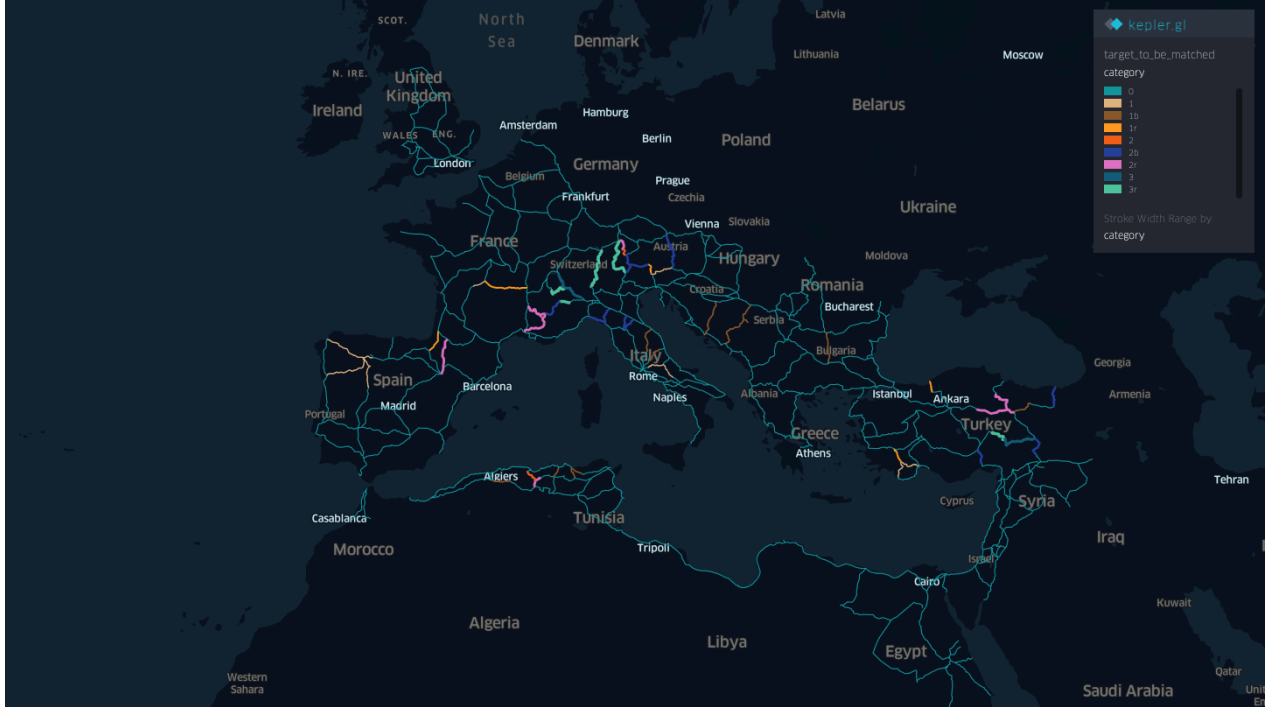
Apart from the two main data source of routes, we also added the Volga trade route, sea routes in the Caspian Sea and sea routes in the Arab world (see below).

During the merge, the geometry of the routes remains unchanged. The only change resulting from the merge is that common locations are treated as identical vertices in the adjacency matrix. All cities are re-indexed and prepared for the computation of least distances and fastest routes after the merge.

Constructing sea routes for the Arab world. We extend [ORBIS's algorithm for sea routes](#) to the Mediterranean Sea and the Black Sea, the Red Sea, the Arabian Sea, the Gulf of Persia, and the Gulf of Oman. Our process begins by creating a grid with a resolution of 0.1 degrees by 0.1 degrees, covering the area of interest in the sea. Each point on the grid can move in eight directions (N, S, W, E, NW, NE, SW, SE). We then manually select Althurayya locations that are close to the coastline as [potential ports](#). Among these candidates, we choose only those whose type is labelled as [capitals](#), [metropoles](#), [sites](#), [towns](#), [villages](#), or [waystations](#), excluding [regions](#) (centroid of a region) and [xroads](#). These selected ports are projected onto the nearest points in the grid, and we calculate the shortest travel time paths along the grid for [given routes](#). The measurement of travel duration is defined below.

Constructing sea routes for Volga trade route Volga trade route plays an important role in connecting northern Europe and northwestern Russia with the Caspian Sea via the Volga River. For the segments within the Caspian Sea, we have extended the method outlined for sea routes. Specifically, we have chosen the following sea routes: Abaskun-Derbent, Derbent-Sasqin, Kuhanrudh-Baku, and Baku-Derbent. To establish a connection between the Caspian Sea and the Black Sea, we have added routes Sasqin-Tanais (via canal), Sarai-Saqsin (via canal), and Sarai-Sarkel (via land). Sasqin-Tanais is represented by a segment in the Don River, which was retrieved from OpenStreetMap [here](#), while Sarai-Saqsin is a segment in the Volga River, retrieved from OpenStreetMap [here](#). Sarai and Sarkel are connected directly since they are in close proximity to each other.

Determining weights and speed.



Appendix Figure C.1: The ORBIS adjustment visualized

Roads. ORBIS categorizes the weight and speed of terrestrial edges in a categorical manner. Table C.4 shows ten different types of adjustments used by ORBIS, and the locations of these edges are illustrated in Figure C.1. The speed of an edge in ORBIS is defined by Equation C.1.

$$\text{speed} = \text{weight} \times 30\text{km}/d, \quad \text{weight} = \frac{\text{unadjusted length}}{\text{adjusted length}} \quad (\text{C.1})$$

ORBIS does not provide explanations for the criteria used to select and categorize edges, otherwise we could simply apply these rules to the Althurayya network. Nevertheless, we have collected various edge-related variables from [Stanford EarthWorks](#) and [2019 ASTER project](#) for both ORBIS and Althurayya edges. We run a regression to explain the ORBIS weight defined in Equation C.1 using these variables. We then extrapolate this linear model to the Althurayya data. To put it simply, we use ORBIS as the training set and Althurayya as the test set.

We collect the following variables for all edges and both directions:

uphill_3d_2d_ratio After properly sampling an edge (as described in Section ??), we identify all segments that ascend along the specified direction (where the height at the end is greater than the height at the beginning), and then compute the ratio.

$$\text{uphill_3d_2d_ratio} = \frac{\sum_s \text{goes uphill length_3D}_s}{\sum_s \text{goes uphill length_2D}_s}, \quad s \text{ is a segment in the edge}$$

A large ratio indicates a steep uphill slope.

downhill_3d_2d_ratio Similar to **uphill_3d_2d_ratio**,

$$\text{downhill_3d_2d_ratio} = \frac{\sum_s \text{goes downhill length_3D}_s}{\sum_s \text{goes downhill length_2D}_s}$$

cityrank_1 We find the intersection of the edge and the 20 km buffer area of rank 1 cities. Find the ratio of the length of the intersection over the length of the entire edge. The rank of the cities are defined as the following:

ORBIS	Cumulative Proportion	Althurayya (w/o quaters, regions)	Cumulative Proportion	Harmonized Rank
6	25.1%	xroads	8.6%	1
		waystations	29.0%	
60	33.9%	sites	31.2%	2
		waters	37.6%	
70	48.2%	villages	48.7%	3
		towns	94.2%	
80	83.2%	capitals	99.4%	4
90	98.2%			5
100	100%	metropoles	100%	6

cityrank_2 Similar to **cityrank_1** but with rank 2 cities.

cityrank_3 Similar to **cityrank_1** but with rank 3 cities.

cityrank_4 Similar to **cityrank_1** but with rank 4 cities.

cityrank_5 Similar to **cityrank_1** but with rank 5 cities.

cityrank_6 Similar to **cityrank_1** but with rank 6 cities.

landfeature_Desert The percentage of the edge's length that intersects desert polygons, retrieved from [Stanford EarthWorks](#), is calculated. A correction has been manually applied to account for the misidentification of the narrow passage along the Nile as desert

landfeature_Plateau Percentage of the edge's length that intersects plateau polygons, retrieved from [Stanford EarthWorks](#).

landfeature_Plain Percentage of the edge's length that intersects plain polygons, retrieved from [Stanford EarthWorks](#).

landfeature_Range/mtn Percentage of the edge's length that intersects mountain polygons, retrieved from [Stanford EarthWorks](#).

near_river Percentage of the edge that intersects the 20 km buffer area of **rivers**.

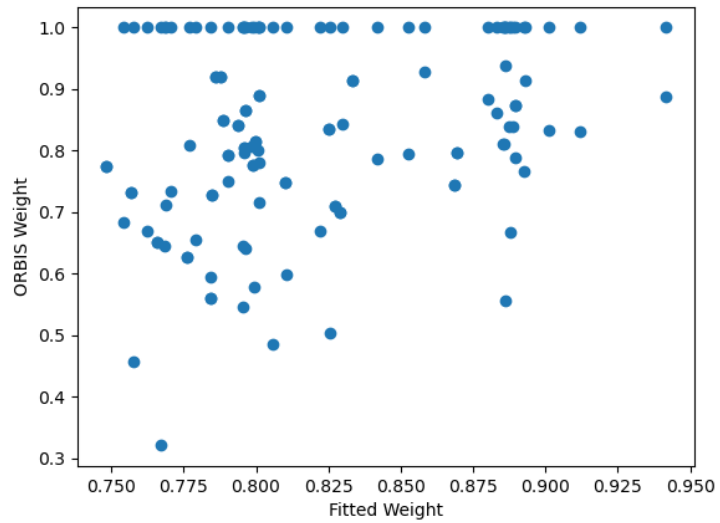
We fit adjusted ORBIS weights using the mentioned variables (except **landfeature_Desert** and **near_river** since ORBIS edges does not traverse desert at all, and rivers are modeled separately from the road in ORBIS). To ensure the plausibility of the coefficients and prevent overfitting, we perform least squares regression with the following constraints: (i) **uphill_3d_2d_ratio** has negative effect on the weight, (ii) The effect of **cityrank_*** has positive effect on the weight, (iii) The magnitudes of the effects for **cityrank_*** should follow the ranking **cityrank_1 < cityrank_2 < cityrank_3 < cityrank_4 < cityrank_5 < cityrank_6**, (iv) The effects of **landfeature_Plateau** and **landfeature_Range/mtn** on the weight should be negative, while the effect of **landfeature_Plain** should be positive. Figure C.2 shows a scatter plot between the fitted weight and the ORBIS weight.

We manually set the coefficient for desert to -0.5 and for river to 0.5. This implies that the marching speed is approximately 18.2 km/day for an edge that is 100% within a desert, and the marching speed is roughly 49.5 km/day for an edge near a river.⁹ The extrapolated weights and the edge locations are displayed in Figure C.3.

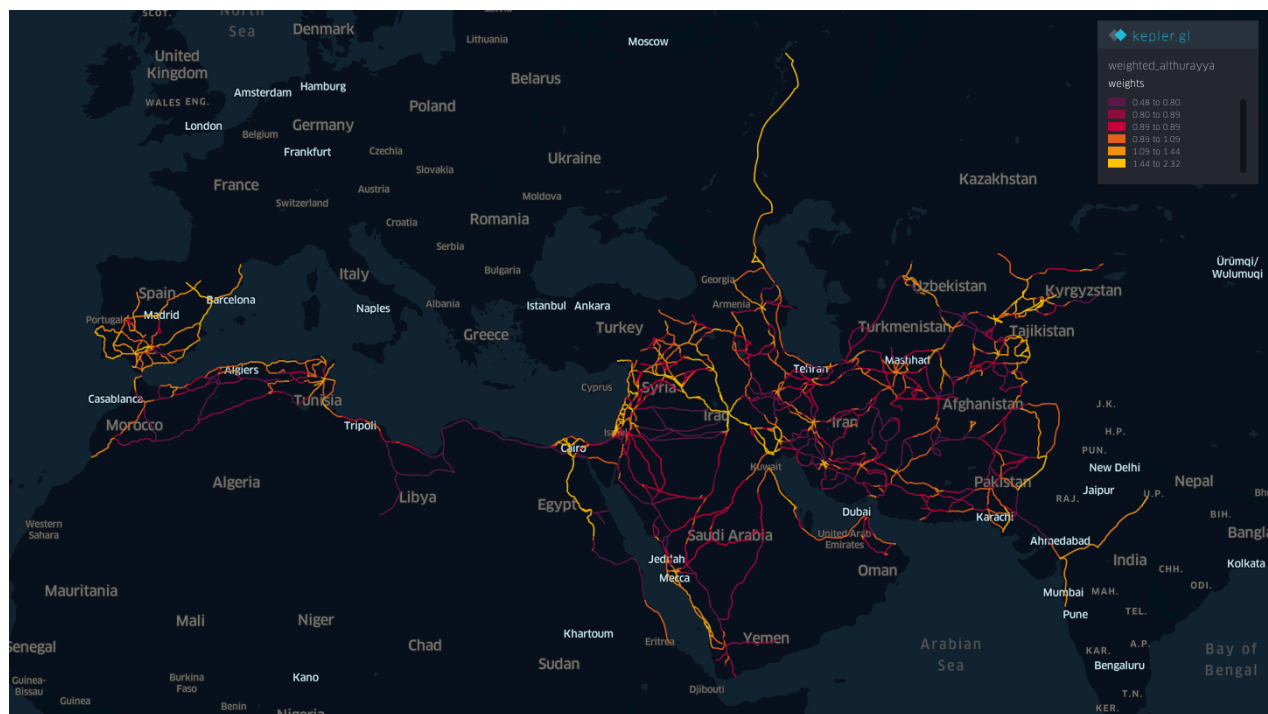
The choice of speed not only impacts the total travel time but also influences the traveler's chosen route. For instance, when considering the unweighted shortest route (Figure C.4) from Dimashq to Baghdad, it passes through the Syrian desert. However, with weighted speed considerations, the preferred route would bypass the desert and follow the Euphrates. Similarly, when traveling from Sana to Isfahan, the preferred route (Figure C.5) runs along the coast and includes a stop in Mecca before crossing the Arabian Peninsula.

Sea: We follow the methodology outlined in [Arcenas \(2015\)](#) to construct sailing speeds at sea, adopting the same steps used by ORBIS. Our data source is the [CCMP wind speed data](#), which provides wind direction and

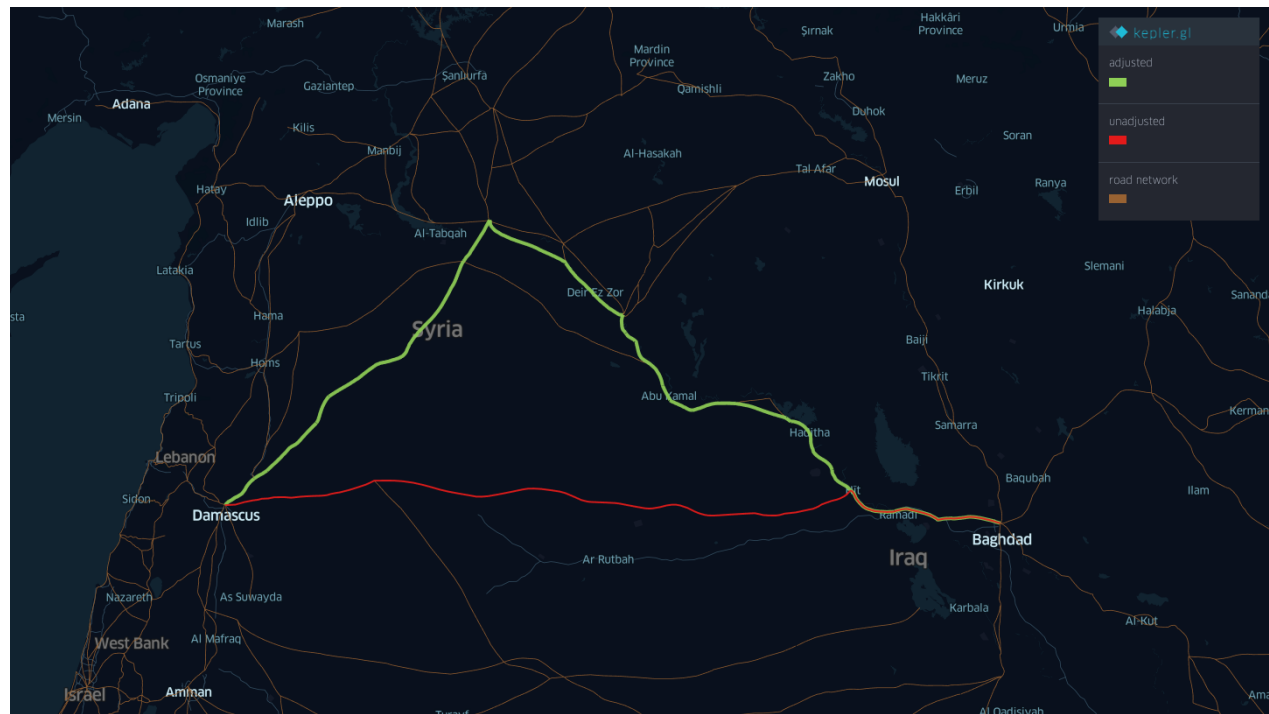
⁹This value is considered suitable since ORBIS indicates that a civilian vessel typically travels at around 65 km/day. Although we do not distinguish between river and road in Althurayya, the speed for a mix of different means of transportation should fall within the range of 30 km/day to 65 km/day



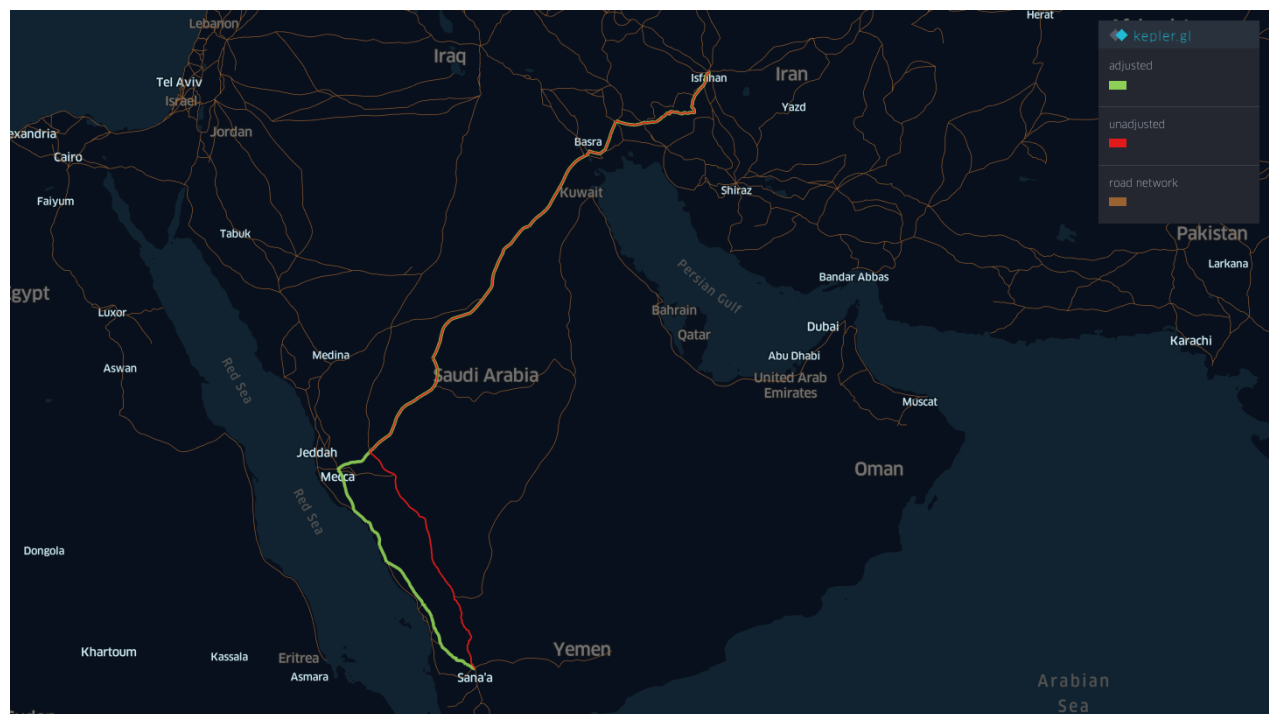
Appendix Figure C.2: Fitted ORBIS weight and actual ORBIS weight



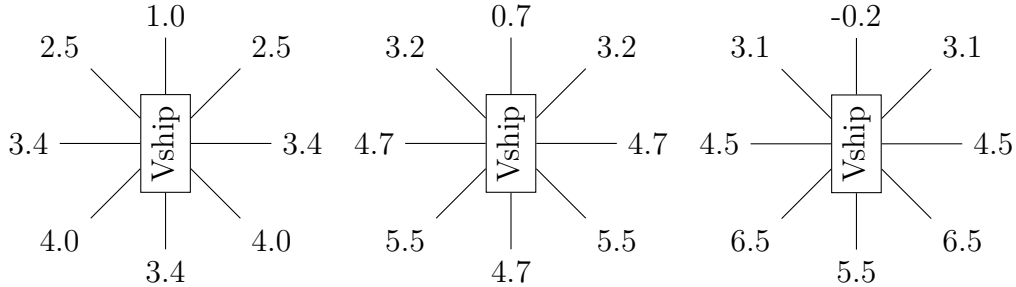
Appendix Figure C.3: Al-thurayya edges and their weight



Appendix Figure C.4: Route comparison from Damascus to Baghdad



Appendix Figure C.5: Route comparison from Sana'a to Isfahan



Appendix Figure C.6: Speed rose in light, moderate, and heavy wind (left to right, unit: knot)

speed information every 6 hours for each cell in a 0.25-degree \times 0.25-degree grid, spanning from 1993 to 2023. To align with ORBIS, we focused on speed data for the month of July.

We categorize the wind direction into eight main directions ("N", "NE", "E", "SE", "S", "SW", "W", and "NW"). At the latitude \times longitude \times direction level, we calculated two key metrics (i) The mean wind speed, and (ii) The proportion of time the wind blew in each direction.

In accordance with Arcenas (2015), scalar wind speeds were classified into four categories: "calm," "light," "moderate," and "heavy," with corresponding Beaufort scale classifications: calm < Beaufort 2; light = Beaufort 2; moderate breeze = Beaufort 3-4; and heavy air \geq Beaufort 5. Each category corresponds to a specific speed rose (see Figure C.6).

In Figure C.6, the figure on thin arrows denote the scalar velocity of the vessel if the wind blows down the direction of the thin arrow. For instance, when the wind speed is "light," the vessel's speed is 1.0 knot when sailing into the wind, 2.5 knots when the wind blows from the front-right, and 3.4 knots when the wind comes directly from the right. For each coordinate, we calculated the weighted mean of the vessel's speed across the eight wind directions, with the weight determined by the proportion of time the wind blew in each direction. We use the mean vessel speed in eight directions for each coordinate.

We create a 0.1-degree \times 0.1-degree mesh grid in the area of interest as described in Section C.3. The vessel can go in eight directions at each vertex. The integration of the vessel speed is essential due to the precarious of the wind speed in the sea. The difference of the least time sailing route under uniform speed and varying speed is shown in Figure C.7.

C.4 Technical details on operations in spherical geometry

Computing 2D distances. Our edges are essentially connecting segments that are characterized by a series of points. To determine the length of each segment, we calculate geodesic distances between the starting point and the ending point. This distance calculation is based on the Haversine equation formula.

$$d_{2D} = 2R \arcsin \sqrt{\text{hav}(\Delta\text{lat}) + \cos(\text{lat}_1) \cos(\text{lat}_2) \text{hav}(\Delta\text{lon})}$$

where

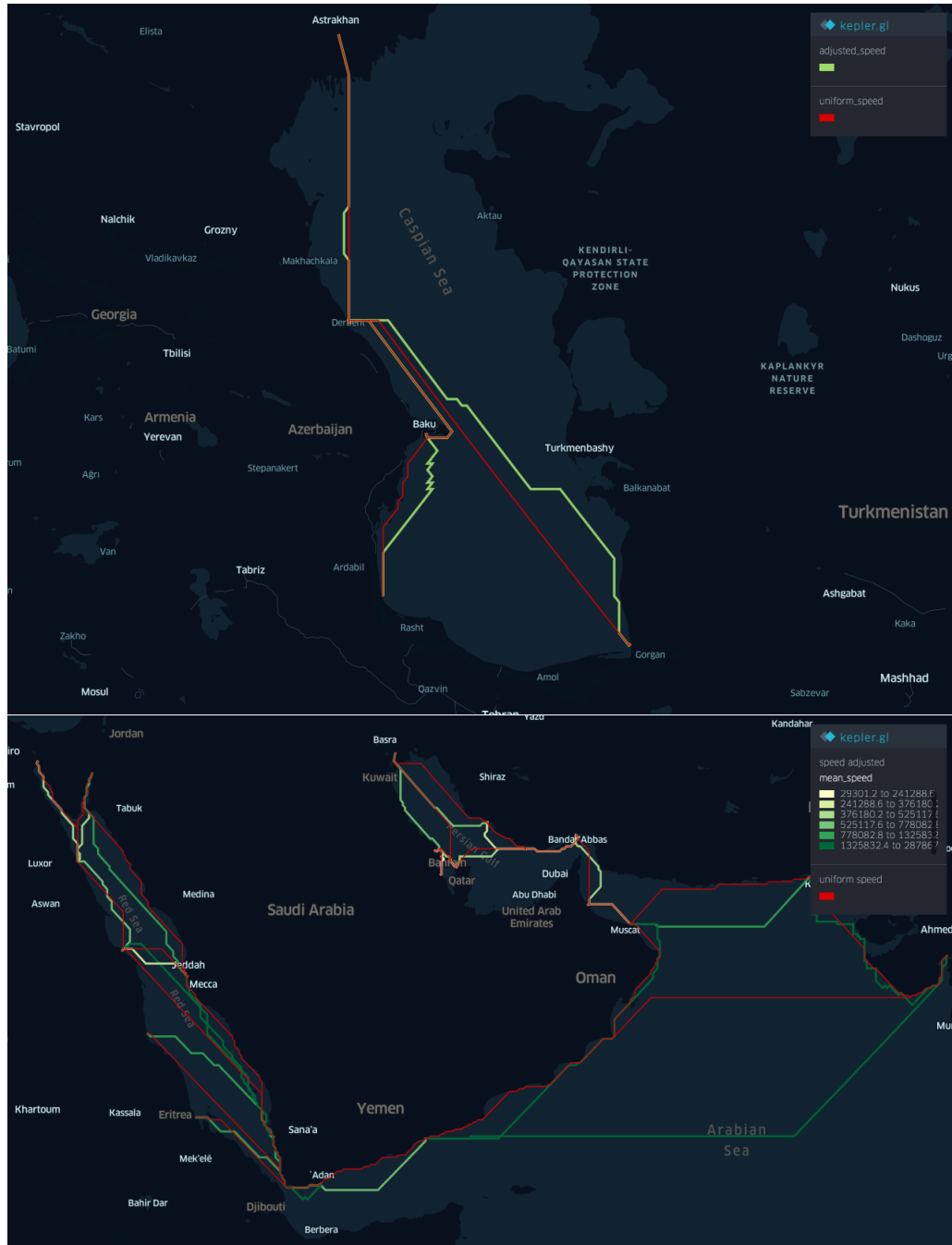
$$\text{hav}(x) = \sin^2\left(\frac{x}{2}\right).$$

Computing 3D distances. Past efforts to incorporate elevation data into the ORBIS dataset, together with the challenges, has been well-documented [here](#) by ORBIS. We follow the documented method, which involves sampling our roads with a series of equidistant points spaced 50 meters apart along the edge. For each sampled point, we retrieve elevation data from the [2019 ASTER project](#).

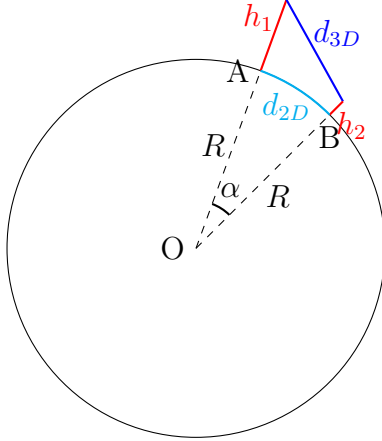
As illustrated in the diagram in Figure C.8, we calculate the angle $\alpha = d_{2D}/R$, with known d_{2D} , R (assumed to be 6371 kilometers), h_1 (the altitude of the start of the line segment) and h_2 (that of the end). Using Law of cosines, we have

$$d_{3D} = \sqrt{(R+h_1)^2 + (R+h_2)^2 - 2(R+h_1)(R+h_2) \cos \alpha}$$

One important consideration of computing the 3D distance is resolution and the sampling technique. It's essential to note that the mesh-grid in the ASTER project does NOT consist of congruent rectangles. As the



Appendix Figure C.7: Changes of the sailing route before and after incorporating wind speed



Appendix Figure C.8: The diagram for 3D distance computation. The circle shown in the graph is the great circle defined by A and B

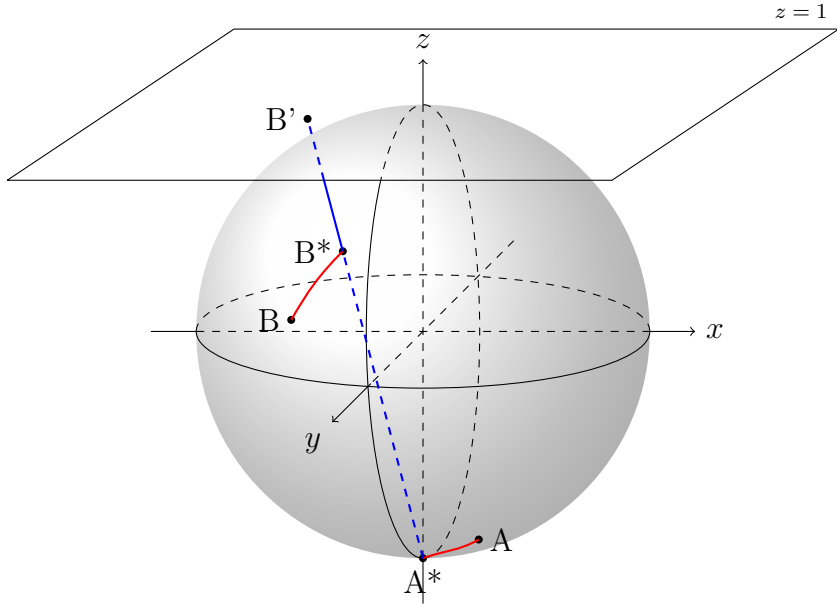
latitude deviates from zero, the rectangles become elongated. When the latitude is close to zero, it resembles more of a square shape. This distortion is due to the spherical shape of the earth.

It would be also unreliable to simply find all intersecting segments of the routes and the grid, and assign the segments with the grid's height data. Some edges are over-sampled than others. A path that goes from east to west and is close to the pole would gain more resolution comparing to a similar path that are closer to the equator, if segments are sampled this way. To address this issue, we interpolate our path each from start to end every 50 meters (in geodesic distance)¹⁰, use these sampled points to find the corresponding height data.

Spherical Voronoi tessellation. Na et al. (2002) proved that the spherical Voronoi tessellation can be computed by computing two planar Voronoi diagrams of sites under stereographic projection in the plane. Following Na et al. (2002) and Patel (2018), our Algorithm is described as the following:

1. Choose one arbitrary location among our sites as the center of projection (point A in C.9), or otherwise called the *anchor*.
2. (Drawn in red in C.9) Rotate the globe such that the anchor (A) meets the South pole (A^*). In the rotation, all other sites are also rotated ($B \rightarrow B^*$).
3. (Drawn in blue in C.9) Connect the South pole with sites that are not the anchor. Find the intersection (B') of the extended line and the plane $z = 1$. We have now created a mapping ($B \rightarrow B'$) that maps all the sites to points in the plane $z = 1$, except the anchor.
4. Perform Delaunay triangulation on the mapped sites. This can be easily done by the Python package `Shapely`'s function `triangulate()`.
5. Since the anchor is not projected, the triangulation is not complete. One needs to choose another arbitrary location as the anchor and repeat step 1-4. Merge the two different results of triangulation.
6. Map the triangulation back to the unrotated sphere. Find the spherical circumcenter of all the mapped-back triangles (The spherical circumcenter and the Euclidean circumcenter and the center of the sphere lies on the same line. The spherical circumcenter is on the surface of the sphere while the Euclidean circumcenter is inside the sphere).
7. Connect all circumcenter pairs whose corresponding triangles touch.

¹⁰The choice of 50 meters serves as an optimal compromise because it ensures that consecutive sampled points are placed in different grid cells because 50 meters slightly exceeds the diagonal length of a 30m x 30m square grid cell



Appendix Figure C.9: Diagram for the stereographic projection

Caveat. Step 6 can potentially cause problems because there are two spherical circumcenters of a triangle. They are antipodal point of each other. If all sites are spaced somewhat evenly around the sphere, it works simply by choosing the spherical circumcenter that is on the same side of the Euclidean circumcenter. However, all our sites can be contained in one hemisphere and Althurayya sites are far from being “placed evenly”. Therefore, we are bound to encounter problems with some spherical circumcenter with the unadjusted algorithm. The remedy is that we add an auxiliary site that is far from our original sites¹¹ when triangulating, and we always choose the spherical circumcenter that is on the same side as the Euclidean circumcenter. Since the auxiliary point is far, the voronoi polygon containing it is outside of our spatial scope of analysis. For instance, in the Voronoi diagram of Althrayya sites, the polygon containing the auxiliary point includes Antarctica, southern part of Australia and South America.

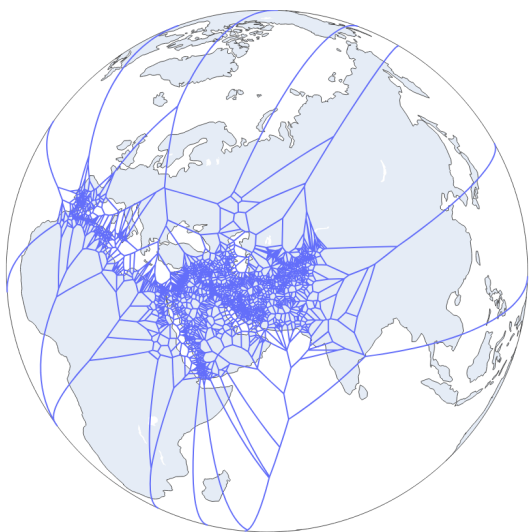
Obtaining the arc between two points. This topic is relevant mainly in terms of visualization. We can obtain an approximation of the arc between two point on the globe with the help of the gnomonic projection, because the gnomonic projection projects all great circles into straight lines. For an arc which we only have its two endpoints, we project them on the plane $z = -1$, fill the projected linestring with additional vertices so that segments divided by these additional vertices are no longer than the choice of maximum segment length. This can be easily achieved by Python package `Shapely`'s `segmentize()`. We then map the processed linestring back to the sphere surface. Note that this method can result in uneven resolution. This method can come in handy when even resolution is not important.

C.5 Other utilities

Since `Shapely` primarily handles shapes in Euclidean space, we had to develop most of our own utilities. For instance, when dealing with the intersection of two lines on the globe, we treat it as the intersection of two great circles. To achieve this, we transform latitude and longitude coordinates into XYZ coordinates. We then determine the planes that pass through these two lines and find their intersection with the spherical surface.

We also developed our own interpolation function for arcs characterized by a start and an end. To achieve this, we first find all the points on the sphere that are at a certain distance from the start point, effectively creating a

¹¹To decide which auxiliary site to add, we find the mean of longitudes and the mean of latitudes of our original sites, then make the auxiliary site the antipodal of the point (mean of longitude, mean of latitude)



Appendix Figure C.10: The voronoi of all sites in Althurayya

circle around the start. We identify the plane that passes through the arc and calculate the intersection points of the plane and the circle. This typically results in two points, and we choose the one inside of the arc.

C.6 Tables and references

Country	Total	City	Crossroad	Country	Total	City	Crossroad
United Kingdom	200	32	168	Cyprus	7	7	0
Italy	119	111	8	Serbia	7	7	0
Turkey	88	86	2	Hungary	6	4	2
Greece	69	69	0	Lebanon	6	5	1
France	50	49	1	Ukraine	6	6	0
Spain	43	42	1	Bosnia & Herzegovina	5	2	3
Egypt	36	36	0	Morocco	5	5	0
Algeria	23	23	0	Jordan	5	5	0
Tunisia	18	18	0	Slovenia	4	3	1
Syria	17	14	3	West Bank	2	2	0
Libya	16	16	0	Gaza Strip	2	2	0
Germany	16	15	1	Macedonia	2	2	0
Romania	15	11	4	Russia	2	2	0
Croatia	15	12	3	Georgia	2	2	0
Austria	11	11	0	Montenegro	1	1	0
Bulgaria	11	10	1	Netherlands	1	1	0
Israel	9	9	0	Iraq	1	1	0
Portugal	8	5	3	Malta	1	1	0
Albania	8	6	2	Total	844	640	204
Switzerland	7	7	0				

Appendix Table C.1: ORBIS cities by their modern country, distinguishing city types (city or crossroad)

Country	Total	capitals	metrop.	quarters	sites	towns	villages	waters	waystns	xroads
Mā-warā ³ -l-nahr	186	17	1	0	3	93	21	0	31	20
Ḩurāsān	139	12	1	0	0	70	16	1	30	9
al-Šām (Greater Syria)	138	7	1	0	0	57	23	0	27	23
Jazīra al-‘arab	122	3	1	0	3	29	16	0	62	8
Fārs(or Fāris)	114	7	1	0	1	45	15	0	42	3
al-Maġrib	110	6	0	0	0	78	5	0	1	20
Aqūr (al-Jazīra)	94	4	0	1	0	45	9	0	25	10
Misr (Egypt)	88	4	1	1	3	44	23	0	7	5
al-Andalus (Spain)	83	0	1	0	0	62	3	0	0	17
al-Jibāl	71	9	1	0	1	16	4	0	31	9
al-‘Irāq	66	5	1	1	1	37	7	0	11	3
al-Rihāb (Caucasus)	62	2	1	0	0	34	10	0	4	11
Badiyya al-‘arab	60	0	0	0	2	4	1	0	48	5
al-Sind	53	4	0	0	0	36	2	0	1	10
al-Daylam	50	3	1	0	0	20	6	0	18	2
al-Mafāza	49	0	0	0	0	3	8	0	33	5
Kirmān	44	3	1	0	0	26	6	0	5	3
Sijistān (Sīstān)	40	4	0	0	0	19	6	0	6	5
Barqa (Lybia)	39	1	0	0	1	8	4	0	24	1
Hūzistān (al-Ahwāz)	39	7	1	0	0	14	2	0	13	2
al-Yaman	31	5	0	0	0	14	2	0	4	6
al-Hazar	8	1	0	0	0	4	0	0	0	3
NoRegion	6	0	0	0	0	0	0	0	0	6
Total	1692	104	13	3	15	758	189	1	423	186

Appendix Table C.2: Althurayya cities by region, distinguishing city types (capitals, metropoles, quarters, sites, towns, villages, waters, waystations, xroads)

	count	mean	std	min	10%	25%	50%	75%	90%	99%	max
ORBIS	1215	144489.0	158012.5	3827.2	31606.2	58006.7	102353.1	168695.0	300377.0	737576.2	2142105.6
Althurayya	2053	55530.4	64952.5	1687.0	13851.8	23842.0	38387.0	62771.0	108031.6	332197.5	861693.0

Appendix Table C.3: Summary statistics of the lengths of the edges in graphs

Type ID	source → target	target → source
0	No adjustment	No adjustment
1	Add 18 km to the length	No adjustment
2	Add 36 km to the length	No adjustment
3	Add 54 km to the length	No adjustment
1r	No adjustment	Add 18 km to the length
2r	No adjustment	Add 36 km to the length
3r	No adjustment	Add 54 km to the length
1b	Add 18 km to the length	Add 18 km to the length
2b	Add 36 km to the length	Add 36 km to the length
3b	Add 54 km to the length	Add 54 km to the length

Appendix Table C.4: Adjustment by ORBIS

References

- ARCENAS, S. (2015): “ORBIS and the sea: A model for maritime transportation under the Roman Empire,” *Retrieved February, 22, 2021.*
- CORNU, G. (1983): *Atlas du monde Arabo-Islamique à l'époque classique: IX.-X. siècles*, Brill.
- NA, H.-S., C.-N. LEE, AND O. CHEONG (2002): “Voronoi diagrams on the sphere,” *Computational Geometry*, 23, 183–194.
- PATEL, A. (2018): “Delaunay+Voronoi on a sphere,” .
- ROMANOV, M. AND M. SEYDI (2022): “al-Thurayyā,” <https://althurayya.github.io/> [Accessed: (1 July 2023)].
- SCHEIDEL, W. (2015): “ORBIS: The Stanford geospatial network model of the Roman world,” Tech. rep.
- TALBERT, R. J. (2000): *Barrington Atlas of the Greek and Roman World: Map-by-map Directory*, vol. 1, Princeton University Press.